

ADAMA SCIENCE AND TECHNOLOGY UNIVERSITY

School Of Mechanical, Chemical and Materials Engineering



The Comparative Analysis of Thermal Stress Variation in Disc Brake

**A Thesis Submitted To the Graduate School of Adama Science and
Technology University**

**In Partial Fulfillment of the Requirements for the Degree of Masters Of
Science**

In

Automotive Engineering

By: Lemi Abebe

Advisor: Dr. N.Anbasagan

Jan, 2016

Declaration

Adama Science and Technology University

School Of Mechanical, Chemical and Materials Engineering

This is to certify that the thesis prepared by **Lemi Abebe**, entitled: **The Comparative Analysis Of Thermal Stress Variation in Disc Brake**, do here by declare this thesis is my original work and that it has not been submitted partially, or in full for a degree in any university/institution, which compiles with the regulations of the university and meets the accepted standards with respect to originality and quality.

Advisor: _____

Signature: _____

Date: _____

ACKNOWLEDGEMENT

During the course of my thesis work, there were many people who were instrumental and morally helping me. Without their guidance, help and patience, I would have never been able to accomplish the work of this thesis. I would like to take this opportunity to acknowledge some of them.

I am grateful to the God for the good health and wellbeing that were necessary to accomplish this work.

I would like to express my special thanks to my advisor, Dr. N.Anbasagan, for his comments, continuous support, guidance and suggestions throughout the entire thesis work.

I also gratefully acknowledge the help, valuable comments and suggestions offered by my co-advisor N. Ramesh Babu (Associate professor) which contribute much in enhancing the quality of my work.

I wish to express my sincere thanks to Bishoftu Automotive Industry specifically design section workers for providing me the necessary facilities for the thesis work.

I would like to thank my wife Emushako for her encouragement, and helped me in many ways.

Finally, I would like to take this opportunity to thank my father and my mother for all their help and understanding. Without my family's encouragement, love and support, this work would never have been accomplished.

Contents

ACKNOWLEDGEMENT	i
List of figures	v
List of tables.....	vii
Nomenclature	viii
Abstract.....	x
CHAPTER ONE.....	1
1. INTRODUCTION.....	1
1.1. Background of the study	1
1.2. Motivation	2
1.3. Statement of the Problem.....	3
1.4. Objective	4
1.4.1. General Objective	4
1.4.2. Specific Objective.....	4
1.5. SCOPE OF STUDY	4
1.6. Organization of the Thesis	5
CHAPTER TWO.....	6
2. LITERATURE REVIEW.....	6
CHAPTER THREE	12
3. Analytical Analysis Methods and Conditions	12
3.1. Material of Rotor Disc of Disc Brake	12
3.1.1. Types of material	13
3.2. Analytical Analysis Conditions.....	24
3.2.1. Geometries and Dimensions of Brake Disk-pad.....	26
3.2.2. Thermal Loading and Boundary Condition	28
3.2.3. Solid Mechanics Aspect and Structural Boundary Condition	34

3.2.3.1.	Circumferential Constraint.....	39
3.2.3.2.	Axial Constraint	39
3.2.3.3.	Radial Constraints	40
3.3.	Analytical Analysis Methods in Disk Brake Temperature Distribution	40
3.3.1.	Heat Partition Coefficient and Energy Input	42
3.4.	Parametric Studies on Rotor Disc for Different Materials.....	48
3.4.1	Analytical Analysis Methods in Disk Brake Temperature Distribution.....	48
3.5.	Methods of Analyzing Disc Stress Components.....	58
3.5.1.	Von Mises Theory Analysis and Fatigue Life Time Estimation	59
CHAPTER FOUR.....		62
4.	Finite Element Analysis Methods and Conditions	62
4.1.	Material properties	62
4.2.	ANALYSIS USING ANSYS.....	62
4.3.	Finite Element Method Conditions	63
4.3.1.	Requirements Of Brake Disc	63
4.3.2.	Structural Analysis.....	63
4.3.3.	Thermal Analysis	64
4.3.4.	Finite Element Method Model.....	64
4.3.5.	Boundary conditions and loading of the disc and pads.....	65
4.3.6.	Thermal boundary conditions	67
4.3.7.	Meshing and Loading Conditions the Disc.....	68
4.4.	Methods of Finite Element Analysis	70
4.4.1.	Coupled-Field Analyses and Methods	71
4.4.2.	Thermal-Structural Analysis.....	73
4.4.3.	Element used in thermal analysis.....	76

4.4.4. Element Used in Stress Analysis	77
CHAPTER FIVE	79
5. Results and Discussion	79
5.1. Results of Thermal Analysis	79
5.1.1. Temperature Distribution for Grey Cast Iron Rotor Disc.....	79
5.1.2. Temperature Distribution for maraging steel Rotor Disc	81
5.1.3. Temperature Distribution for ALMMC Rotor Disc.....	82
5.1.4. Temperature Distribution for E-Glass Rotor Disc	83
5.1.5. Total heat flux analysis for gray cast iron.....	84
5.1.6. Total heat flux analysis for ALMMC	85
5.2. RESULTS OF STRUCTURAL ANALYSIS	85
5.2.1. principal stress and deformation through surface and thickness of the disc.....	85
CHAPTER SIX.....	89
6. Conclusions and Recommendation	89
6.1. Conclusion.....	89
6.2. Recommendation.....	90
6.3. Future Work	91
REFERANCE	92
Appendix I: Specification of SUV Car	94

List of figures

Figure 1:Disc brake parts	1
Figure 2:Huanghai SUV car of model DD6470C.....	25
Figure 3:Measuring dimensions of disc and pad	26
Figure 4:Cross sectional view of the disc	27
Figure 5:Dimensioning disc and pad	28
Figure 6:Braking conditions	29
Figure 7:Energy balance at the surface of a solid parts	31
Figure 8:Heat Dissipation from Disc Rotor	31
Figure 9:Boundary condition of the disk (a) uniform wear (b) uniform pressure	33
Figure 10:Stress components in cylindrical coordinates.	36
Figure 11:Circumferential Constraint (zero displacement)	39
Figure 12:Axial compressive stresses.....	40
Figure 13:Radial Displacement Constraints	40
Figure 14:Schematic shapes of the disk and the pad in sliding contact.....	41
Figure 15:Contac surface elements of two components a) the disc and b) the pad.	45
Figure 16:Vehicle dimensions	49
Figure 17:Plot for brake power vs. Time	53
Figure 18:Schematic illustration of a constant life or Goodman diagram	60
Figure 19:FEM odel creation on ANSYS WB of 24mm Disc Brake.	65
Figure 20:Boundaitions and loading imposed on model the disc-pads	67
Figure 21:Therndary conditions applied on disc brake.....	68
Figure 22:Heat Flux versus time.....	68
Figure 23>Contact zone of the disc and pad.....	69
Figure 24:SOLID90 Geometry	76
Figure 25:SOLID186 Homogenous Structural Solid Geometry.....	77
Figure 26:Temperature Distribution for Grey Cast Iron Rotor Disc	80
Figure 27:Temperature Distribution for maraging steel Rotor Disc.....	81
Figure 28:Temperature Distribution for ALMMCRotor Disc	82
Figure 29:Temperature Distribution for E-Glass Rotor Disc	83
Figure 30:Total heat flux analysis.....	84

Figure 31:Total heat flux analysis.....	85
Figure 32:Maximum principle stress	86
Figure 33:Total deformation of cast iron	86
Figure 34:Maximum principle stress	87
Figure 35:Total deformation of ALMMC.....	87

List of tables

Table 1:Table of comparative qualities of cast irons	14
Table 2: Measured dimensions of disc rotor and pad	26
Table 3: The Material Property of the Pad.....	42
Table 4: The Material Property of the Brake Assembly	42
Table 5: coefficient of adhesion.....	51
Table 6:Cast Iron Properties	55
Table 7:Maraging Steels Properties	55
Table 8:ALMMC(Aluminum metal matrix composites) Properties.....	56
Table 9:E-Glass Properties	56
Table 10:Temperature Distribution during Braking in Various Materials: Results Comparison.	83
Table 11:Results Comparison of materials	88
Table 12:Comparison the Results of brake Disc by analytical and FEM.....	88

Nomenclature

k Thermal conductivity

δ Disc thickness

ρ Density

c Specific heat

ν Poisson's ratio

α Thermal expansion

E Elastic modulus,

μ Coefficient of friction μ

p Hydraulic pressure

ϕ_0 The cover angle of pad in degrees

r, z, θ Radial circumferential and axial coordinate

δ_d Disk thickness

δ_p Pad thickness

R_p External radius of the pad

r_d Internal radius of the disk

R_d External radius of the disk

M Total mass of the vehicle

V_0 Initial speed of the vehicle

m Amount of the distributed mass on the front axle of the vehicle

ξ_d Disc thermal effusivity

ξ_p Pad thermal effusivity

S_d Frictional contact surfaces of the disc

S_p Frictional contact surfaces of the pad

γ Heat partition coefficient

dE Rate of heat generated due to friction between two sliding components,

V Relative sliding velocity and

dF_f Friction force.

dE_p Amount of absorbed heat by the pad

dE_d Amount of absorbed heat by disk

ω Angular velocity of the disc

q_d Heat flux of disc
 q_p Heat flux of pad
 q_{0d} Heat flux of disc at $t=0$ sec.
 t_b Braking time
 h Convection coefficient
 T_i Initial temperature
 T_∞ Ambient temperature
 σ Stefan-Boltzmann constant
 ε Emissivity of the surface
 α_d Thermal diffusivity of disc
 λ_n Eigenvalue
 $\varphi_n(z)$ Eigen function
 ε_t Thermal strain
 σ_r Normal stress in radial direction.
 σ_θ Normal stress in circumferential direction
 σ_z Normal stress in axial direction.
 $\tau_{r\theta}$ Shearing stress in $r \theta$ plane
 τ_{rz} Shearing stress in $r z$ plane
 $\tau_{r\theta}$ Shearing stress in $z \theta$ plane
 F_r Component of the body forces in the radial direction
 F_θ Component of the body forces in the tangential direction
 F_z Component of the body forces in the tangential direction
 α The coefficient of the linear thermal expansion
 ν The Poisson's ratio
 G Shear modulus
 ΔT Temperature change from the reference temperature T_0
 ε_r Radial deformation strain
 ε_θ Circumferential deformation strain
 ε_z Axial deformation strain
 γ_{rz} Shear deformation strain

Abstract

An automotive brake disc or rotor is a device for slowing or stopping the motion of a wheel while it runs at a certain speed. The widely used brake rotor material is cast iron which consumes much fuel due to its high specific gravity. The aim of this paper is to develop the material selection method and select the optimum material for the application of brake disc system emphasizing on the substitution of this cast iron by any other lightweight material. Two methods are used for this thesis work i.e Analytical and FE Analysis. Material performance requirements were analyzed and alternative solutions were evaluated among cast iron, maraging steel, aluminium metal matrix composites and E-Glass. Mechanical properties including compressive strength, friction coefficient, wear resistance, thermal conductivity and specific gravity, were used as the key parameters in the material selection stages. The analysis led to Aluminium metal matrix composite as the most appropriate material for brake disc system.

Index Terms— Brake disc; Material selection, Analytical analysis, Heat flux, Finite element method, Stress components

CHAPTER ONE

1. INTRODUCTION

1.1. Background of the study

A brake disc rotor is the rotating part of a disc brake assembly normally located on the front axle which is most important safety feature of an automobile. The ability of a braking system to provide safe, repeatable stopping is the key to safe motoring. To stop the wheel, friction material in the form of brake pads (mounted in a device called a brake caliper) is forced hydraulically, against both sides of the disc. The purpose of friction brakes is to decelerate a vehicle by transforming the kinetic energy of the vehicle to heat, via friction, and dissipating that heat to the surroundings. So friction based braking systems are still the common device to convert kinetic energy into thermal energy, through friction between the brake pads and the rotor faces. Braking system is performed by combination of different components of disc brake assembly such as caliper, piston and cylinder, pads and rotor .

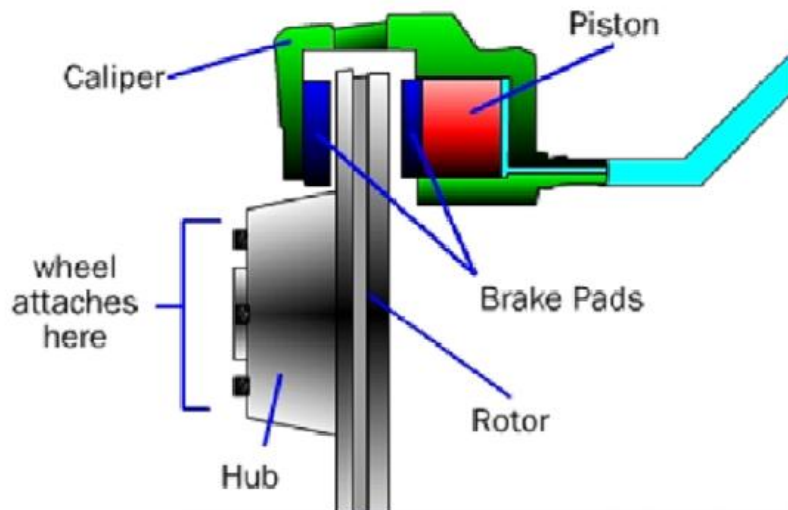


Figure 1: Disc brake parts

Based on the design configurations, vehicle friction brakes can be grouped into drum and disc brakes. The drum brakes use brake shoes that are pushed in a radial direction against a brake drum. The disc brakes use pads that are pressed axially against a rotor or disc. Under extreme conditions, such as descending a steep hill with a heavy load, or repeated high-speed decelerations, drum brakes would often fade and lose effectiveness. Compared with their counterpart, disc brakes would operate with less fade under the same conditions. An additional

advantage of disc brakes is their linear relationship between brake torque and pad/rotor friction coefficient. Advantages of disc brakes over drum brakes have led to their universal use on passenger-car and light-truck front axles, many rear axles, and medium-weight trucks on both axles.

Disc-style brakes development and use start at England in the 1890's which is the first ever automobile disc brakes were patented by F.W. Lanchester . It was patented at Birmingham factory in 1902, though it took another half century for the innovation to be widely adopted. The first designs resembling modern style disc brakes began to appear in Britain in the late 1940 and early 1950. The first appeared on the low volume Crosley Hotshot in 1949, although it had to be discontinued in 1950 due to design problems. Modern style disc brakes offered much greater stopping performance than comparable drum brakes, including much greater resistance to "brake fade" which is caused by the overheating of brake components. Meanwhile, from the late 1990 to present, North American automotive industry accelerated the pace on brake research and application to catch up with Japanese quality performance. It has been more tailored towards American vehicle brake designs which often have more challenges to balance between the brake performances and quality.

Disk brakes were most popular on sport cars when they were first introduced, since these vehicles are more demanding about brake performance. Disks have now become the more common form in most passenger vehicles.

1.2. Motivation

Excessive thermal deformation of cast iron rotors is one of the most serious problems facing automotive brake designers as they try to enhance disc brake performance for faster and heavier vehicles within tight packaging constraints. In addition, cracking sometimes occurs as a result of repeated high speed stops when the brake rotor is subject to rapid and severe thermal cycling.

The thermal structural analysis is a primordial stage in the study of the brake systems, because the temperature determines thermo-mechanical behavior of the structure. In the braking phase, temperatures and thermal gradients are very high which produces high thermal stress. This generates disc thickness variations and deformations whose consequences are manifested by the appearance and the accentuation of cracks. Under the influence of temperature, the friction elements hence, the conditions of operation of the friction patches become less favorable: their wear intensifies and the friction coefficient decreases, material strength decrease due to thermal

stress which may lead to emergency situations. Thus, experimental, mathematical and software modeling of the temperature is the important problem at a design stage of brake systems.

This study tries to presents the result comparison of analytical and ANSYS 14.0 and carry out a concise summary of the information about the tensile, compressive, axial, and von mises stress developed during braking. The front disc brake of Huanghai SUV car of model DD6470C will be used for analysis. Due to sliding of disc and pad with each other wear is developed, which is not included in the analysis. The temperature field is obtained considering constant angular velocity, which means heat flux applied on disc surface is constant. Temperature variation occurs only along thickness of the disc, so that thermal and structural analysis is focused only along the thickness of the disc. The material properties are assumed to be temperature independent. Only areas which are exposed to high thermal stress are selected for analysis, which excludes vanes and hub of the disc. Only thermal stresses were considered because the mechanical loads due to the pad normal pressure, centrifugal force and inertia force are insignificant in comparison.

1.3. Statement of the Problem

There were so many researches done on transient thermal-structural analysis of disc brake, which are described in literatures. Most of the researches are concentrated on analytical (theoretical method), experimental or finite element method. In each study only one of the methods was applied, which is not satisfactory for accuracy of the analysis. But, this thesis is done both analytical and by finite elements which strengthens the result obtained.

Experimental analysis is accurate as far as instruments are fully available, sufficient knowledge of using instruments, and good conditions to apply instruments. And this is difficult to estimate thermal structural analysis between disc and pads, where there is heat dissipation over time and high speed rotation of disc. Experimental determination of temperature and stress of a surface of contact concerning authentic objects in most cases causes significant technical difficulties and is connected with essential material and time expenses. Instruments which pass these obstacles face another obstacle which is expensiveness of these instruments. Taking this in to consideration, the aim of this paper is studying and comparing analytical analysis and finite element /ANSYS software analysis of a temperature and stress along the thickness of the front disc brake. This is done by applying mathematical analysis of heat transfer and stress boundary conditions.

1.4. Objective

1.4.1. General Objective

The General objective of the thesis work is to study analytical analysis and finite element analysis of automotive disc brake rotor for its thermal stress distribution by using different materials.

1.4.2. Specific Objective

- ✓ Developing thermal boundary condition and thermal equation governing temperature distribution through the disc thickness
- ✓ 3-D modeling of disc brake using ANSYS 14.0 or CATIA V5 R19 software to study temperature distribution through thickness of the rotor
- ✓ Comparing analytical and ANSYS temperature distribution to check whether input for thermal stress is same or not for analytical and finite element method (ANSYS)

1.5. SCOPE OF STUDY

This research work covers analytical analysis and finite element analysis of thermal stress distribution in disc thickness caused by temperature distribution, and its effect on life and brake fading.

For comparison of thermal structural analysis between analytical and finite element, the dimensions and specifications of SUV (Sport Utility Vehicle) car of model DD6470C is selected. Dimensions and specifications of this car are taken from Bishoftu Automotive Industry. SUV car is manufactured by Huanghai Company in China, and Bishoftu Automotive Industry imports the disassembled parts and assembles it locally. The demand of this car is increasing worldwide due to its quality in fuel economy, less expensive, and varying amount of towing capacity with an all-wheel drive or four wheel drive system. The maximum high speed set for this car is as high as 36m/s which is higher than pickup car (30m/s). This high speed makes this car to be selected for the analysis of thermal-structural analysis of its disc brake. They also provide extra traction in slippery conditions and the ability to tackle at least moderate off-road terrain.

Taking these in to consideration Bishoftu Automotive Industry imported the disassembled parts from Huanghai Company. The demand of this car is highly increased now days in government officials, as well as in private company.

This thesis is focused on a study of ventilated disc brake rotor of SUV Huanghai vehicle with full load of capacity with selected positions for study of thermal stress analysis. Vent and hub are excluded from analysis because hub is far from position of high temperature gradient, and vent is not exposed to high temperature because of convection heat transfer. Therefore only thickness of a rotor is the main concentration of this thesis. Cylindrical cordite system is used to describe the dimensions. For analysis we focus on front wheel rotor only. Therefore front disc brake of Huanghai SUV car of model DD6470C will be used for analysis.

1.6. Organization of the Thesis

This thesis is organized in to six chapters. In the first chapter, background and justification of this thesis work and the objectives to be achieved are discussed. In chapter two, a review of literature relevant to this thesis work, which has been investigated by different researchers, is given. Chapter three is about analytical method in temperature and thermal stress analysis. In chapter four, finite element method (FEM) is used, to develop 3-D model of disc brake. Also different thermal and structural boundary conditions are discussed in detail. In addition application of symmetry is justified here. In chapter five results of the analysis are summarized and discussions are made based on the outputs of the FEM. In addition, comparison of analytical and numerical solutions is made. Finally, chapter six gives conclusion achieved from this thesis work and propose future work in this field of study.

CHAPTER TWO

2. LITERATURE REVIEW.

Due to the application of brakes on the car disk brake rotor, heat generation takes place due to friction and this thermal flux has to be conducted and dispersed across the disk rotor cross section. The condition of braking is very much severe and thus the thermal and structural analysis has to be carried out. Taking this in to consideration, many researchers have been done about the brake disc thermo-mechanical coupling analysis.

(S.Koetniyom, 2014) Studied thermal stress analysis of automotive disc brakes to develop material properties of gray cast cast iron brake disc model of the Rover disc subjected to severe thermal cycles using the commercial package ABAQUS. One particular existing brake disc design for a medium passenger car was chosen for the investigation. Due to symmetry, the final model of the disc was a 20° segment of the brake disc and hub meshed using nearly three thousand 20 noded solid elements with a quadratic interpolation function. In addition, experimental work was undertaken to derive the rotor material properties in tension and compression as a function of temperature. This data was used to generate suitable FE material model routines which accurately allow for the different temperature dependent yield properties of cast iron in tension and compression. Using the most accurate user developed material subroutine, the thermal response of the back-and front-vented disc designs are compared: the back-vented disc suffers lower thermal distortion but at the expense of higher plastic strain accumulation, particularly near the point of attachment of the vanes. The result indicates that temperatures increase non-uniformly with the braking time and the disc is subjected to maximum temperatures up to around 380 °C at the end of the brake application. Thermal stress result shows maximum von Mises elastic stresses at the neck was 273 MPa and near the inner fillet radius of the long vane 442 MPa due to the constraints applied to the free expansion of the rotor rubbing surfaces. If these stresses are beyond the proportional limit, plastic strains would occur in the brake disc.

(Hogskolan, 2012) Studied simulation of thermal fatigue stresses in a disc brake by taking as an input the heat flux produced from the friction between a disc and pad system for a number of repeated braking cycles. He used the finite element analysis (FEA) to determine the temperatures profile in the disc and to analyze the stresses for the repeated braking, which could be used to

calculate the fatigue life of a disc. Sequentially coupled approach was used for thermomechanical problem and the problem was divided into two parts, heat analysis and thermal stress analysis. The heat analysis was obtained by including frictional heat and adopting an Eulerian approach. The thermal stress analysis, which was the main focus of his thesis, was followed using Abaqus. The plasticity theory as background for stress analysis was discussed in detail and temperature independent material properties were considered throughout the thesis work. The linear kinematic hardening model with rate independent elastic-plastic plasticity is used for benchmark and real disc-pad model. The results of the benchmark model and the real model were observed to be similar in terms of plasticity theory. First brake application stays for 6 second, and the result shows maximum temperature of 220°C at 2.5 seconds. After first brake application mean equivalent stress of 180Mpa was shown.

(Samic & Sheridan, 2012) Investigated the effects of friction on the pressure distribution between the rotor and the pads with a floating caliper using the finite element technique. The computational results without the friction forces (static case) revealed that the inboard and outboard pressure distributions varied because the locations of the normal forces acting on the pads were different on the piston and finger sides of the floating caliper. Furthermore, the pressure distributions with the friction forces taken into account were different from the static case due to the moment set up between the abutment and the friction interface.

(lee, 2012) Studied the pressure distribution between the rotor and the pads including the friction force with a floating caliper in order to investigate the motion at the friction interface that could be used to determine the onset of disc brake squeal using the finite element technique. The computed result revealed that the pressure distributions acting on the pads were different on the piston and finger sides of the floating caliper. Moreover, the axial displacements at the friction interface on the two sides were different.

The heat flux generated at the rubbing surface can transfer to both the rotor and the pad. The amount of thermal energy transferred into the brake rotor depends on the specification of the friction and disc materials.

(Yano & Murata, 2000) Performed experimental work to determine the amount of heat flow from the frictional interface into the rotor by conduction. The volume or quantity of heat

transferring to the pads, the rotor and the ambient air was obtained from the measured temperature gradients and heat transfer coefficients. According to their experiments, the heat conduction from the rubbing surfaces to the rotor was approximately 72% of the heat generated. (Belhocine & Bouchetara, 2010) Studied simulation of fully coupled thermo mechanical analysis of disc brake rotor caused by frictional heat generated during braking application. They studied surface roughness and wear at the pad interface using finite element method by building 3D model of ventilated pad-disc brake assembly with a thermo mechanical coupling boundary condition and multi-body model technique. The numerical simulation for the coupled transient thermal field and stress field was carried out by sequentially thermal structural coupled method based on ANSYS to evaluate the stress fields and of deformations which were established in the disc had with the pressure of the pads and in the conditions of tightening of the disc thus the contact pressures distributions field in the pads which was another significant aspect in their research paper. In addition effects of materials on mechanical properties are studied by using three different types of gray cast iron materials.

(Noyes & Vickers, 2013) Predicted the temperature response on the rubbing surfaces of a brake disc, using the assumption of a uniform heat flux. The computational results were compared with the temperatures measured at the rotor surface on entry to and exit from the pad area. It was found that the measured temperature on exit from the pad was higher than the temperature calculated using the assumption of uniform heat flux by approximately 55°C. However, for many applications, the effect of this circumferential temperature variation, the so-called "rotating heat source" effect, can be ignored.

(Nackatsuji, 2013) Did a study on the initiation of hair-like cracks which formed around small holes in the flange of one-piece discs during overloading conditions. The study showed that thermally induced cyclic stress strongly affects the crack initiation in the brake discs. Using the finite element method, the temperature distribution under overloading was analyzed. 3D unsteady heat transfer analyses were conducted using ANSYS. A 1/8 of the one piece disc was divided into finite elements, and the model had a half thickness due to symmetry in the thickness direction.

(Babukanth & Vimal, 2013) Studied transient Analysis of disk brake using ANSYS Software by choosing element type solid 90, which is higher order version of the 3-D eight node thermal element (Solid 70). The element has 20 nodes with single degree of freedom, temperature, at each node. The 20-node elements have compatible temperature shape and are well suited to model curved boundaries. The 20-node thermal element is applicable to a 3-D state or transient thermal analysis. If the model containing this element is also to be analyzed structurally, the element should be replaced by the equivalent structural element (Solid 95)

(A.Floquet , 2010) Determined of temperature distribution and comparison of simulation results and experimental results in the disc by 2D thermal analysis using axis-symmetric model.

The disc brake used in the automobile is divided into two parts; a rotating axis-symmetrical disc, and the stationary pads. The friction heat, which is generated on the interface of the disc and pads, can cause high temperature during the braking process. The influence of initial velocity and deceleration on cooling of the brake disc was also investigated. The thermal simulation is used to characterize the temperature field of the disc with appropriate boundary conditions.

A Finite-element method was developed for determining the critical sliding speed for thermo elastic instability of an axis-symmetric clutch or brake. Linear perturbations on the constant-speed solution were sought that vary sinusoidally in the circumferential direction and grow exponentially in time.

These factors cancel in the governing thermo elastic and heat-conduction equations, leading to a linear Eigen value problem on the two-dimensional cross-sectional domain for the exponential growth rate for each Fourier wave number. The imaginary part of this growth rate corresponds to a migration of the perturbation in the circumferential direction.

The algorithm was tested against an analytical solution for a layer sliding between two half-planes and provided excellent agreement, for both the critical speed and the migration speed. Criteria were developed to determine the mesh refinement required to give an adequate discrete description of the thermal boundary layer adjacent to the sliding interface.

The method was then used to determine the unstable mode and critical speed in geometries approximating current multi-disc clutch practice.

(Kim, 2012) Investigated the temperature distribution, the thermal deformation, and the thermal stress of automotive brake disks have quite close relations with car safety; therefore, much research in this field has been performed. based on the review of researches on the vibration and

noise related to automobile brake, the four degrees of freedom nonlinear dynamics model of brake disk and pads is established, the stability of vibration system at the equilibrium points is analyzed. The main idea is to express the thermal energy that the disc stores when a braking action is performed. In order to express this energy, the global system that influences the slowing down of the vehicle has to be considered. This system is composed by the following technical braking components: brake discs, transmission retarders, controlled engine brakes and exhaust brakes. Jadon carries out a transient analysis for the thermo elastic contact problem of the disk brakes with heat generation is performed using the finite element analysis. To analyze the thermo elastic phenomenon occurring in the disk brakes, the occupied heat 12 conduction and elastic equations are solved with contact problems.

(Kang & Cho , 2010) Analyzed the geometry of vents in motorcycle disc brakes which affects the surface of the disc and the thermal characteristics of disc brakes. Thermal deformation analysis and thermal stress analysis due to heat transfer were carried out through the finite element analysis for ventilated disc and solid disc. For 3-dimensional modeling and finite element analysis of the discs, the commercial code ANSYS Workbench was used.

(Hassan & Li , 2011) Have predicted the temperature distribution for disc brakes by carrying out a coupled thermal–mechanical analysis as a part of their works. They have applied angular displacements to the rotor to maintain a specific velocity and calculated the heat generation at the interface from contact pressure. However, in reality, the wheel is in deceleration during braking.

(Choi & Lee, 1998) Presented a paper on finite element analysis of transient thermo-elastic behaviors in disc brakes. A transient analysis for thermo-elastic contact problem of disc brakes with frictional heat generation is performed using the finite element method. To analyze the thermo-elastic phenomenon occurring in disc brakes, the coupled heat conduction and elastic equations are solved with contact problems. The numerical simulation for the thermo-elastic behavior of disc brake is obtained in the repeated brake condition. The computational results are presented for the distributions of pressure and temperature on each friction surface between the contacting bodies.

Recent numerical models, presented to deal with thermal stress have shown that the thermal gradients can attain important levels which depend on the heat dissipated by friction, the sliding speed and the heat convection coefficient. Many other works dealt with the evaluation of

temperature in solid disks subjected to frictional heating. The temperature distribution due to friction process necessitates a good knowledge of the stress parameters. In fact, the interface is always imperfect due to the roughness from a mechanical and thermal point of view.

In the scope of the present work both finite element method and analytical analysis are done and compared with different rotor materials. None of the above approaches were available found to be fully compared with other result. In some cases the geometry boundary conditions were inappropriate; in others the published information was insufficient to allow direct implementation. As a result, it is decided to develop a new solution to meet our requirements.

CHAPTER THREE

3. Analytical Analysis Methods and Conditions

3.1. Material of Rotor Disc of Disc Brake

In automotive industries, to achieve reduced fuel consumption as well as greenhouse gas emission is a current issue of utmost importance. To reduce automobile weight and improve fuel efficiency, the auto industry has dramatically increased the use of aluminum in light vehicles in recent years. Aluminum alloy based metal matrix composites (MMCs) with ceramic particulate reinforcement have shown great promise for such applications. These materials having a lower density and higher thermal conductivity as compared to the conventionally used gray cast irons are expected to result in weight reduction of up to 50 – 60 % in brake systems. Moreover, these advanced materials have the potential to perform better under severe service conditions like higher speed, higher load etc. which are increasingly being encountered in modern automobiles. Since brake disc or rotor is a crucial component from safety point of view, materials used for brake systems should have stable and reliable frictional and wear properties under varying conditions of load, velocity, temperature and environment, and high durability. There are several factors to be considered when selecting a brake disc material. The most important consideration is the ability of the brake disc material to withstand high friction and less abrasive wear. Another requirement is to withstand the high temperature that evolved due to friction. The brake disc must have enough thermal storage capacity to prevent distortion or cracking from thermal stress until the heat can be dissipated. This is not particularly important in a single stop but it is crucial in the case of repeated stops from high speed.

And also the Disc brake discs are commonly manufactured out of grey cast iron. The SAE maintains a specification for the manufacture of grey iron for various applications. For normal car and light truck applications, the SAE specification is J431 G3000 (superseded to G10). This specification dictates the correct range of hardness, chemical composition, tensile strength, and other properties necessary for the intended use. Some racing cars and airplanes use brakes with carbon fiber discs and carbon fiber pads to reduce weight. Wear rates tend to be high, and braking may be poor or grabby until the brake is hot. The materials used for rotor disc are explained in detail. It is investigated the temperature distribution, the thermal deformation, and the thermal stress of automotive brake disks have quite close relations with car safety.

Performance evaluation: Due to the application of brakes on the car disk brake rotor, heat generation takes place due to friction and this thermal flux has to be conducted and dispersed across the disk rotor cross section. The condition of braking is very much severe and thus the thermal analysis has to be carried out.

The thermal structural stability of the disc brake is influenced by the thermal and elastic property of material properties, rate of hydraulic pressure applied on pad and the basic design for the disc rotor.

Some of the thermally most important properties of disc brake rotor are as follows:-

- Thermal capacitance (density and specific heat) is the ability to store the heat. Initially on braking process, a significant amount of frictional heat is stored and during short braking, this thermal capacitance is dominates
- Thermal conductivity is the ability to re-distribute the thermal energy. During long and low intensity braking, the peak temperature is largely depends on the disc material's conductivity. However, the thermal conductivity has a little effect during short braking.
- Thermal expansion coefficient (related to location of friction contact due to the thermal deformation) affects the tendency towards hot spotting and thermal disc thickness variation (DTV) generation. The temperature gradients of the disc brake can cause to temporary DTV owing to the uneven thermal expansion of the material

Here for thermal analysis we have considered 4 rotor disc materials cast iron, maraging steel , Aluminum metal matrix composites, & E -glass fiber.

3.1.1. Types of material

Classes of steel

- Crucible steel
- Carbon steel
- Spring steel
- Alloy steel
- Maraging steel
- Stainless steel
- Weathering steel
- Tool steel

Other iron-based materials

- Cast iron
- White iron
- Ductile iron
- Malleable iron
- Wrought iron

Table 1: Table of comparative qualities of cast irons

Name	Nominal composition [% by weight]	Form and condition	Yield strength [Ksi(0.2% offset)]	Tensile strength [ksi]	Elongation [% (in 2 inches)]	Hardness [Brinell scale]	Uses
Grey cast iron (ASTMA48)	C 3.4, Si 1.8, Mn 0.5	Cast	—	50	0.5	260	Engine cylinder blocks, flywheels, gearbox, cases, machine-tool bases, Brake components
White cast iron	C 3.4, Si 0.7, Mn 0.6	Cast (as cast)	—	25	0	450	Bearing surfaces
Malleable iron (ASTM A47)	C 2.5, Si 1.0, Mn 0.55	Cast (annealed)	33	52	12	130	Axle bearings, track wheels, automotive crankshafts
Ductile or nodular iron	C 3.4, P 0.1, Mn 0.4, Ni 1.0, Mg 0.06	Cast	53	70	18	170	Gears, camshafts, crankshafts
Ductile or nodular iron (ASTM A339)	—	cast (quench tempered)	108	135	5	310	—

Following material Properties were selected for the modified Disc Brakes.

A. Cast Iron and its Properties:

Cast iron usually refers to grey cast iron, but identifies a large group of ferrous alloys, which solidify with a eutectic. Iron accounts for more than 95%, while the main alloying elements are carbon and silicon. The amount of carbon in cast iron is the range 2.1-4%, as ferrous alloys with less are denoted carbon steel by definition. Cast irons contain appreciable amounts of silicon, normally 1-3%, and consequently these alloys should be considered ternary Fe-C-Si alloys. Here graphite is present in the form of flakes. Disc brake discs are commonly manufactured out of a material called grey cast iron.

Cast iron is a group of iron-carbon alloys with a carbon content greater than 2%.The alloy constituents affect its colour when fractured: white cast iron has carbide impurities which allow

cracks to pass straight through; grey cast iron has graphite flakes which deflect a passing crack and initiate countless new cracks as the material breaks.

Carbon (C) and silicon (Si) are the main alloying elements, with the amount ranging from 2.1–4 wt% and 1–3 wt%, respectively. Iron alloys with less carbon content are known as steel. While this technically makes these base alloys ternary Fe–C–Si alloys. Since the compositions of most cast irons are around the eutectic point of the iron–carbon system, the melting temperatures closely correlate, usually ranging from 1,150 to 1,200 °C (2,100 to 2,190 °F), which is about 300 °C (572 °F) lower than the melting point of pure iron.

Cast iron tends to be brittle, except for malleable cast irons. With its relatively low melting point, good fluidity, cast ability, excellent machinability, resistance to deformation and wear resistance, cast irons have become an engineering material with a wide range of applications and are used in pipes, machines and automotive industry parts, such as cylinder heads (declining usage), cylinder blocks and gearbox cases (declining usage). It is resistant to destruction and weakening by oxidation (rust).. Cast iron is also used in the construction of buildings.

Mechanical property reference data for various grey cast irons, includes Tensile strength, Compressive Strength, Shear Modulus of Rupture, Tensile Modulus of Elasticity, Torsional Modulus of Elasticity, Endurance Limit and Brinell hardness data. The American Society for Testing Materials (ASTM) numbering system for grey cast iron is established such that the numbers correspond to the minimum tensile strength in KPSI. Thus an ASTM No. 20 cast iron has a minimum tensile strength of 20 KPSI. Note particularly that the tabulations are typical values. Multiply strength in KPSI by 6.89 to get strength in MPa. Steels given for comparison purposes. Tensile and hardness given as rolled and heat treated by water quench and tempered at 425°F. The SAE 1050 heat treated is roughly the properties of most anvils. However the temper condition given is softer. Use the SAE 1095 temper for anvils. Cast iron is a brittle virtually non-malleable metal that is considered generally inflexible. Cast iron is NOT the metal worked by blacksmiths. It cannot be forged. Cast iron is worked by melting to a liquid and pouring in molds, then by sawing, filing, machining (chip making methods). The stiffness and dampening properties of cast iron make it an excellent material for machine tool frames and parts.

B. Maraging Steels and its Properties:

Maraging steels (a portmanteau of "martensitic" and "aging") are steels (iron alloys) that are known for possessing superior strength and toughness without losing malleability, although they cannot hold a good cutting edge. *Aging* refers to the extended heat-treatment process. These steels are a special class of low-carbon ultra-high-strength steels that derive their strength not from carbon, but from precipitation of intermetallic compounds. The principal alloying element is 15 to 25 wt. % nickel. Secondary alloying elements, which include cobalt, molybdenum, and titanium, are added to produce intermetallic precipitates,. Original development (by Bieber of Inco in the late 1950s) was carried out on 20 and 25 wt.% Ni steels to which small additions of Al, Ti, and Nb were made; a rise in the price of cobalt in the late 1970s led to the development of cobalt-free maraging steels.

The common, non-stainless grades contain 17–19 wt. % nickel, 8–12 wt.% cobalt, 3–5 wt.% molybdenum, and 0.2–1.6 wt.% titanium. Addition of chromium produces stainless grades resistant to corrosion. This also indirectly increases hardenability as they require less nickel: high-chromium, high-nickel steels are generally austenitic and unable to transform to martensite when heat treated, while lower-nickel steels can transform to martensite. Alternative variants of Ni-reduced maraging steels are based on alloys of Fe and Mn plus minor additions of Al, Ni, and Ti where compositions between Fe-9wt.%Mn to Fe-15wt.% Mn have been used. The Mn has a similar effect as Ni, i.e. it stabilizes the austenite phase. Hence, depending on their Mn content, Fe-Mnmaraging steels can be fully martensitic after quenching them from the high temperature austenite phase or they can contain retained austenite. The latter effect enables the design of maraging-TRIP steels where TRIP stands for Transformation-Induced-Plasticity

Properties: Due to the low carbon content maraging steels have good machinability. Prior to aging, they may also be cold rolled to as much as 90% without cracking. Maraging steels offer good weld ability, but must be aged afterward to restore the original properties to the heat affected zone. When heat-treated the alloy has very little dimensional change, so it is often machined to its final dimensions. Due to the high alloy content maraging steels have a high hardenability. Since ductile FeNi martensites are formed upon cooling, cracks are non-existent or negligible. The steels can be nitrided to increase case hardness, and polished to a fine surface finish. Non-stainless varieties of maraging steel are moderately corrosion-resistant, and

resist stress corrosion and hydrogen embrittlement. Corrosion-resistance can be increased by cadmium plating or phosphating.

Several desirable properties of maraging steels are:

- Ultra-high strength at room temperature
- Simple heat treatment, which results in minimum distortion
- Superior fracture toughness compared to quenched and tempered steel of similar strength level
- Low carbon content, which precludes decarburization problems
- Section size is an important factor in the hardening process
- Easily fabricated
- Good weldability.

These factors indicate that maraging steels could be used in applications such as shafts, and substitute for long, thin, carburized or nitrided parts, and components subject to impact fatigue, such as print hammers or clutches.

Uses: Maraging steel's strength and malleability in the pre-aged stage allows it to be formed into thinner rocket and missile skins than other steels, reducing weight for a given strength. Maraging steels have very stable properties, and, even after overaging due to excessive temperature, only soften slightly. These alloys retain their properties at mildly elevated operating temperatures and have maximum service temperatures of over 400 °C (752 °F). They are suitable for engine components, such as crankshafts and gears, and the firing pins of automatic weapons that cycle from hot to cool repeatedly while under substantial load. Their uniform expansion and easy machinability before aging make maraging steel useful in high-wear components of assembly lines and dies. In the sport of fencing, blades used in competitions run under the auspices of the Federation are usually made with maraging steel. Maraging blades are superior for foil and épée because crack propagation in maraging steel is 10 times slower than in carbon steel, resulting in less blade breakage and fewer injuries. Stainless maraging steel is used in bicycle frames and golf club heads. It is also used in surgical components and hypodermic syringes, but is not suitable for scalpel blades because the lack of carbon prevents it from holding a good cutting edge. Maraging steel production, import, and export by certain states, such as the United States, is closely monitored by international authorities because it is particularly suited

for use in gas centrifuges for uranium enrichment; lack of maraging steel significantly hampers this process. Older centrifuges used aluminum tubes; modern ones, carbon fiber composite.

C. ALMMC(Aluminum metal matrix composites) and its Properties:

A metal matrix composite (MMC) is composite material with at least two constituent parts, one being a metal necessarily, the other material may be a different metal or another material, such as a ceramic or organic compound. When at least three materials are present, it is called a hybrid composite.

Aluminum is the most popular matrix for the metal matrix composites (MMCs). The Al alloys are quite attractive due to their low density, their capability to be strengthened by precipitation, their good corrosion resistance, high thermal and electrical conductivity, and their high damping capacity. Aluminum matrix composites (AMCs) refer to the class of light weight high performance aluminum centric material systems. The reinforcement in AMCs could be in the form of continuous or discontinuous fibers, whisker or particulates, in volume fractions ranging from a few percent to 70%. In the last few years, AMCs have been utilized in high-tech structural and functional applications including aerospace, defense, automotive, and thermal management areas, as well as in sports and recreation. There has been interest in using aluminum based metal matrix composites for brake disc and drum materials in recent years. While much lighter than cast iron they are not as resistant to high temperatures and are sometimes only used on rear axles of automobiles because the energy dissipation requirements are not high as compared to front axle. While the friction and wear of almmc were high speeds and loads the behavior could be greatly improved beyond that of iron discs, given the correct match of pad and disc material.

Composition: MMCs are made by dispersing a reinforcing material into a metal matrix. The reinforcement surface can be coated to prevent a chemical reaction with the matrix. For example, carbon fibers are commonly used in aluminium matrix to synthesize composites showing low density and high strength. However, carbon reacts with aluminium to generate a brittle and water-soluble compound Al_4C_3 on the surface of the fibre. To prevent this reaction, the carbon fibres are coated with nickel or titanium boride.

Matrix: The matrix is the monolithic material into which the reinforcement is embedded, and is completely continuous. This means that there is a path through the matrix to any point in the material, unlike two materials sandwiched together. In structural applications, the matrix is usually a lighter metal such as aluminum, magnesium, or titanium, and provides a compliant support for the reinforcement. In high-temperature applications, cobalt and cobalt–nickel alloy matrices are common.

Reinforcement: The reinforcement material is embedded into a matrix. The reinforcement does not always serve a purely structural task (reinforcing the compound), but is also used to change physical properties such as wear resistance, friction coefficient, or thermal conductivity. The reinforcement can be either continuous, or discontinuous. Discontinuous MMCs can be isotropic, and can be worked with standard metalworking techniques, such as extrusion, forging, or rolling. In addition, they may be machined using conventional techniques, but commonly would need the use of polycrystalline diamond tooling (PCD).

Continuous reinforcement uses monofilament wires or fibers such as carbon fiber or silicon carbide. Because the fibers are embedded into the matrix in a certain direction, the result is an anisotropic structure in which the alignment of the material affects its strength. One of the first MMCs used boron filament as reinforcement. Discontinuous reinforcement uses "whiskers", short fibers, or particles. The most common reinforcing materials in this category are alumina and silicon carbide.

The automotive industry recognizes that weight reduction and improved engine efficiency will make the greatest contribution to improved fuel economy with current powertrains. This is evidenced by the increased use of aluminum alloys in engine and chassis components. Aluminum and magnesium castings in this sector have grown in leaps and bounds over the past five years to help engineers design and manufacture more fuel efficient cars.

The low density and high specific mechanical properties of aluminum metal matrix composites (MMC) make these alloys one of the most interesting material alternatives for the manufacture of lightweight parts for many types of vehicles. With wear resistance and strength equal to cast iron, 67% lower density and three times the thermal conductivity, aluminum MMC alloys are ideal materials for the manufacture of lightweight automotive and other commercial parts.

MMC's desirable properties result from the presence of small, high strength ceramic particles, whiskers or fibers uniformly distributed throughout the aluminum alloy matrix. Aluminum MMC castings are economically competitive with iron and steel castings in many cases. However, the presence of these wear resistant particles significantly reduces the machinability of the alloys, making machining costs higher due mainly to increased tool wear. As a result, the application of cast MMCs to components requiring a large amount of secondary machining has been somewhat stifled.

Most components do not require the high performance capability of aluminum MMCs throughout their entirety. An un-reinforced cast alloy may accommodate the stresses in these areas. Reinforcement of only the high stress regions of a component is referred to as selective reinforcement. This approach to component design and manufacture optimizes the material for the application, reduces the cost of the cast MMC part and lowers machining costs.

Applications:

- High performance tungsten carbide cutting tools are made from a tough cobalt matrix cementing the hard tungsten carbide particles; lower performance tools can use other metals such as bronze as the matrix.
- Some tank armors may be made from metal matrix composites, probably steel reinforced with boron nitride, which is a good reinforcement for steel because it is very stiff and it does not dissolve in molten steel.
- Some automotive disc brakes use MMCs. Early Lotus Elise models used aluminum MMC rotors, but they have less than optimal heat properties and Lotus has since switched back to cast-iron. Modern high-performance sport cars, such as those built by Porsche, use rotors made of carbon fiber within a silicon carbide matrix because of its high specific and thermal conductivity. 3M sells a preformed aluminum matrix insert for strengthening cast aluminum disc brake calipers, allowing them to weigh as much as 50% less while increasing stiffness. 3M has also used alumina preforms for AMC pushrods.
- Ford offers a Metal Matrix Composite (MMC) driveshaft upgrade. The MMC driveshaft is made of an aluminum matrix reinforced with boron carbide, allowing the critical speed of the driveshaft to be raised by reducing inertia. The MMC driveshaft has become a common modification for racers, allowing the top speed to be increased far beyond the safe operating speeds of a standard aluminum driveshaft.

- Honda has used aluminum metal matrix composite cylinder liners in some of their engines, including the B21A1, H22A and H23A, F20C and F22C, and the C32B used in the NSX.
- Toyota has since used metal matrix composites in the Yamaha-designed 2ZZ-GE engine which is used in the later Lotus Lotus Elise S2 versions as well as Toyota car models, including the eponymous Toyota Matrix. Porsche also uses MMCs to reinforce the engine's cylinder sleeves in the Boxster and 911.
- The F-16 Fighting Falcon uses monofilament silicon carbide fibers in a titanium matrix for a structural component of the jet's landing gear.
- Specialized Bicycles has used aluminum MMC compounds for its top of the range bicycle frames for several years. Griffen Bicycles also made boron carbide-aluminum MMC bike frames, and Univega briefly did so as well.
- Some equipment in particle accelerators such as Radio Frequency Quadrupoles (RFQs) or electron targets use copper MMC compounds such as Glidcop to retain the material properties of copper at high temperatures and radiation levels.
- Copper-silver alloy matrix containing 55% by volume diamond particles, known as Dymalloy, is used as a substrate for high-power, high-density multi-chip modules in electronics for its very high thermal conductivity.
- Aluminum-Graphite composites are used in power electronic modules because of their high thermal conductivity, the adjustable coefficient of thermal expansion and the low density.

MMCs are nearly always more expensive than the more conventional materials they are replacing. As a result, they are found where improved properties and performance can justify the added cost. Today these applications are found most often in aircraft components, space systems and high-end or "boutique" sports equipment. The scope of applications will certainly increase as manufacturing costs are reduced.

In comparison with conventional polymer matrix composites, MMCs are resistant to fire, can operate in wider range of temperatures, do not absorb moisture, have better electrical and thermal conductivity, are resistant to radiation damage, and do not display out gassing. On the other hand, MMCs tend to be more expensive, the fiber-reinforced materials may be difficult to fabricate, and the available experience in use is limited.

D. (Electrical)E-Glass Fiber and its Properties:

E-Glass or electrical grade glass was originally developed for standoff insulators for electrical wiring. It was later found to have excellent fiber forming capabilities and is now used almost exclusively as the reinforcing phase in the material commonly known as fiberglass.

The use of E-Glass as the reinforcement material in polymer matrix composites is extremely common. Optimal strength properties are gained when straight, continuous fibers are aligned parallel in a single direction. To promote strength in other directions, laminate structures can be constructed, with continuous fibers aligned in other directions. Fiber dimension and to some extent proper-ties can be controlled by the process variables such as melt temperature (hence viscosity) and draw-ing/spinning rate. The temperature window that can be used to produce a melt of suitable viscosity is quite large, making this composition suitable for fiber forming.

Composition:E-Glass is a low alkali glass with a typical nominal composition of SiO₂ 54wt%, Al₂O₃ 14wt%, CaO+MgO 22wt%, B₂O₃ 10wt% and Na₂O+K₂O less than 2wt%. Some other materials may also be present at impurity levels.

Key Properties

Properties that have made E-glass so popular in fibreglass and other glass fibre reinforced composite include:

- Low cost
- High production rates
- High strength,
- High stiffness
- Relatively low density
- Non-flammable
- Resistant to heat
- Good chemical resistance
- Relatively insensitive to moisture
- Able to maintain strength properties over a wide range of conditions

- Good electrical insulation

The advantageous properties of E-glass generally outweigh the disadvantages which include:

- Low modulus
- Self-abrasiveness if not treated appropriately leading to reduced strength
- Relatively low fatigue resistance
- Higher density compared to carbon fibers and organic fibers.

Uses: Uses for regular glass fiber include mats and fabrics for thermal insulation, electrical insulation, sound insulation, high-strength fabrics or heat- and corrosion-resistant fabrics. It is also used to reinforce various materials, such as tent poles, pole vault poles, arrows, bows and crossbows, translucent roofing panels, automobile bodies, hockey sticks, surfboards, boat hulls, and paper honeycomb. It has been used for medical purposes in casts. Glass fiber is extensively used for making FRP tanks and vessels.

Open-weave glass fiber grids are used to reinforce asphalt pavement. Non-woven glass fiber/polymer blend mats are used saturated with asphalt emulsion and overlaid with asphalt, producing a waterproof, crack-resistant membrane. Use of glass-fiber reinforced polymer rebar instead of steel rebar shows promise in areas where avoidance of steel corrosion is desired.

Thermal; Glass fibers are useful thermal insulators because of their high ratio of surface area to weight. However, the increased surface area makes them much more susceptible to chemical attack. By trapping air within them, blocks of glass fiber make good thermal insulation, with a thermal conductivity of the order of $0.05 \text{ W}/(\text{m}\cdot\text{K})$

The strength of glass is usually tested and reported for "virgin" or pristine fibers—those that have just been manufactured. The freshest, thinnest fibers are the strongest because the thinner fibers are more ductile. The more the surface is scratched, the less the resulting tenacity. Because glass has an amorphous structure, its properties are the same along the fiber and across the

fiber. Humidity is an important factor in the tensile strength. Moisture is easily adsorbed and can worsen microscopic cracks and surface defects, and lessen tenacity.

In contrast to carbon fiber, glass can undergo more elongation before it breaks. There is a correlation between bending diameter of the filament and the filament diameter. The viscosity of the molten glass is very important for manufacturing success. During drawing (pulling of the glass to reduce fiber circumference), the viscosity must be relatively low. If it is too high, the fiber will break during drawing. However, if it is too low, the glass will form droplets rather than drawing out into fiber.

3.2. Analytical Analysis Conditions

For comparison of thermal structural analysis between analytical and finite element, the dimensions and specifications of SUV (Sport Utility Vehicle) car of model DD6470C is selected. The detail of this specification is in appendix I. Dimensions and specifications of this car are taken from Bishoftu Automotive Industry. SUV car is manufactured by Huanghai Company in China, and Bishoftu Automotive Industry imports the disassembled parts and assembles it locally. The demand of this car is increasing worldwide due to its quality in fuel economy, less expensive, and varying amount of towing capacity with an all-wheel drive or four wheel drive system. The maximum high speed set for this car is as high as 200km/hr or 36m/s which is higher than pickup car 180km/hr. or (30m/s). This high speed makes this car to be selected for the analysis of thermal structural-structural analysis of its disc brake.

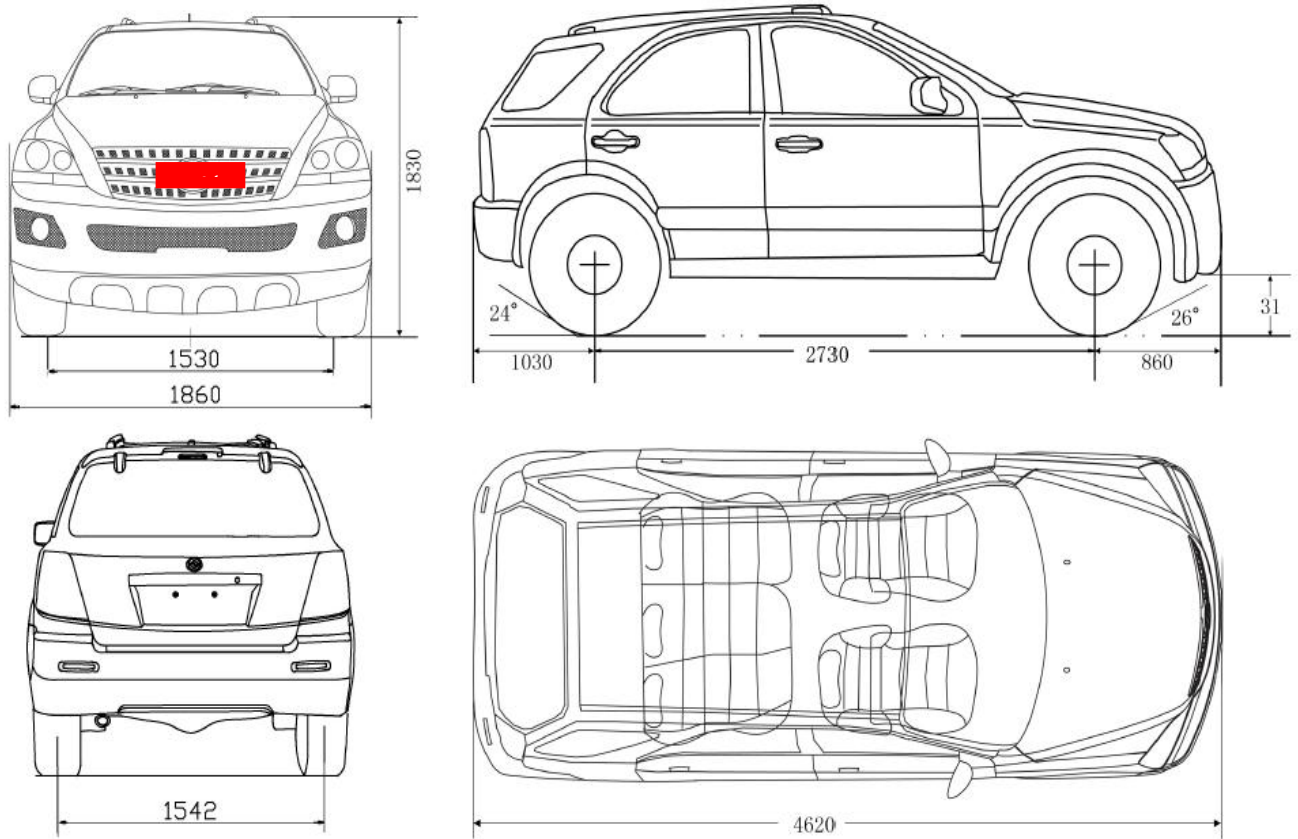


Figure 2:Huanghai SUV car of model DD6470C

They also provide extra traction in slippery conditions and the ability to tackle at least moderate off-road terrain. Taking these in to consideration Bishoftu Automotive Industry imported the disassembled parts from Huanghai Company. The demand of this car is highly increased now days in government officials, as well as in private company.

This thesis is focused on a study of ventilated disc brake rotor of SUV Huanghai vehicle with full load of capacity with selected positions for study of thermal stress analysis. Vent and hub are

excluded from analysis because hub is far from position of high temperature gradient, and vent is not exposed to high temperature because of convection heat transfer. Therefore only thickness of a rotor is the main concentration of this thesis. Cylindrical coordinate system is used to describe the dimensions. For analysis we focus on front wheel rotor only. Therefore front disc brake of Huanghai SUV car of model DD6470C will be used for analysis.



Figure 3: Measuring dimensions of disc and pad

3.2.1. Geometries and Dimensions of Brake Disk-pad

Dimensions of disc and pads are used for development of 3-D drawing. Radius and thickness, as well as other complex structures are used as an input for analysis. These dimensions are taken by measuring the disc by caliper. In addition maximum speed is used for thermal analysis. This and other necessary data are found on SUV specification (appendix I).

Table 2: Measured dimensions of disc rotor and pad

Symbols	Meaning	Value
φ_0	The cover angle of pad (in degrees)	65
r, z, θ	Radial circumferential and axial coordinate	-
r_p	The internal radius of the pad, mm	60
R_p	External radius of the pad, mm	120
r_d	Internal radius of the disk, mm	60
R_d	External radius of the disk, mm	120
δ_d	Disk thickness, mm	24

δt	Vent thickness	6
δp	pad thickness, mm	12

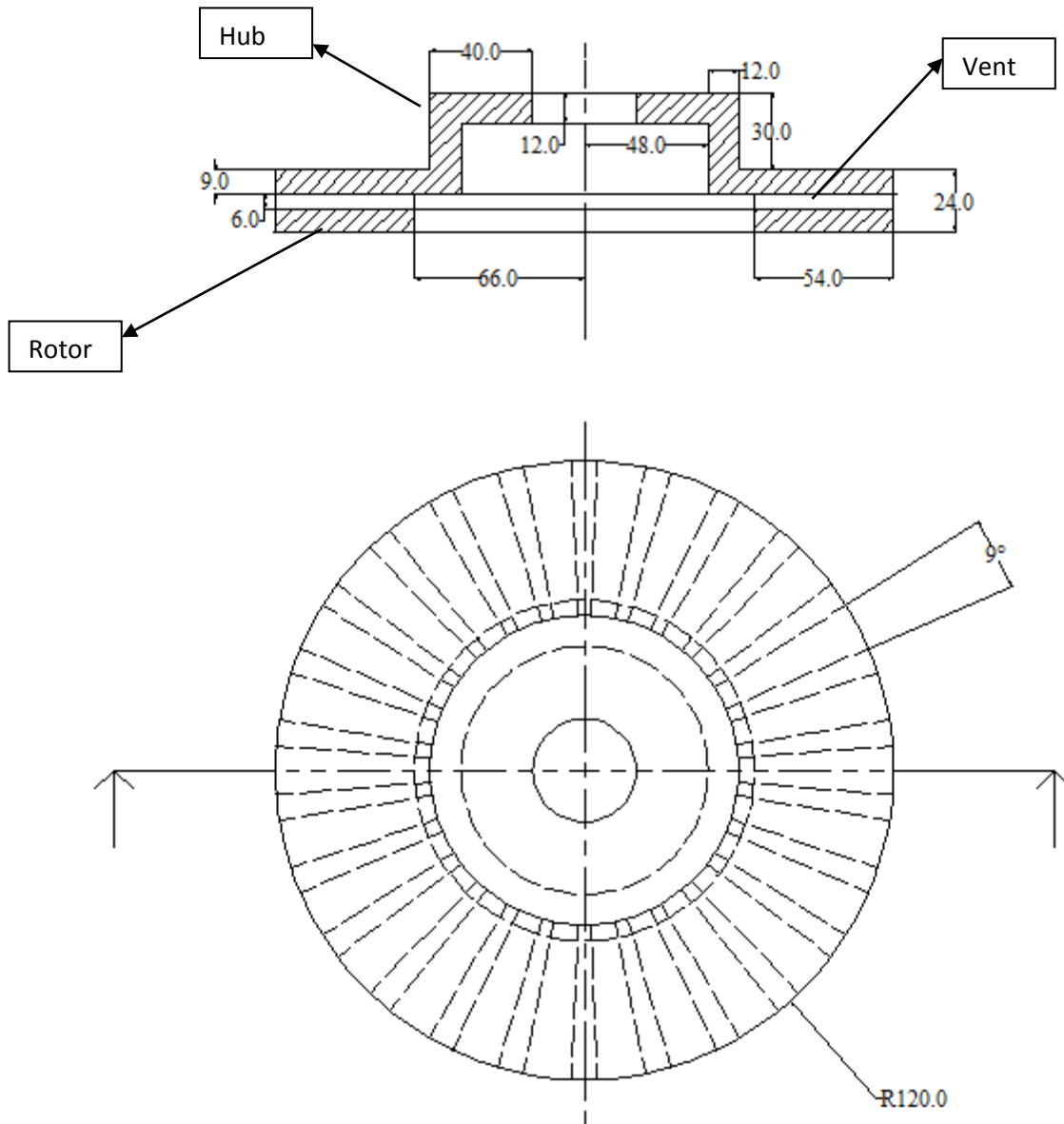


Figure 4: Cross sectional view of the disc

The values displayed in table 3.4 are found on figure 3.3 and figure 3.4. This thesis is focused on a study of ventilated disc brake rotor of SUV Huanghai vehicle with full load of capacity with selected positions for study of thermal stress analysis. Therefore only thickness of a rotor is the main concentration of this thesis. Cylindrical cordite system is used to describe the dimensions.

Different surfaces of disc or pad shown in figure 3.4 are designated by the following symbols.

Ω_1 Contact surface area between pads and disc (upper)

Ω_2 External radius surface area

Ω_3 Internal radius surface area

Ω_4 Contact surface area between pads and disc (lower)

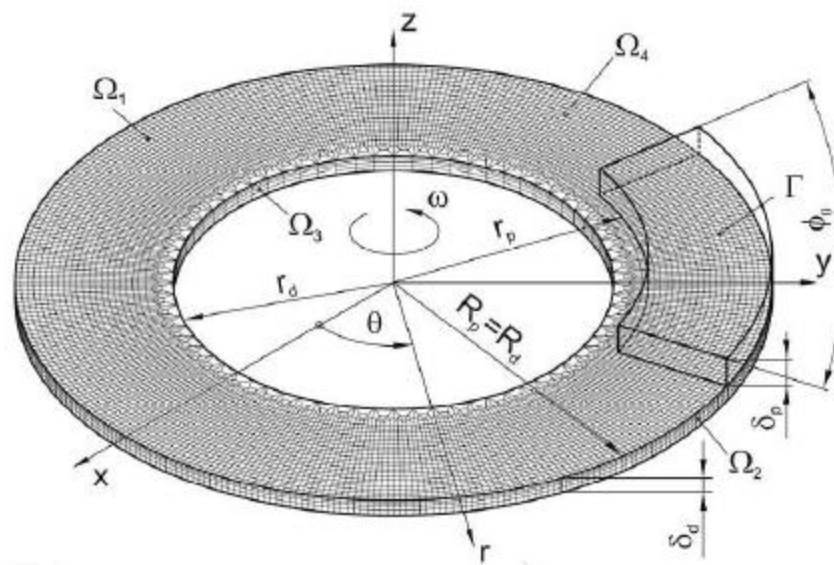


Figure 5: Dimensioning disc and pad

3.2.2. Thermal Loading and Boundary Condition

Thermal analysis is used to determine the temperature distribution, thermal gradient, rate of heat flow and heat flux in an object that occurred due to thermal loads. Such load includes the following parameters:-

- Convection
- Radiation
- Heat flow rates
- Heat flow per unit is i.e. Heat Flux.
- Heat flow per unit volume i.e. Heat Generation Rate.
- Constant temperature boundaries.

The thermal analysis may be either linear or nonlinear. Linear includes with material properties and nonlinear includes material properties that depend on temperature. The thermal properties of most material vary with nonlinear.

Based on the information of the Vehicle Research & Test Center of Huanghai SUV car specification (appendix I), the average of stopping distance with fully loaded disc brake (30°C ambient temperature) traveling at a speed of 200 km/hr (56m/s) under the roller test conditions, required an average of 81m stopping distance with the deceleration rate 12 m/s² in 4.6 second. For the analysis, speed of the car reduced from 56m/s to zero within 4.6 seconds (figure 3.5). In this thesis, the single stop cycles of braking were used to analyze thermal structural analysis, because the material regains its original condition (elastic) after force is removed.

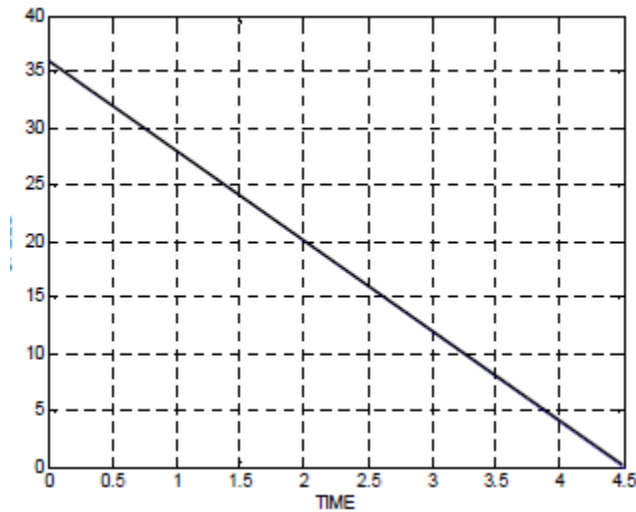


Figure 6: Braking conditions

In actually, variation of the rotating speed during braking must be determined through vehicle dynamics. However, in this study, the rotating speed of disk was considered to be a 300rad/sec. at t=0, which is maximum speed divided by external radius of disk. The final velocity is zero. For the purpose of comparison of obtained results, pressures of 1Mpa are taken from specification of the SUV car (appendix I). The heat dissipated through the brake disc surface during the heat flux applied to the both surface are ignored and only can be considered during the idle time.

Heat transfer convection is only considered after brake application is completed, and the car accelerated to regain its original speed. The remaining surface area of the disc is considered to be insulated. These areas include circumferential areas, inner and external radius areas of the disc.

Several assumptions have been made to simplify the analysis complexity and at the same time allow the reasonable output is obtained from the result of the analysis. In the temperature analysis for repeated braking, for both types' models (FE and analytical) it has been assumed as follows:

- ✓ Material properties are isotropic and independent of the temperature
- ✓ The nominal surface of contact between the disc brake and the pad in operation is equal to the apparent surface in the sliding motion.
- ✓ The contact pressure is uniformly distributed over all friction surfaces hence the heat generation of the midplane is considered as symmetric
- ✓ Radiation is neglected by virtue of short braking time and hence relatively low temperature
- ✓ The wear on the contact surface is negligible.
- ✓ Temperature vary only along thickness and constant heat flux is applied radially.

The differential equation of heat conduction will have numerous solutions unless a set of boundary conditions and an initial condition (for the time-dependent problem) are prescribed. Boundary conditions specify the temperature or the heat flow at the boundaries of the region. For example, at a given boundary surface, the temperature distribution may be prescribed, or the heat flux distribution may be prescribed, or there may be heat exchange by convection and/or radiation with an environment at a prescribed temperature. The boundary condition can be derived by writing an energy balance equation at the surface of the solid.

We consider a surface element having an outward-drawn unit normal vector \mathbf{n} , subjected to convection, radiation, and external heat supply as illustrated in figure 7. The physical significance of various heat fluxes shown in this figure is as follows.

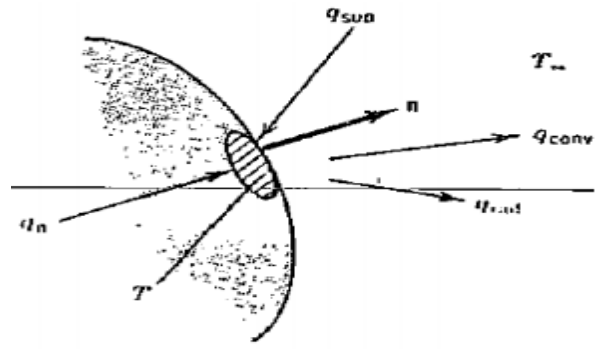


Figure 7: Energy balance at the surface of a solid parts

A simplified energy balance of the process is shown in Figure below;

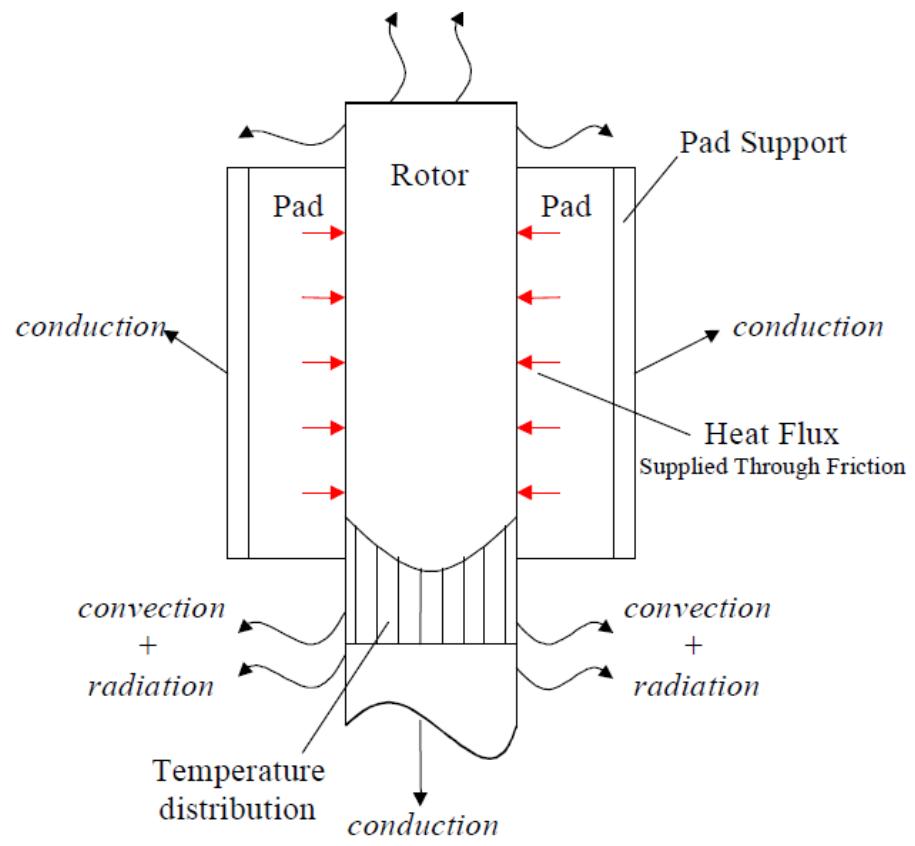


Figure 8: Heat Dissipation from Disc Rotor

The quantity q_{sup} represents energy supplied to the surface, in W/m^2 , from an external source.

The quantity q_{conv} represents heat loss from the surface at temperature T by convection with a heat transfer coefficient h into an external ambient at a temperature T_{∞} , and is given by

$$q_{conv} = h(T - T_{\infty}) \text{ W/m}^2 \dots\dots\dots 3.1$$

Here the heat transfer coefficient h varies with the type of flow (laminar, turbulent, etc.), the geometry of the body and flow passage area, the physical properties of the fluid, the average temperature, and many others.

The quantity q_{rad} represents the heat loss from the surface by radiation in to an ambient at an effective temperature T_∞ , and is given by

$$q_{rad} = \epsilon \sigma (T^4 - T_\infty^4) \dots \dots \dots 3.2$$

Where ϵ is the emissivity of the surface and σ is the Stefan-Boltzmann constant, that is, $\sigma = 5.6697 \times 10^{-8} \text{ W}/(\text{m}^2 \cdot \text{K}^4)$.

The quantity q_n represents the component of the conduction heat flux vector normal to the surface element and is

$$q_n = -k \frac{\partial T}{\partial n} \dots \dots \dots 3.3$$

To develop the boundary condition, we consider the energy balance at the surface as

Heat supply = heat loss

$$q_n + q_{supp} = q_{conv} + q_{rad} \dots \dots \dots 3.4$$

Introducing the expressions 3.1, 3.2, and 3.3 into 3.4, the boundary condition becomes

$$-k \frac{\partial T}{\partial n} + q_{supp} = h(T - T_\infty) + \epsilon \sigma (T^4 - T_\infty^4) \dots \dots \dots 3.5a$$

$$k \frac{\partial T}{\partial n} + hT + \epsilon \sigma T^4 = q_{supp} + hT_\infty + \epsilon \sigma T_\infty^4 \dots \dots \dots 3.5b$$

Where all the quantities on the right hand side of equation 3.5b are known and the surface temperature T is unknown. The general boundary condition given by equations 3.5b is nonlinear because it contains the fourth power of the unknown surface temperature T^4 . In addition, the absolute temperatures need to be considered when radiation is involved.

In this thesis, for the analytic solution of linear heat conduction problems, three different types of linear boundary conditions are considered: boundary condition of the first kind, second kind and third kind.

Boundary condition of the first kind is the situation when the temperature distribution is prescribed at the boundary surface, that is $T=f(z, t)$ on S where the prescribed surface temperature $f(z, t)$ is, in general, a function of position and time. The special case $T=0$ on S is called homogeneous boundary condition of first kind.

Boundary condition of the second kind is the situation in which the heat flux is prescribed at the surface, that is $k \frac{\partial T}{\partial n} = f(z, t)$ on S , where, $\frac{\partial T}{\partial n}$ is the derivative along the outward drawn normal to the surface. Here $f(z, t)$ is the prescribed heat flux, W/m². The special case $\frac{\partial T}{\partial n} = 0$ on S is called the homogeneous boundary condition of the second kind.

Boundary condition of the third kind is the convection boundary condition which is readily obtained from equation 3.5b by setting the radiation term and the heat supply equal to zero, that is $k \frac{\partial T}{\partial n} + hT = h T_{\infty}(z, t)$ on S . where, for generality, the ambient temperature $T_{\infty}(z, t)$ is assumed to be a function of position and time. The special case $k \frac{\partial T}{\partial n} + ht = 0$ On S is called the homogeneous boundary condition of the third kind. It represents convection into a medium at zero temperature.

Figure 9 shows the boundary conditions of the disk for two types of pressure distribution; uniform wear and uniform pressure in figure a and b respectively. As it can be seen, since the thermal problem in the disk is symmetric in z direction, only the half of the disk ($z=\delta/2$) is considered. So the transient heat equation for the disk and the related boundary conditions that have been shown in the figure is formulated as follows.

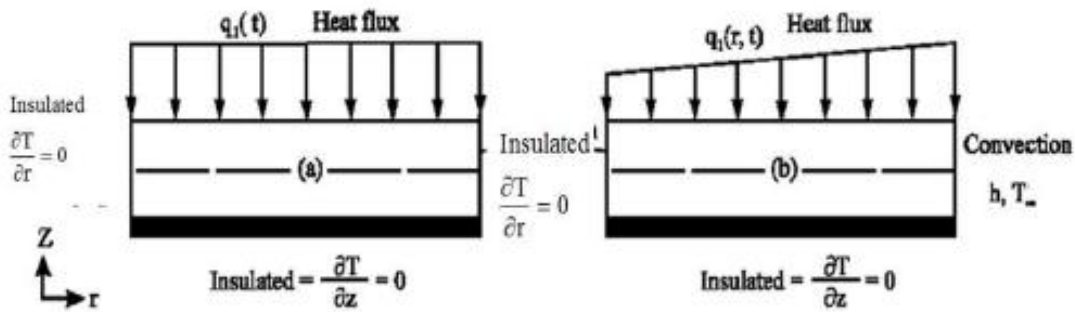


Figure 9: Boundary condition of the disk (a) uniform wear (b) uniform pressure

Where

r - is the radial coordinate,

z - is the axial coordinate,

The location of first boundary condition on rotor is found at $z=0$, which is insulated surface. It is homogeneous boundary condition of the second kind (special case). This boundary condition is

resulted due to axial symmetry (half thickness of the disc).

$$\frac{\partial T}{\partial z} = 0 \dots\dots\dots 3.6a$$

$$z=0$$

$$r_d \leq r \leq R_d$$

$$t \geq 0$$

The second boundary condition is found at $z=\delta$ (surface of the rotor). This boundary should be considered in two sections, one of them is exposed to the boundary condition of the third kind or convection, and the other is exposed to the boundary condition of the second kind, or prescribed heat flux. Heat flux is specified in contact zone of disk-pad due to the frictional heating between the pads and disk. Boundary condition of the third kind is ignored here due to first brake application.

$$\frac{\partial T}{\partial z} = q_o \dots\dots\dots 3.6b$$

$$z=\delta$$

$$r_d \leq r \leq R_d$$

$$t \geq 0$$

With initial condition of

$$T(r,z,0)=T_o \quad r_p \leq r \leq R_p \quad 0 \leq z \leq \delta_p \dots\dots\dots 3.6c$$

3.2.3. Solid Mechanics Aspect and Structural Boundary Condition

Thermal stresses are defined as self-balancing stresses produced by a non-uniform distribution of temperature or by differing coefficients of thermal expansion . These thermal stresses are developed in a solid body whenever any part is prevented from assuming the size and shape that it would freely assume under a change in temperature. Time dependent thermal boundary conditions are assumed to act on the disc surfaces axially. The transient temperature response of the brake disc is first required in order to be used as a load input for the thermal stress analysis.

In the first step, the general relation and analytical solution for the temperature distribution is derived by means of dimensionless parameter followed by separation of variables in disc thickness using transient dimensionless variable. In second step the thermal stress components are extracted by means of the displacement technique applied to a one dimensional problem of disc bodies. Specific solutions were determined for the case of transient thermal loading case applied to disc.

One of the causes of initial stresses in a body is no uniform heating. With rising temperature the elements of a body expand. Such an expansion generally cannot proceed freely in a continuous body, and stresses due to the heating are set up. In many cases of machine design, such as in the design of brakes, steam turbines and diesel engines thermal stresses are of great practical importance and must be considered in more detail. Solution of thermal stress problems requires reformulation of the stress-strain relationships accomplished by superposition of the strain attributable to stress and that due to temperature.

For a change in temperature $T(z)$, the change of length δL , of small linear element of length L in an unconstrained body is $\delta L = \alpha L T$. Here α , is the coefficient of linear thermal expansion. The thermal strain ϵ_t associated with the free expansion at a point is then

$$\epsilon_t = \alpha T \dots\dots\dots 3.7$$

To ascertain the distribution of stress, strain, and displacement with in an elastic body subjected to a prescribed system of forces requires consideration of a number of conditions relating to certain physical laws, material properties, and geometry. These fundamental principles of analysis also referred to as the three aspects of solid mechanics problems: Condition of equilibrium, condition of compatibility and Condition of equilibrium is related to statistics equation. The equation of statistics must be satisfied throughout the body. The stress field in an elastic solid is continuously distributed within the body and uniquely determined from the applied loadings. Because we are dealing primarily with bodies in equilibrium, the applied loadings satisfy the equations of static equilibrium; that is, the summation of forces and moments is zero. If the entire body is in equilibrium, then all parts must also be in equilibrium. Thus, we can partition any solid into an appropriate sub domain and apply the equilibrium principle to that region. Following this approach, equilibrium equations can be developed that express the vanishing of the resultant force and moment at a continuum point in the material. These

equations can be developed by using either an arbitrary finite subdomain or a special differential region with boundaries coinciding with coordinate surfaces.

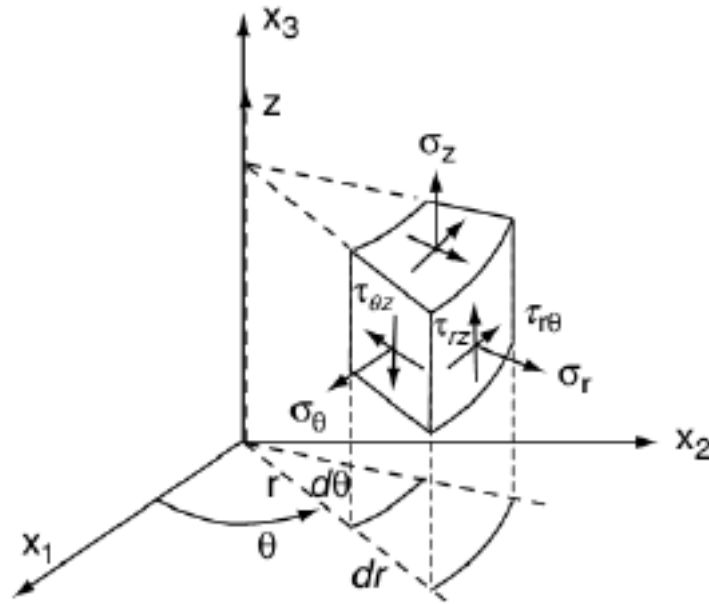


Figure 10: Stress components in cylindrical coordinates.

In order to solve many elasticity problems, formulation must be done in curvilinear coordinates typically using cylindrical or spherical systems. The stress components are defined on the differential element shown in Figure 3.8, and thus the stress matrix is given by.

$$\boldsymbol{\sigma} = \begin{bmatrix} \sigma_r & \tau_{r\theta} & \tau_{rz} \\ \tau_{r\theta} & \sigma_\theta & \tau_{\theta z} \\ \tau_{rz} & \tau_{\theta z} & \sigma_z \end{bmatrix} \dots\dots\dots 3.8$$

Now wish to develop expressions for the equilibrium equations in curvilinear cylindrical and spherical coordinates. By using a direct vector/matrix notation, the equilibrium equations can be expressed as [20]

$$\frac{\partial \sigma_r}{\partial r} + \frac{1}{r} \frac{\partial \tau_{r\theta}}{\partial \theta} + \frac{\partial \tau_{rz}}{\partial z} + \frac{\sigma_r - \sigma_\theta}{r} + F_r = 0$$

$$\frac{1}{r} \frac{\partial \sigma_\theta}{\partial \theta} + \frac{\partial \tau_{r\theta}}{\partial r} + \frac{\partial \tau_{\theta z}}{\partial z} + 2 \frac{\tau_{r\theta}}{r} + F_\theta = 0 \dots\dots\dots 3.9$$

$$\frac{\partial \tau_{rz}}{\partial r} + \frac{1}{r} \frac{\partial \tau_{\theta z}}{\partial \theta} + \frac{\partial \sigma_z}{\partial z} + \frac{1}{r} \tau_{rz} + F_z = 0$$

σ_r -Normal stress in radial direction.

σ_θ - Normal stress in circumferential direction

σ_z - Normal stress in axial direction.

$\tau_{r\theta}$ -Shearing stress in r θ plane

τ_{rz} -Shearing stress in r z plane

$\tau_{z\theta}$ -Shearing stress in z θ plane

F_r -Component of the body forces in the radial direction

F_θ - Component of the body forces in the circumferential direction

F_z -Component of the body forces in the axial direction

The second aspect of solid mechanics is condition of compatibility. The geometry of deformation and the distribution of strain must be consistent with the preservation of body continuity. The true solutions satisfy also the compatibility equation (bi-harmonic equation in polar coordinate):

$$\left(\frac{\partial^2}{\partial r^2} + \frac{1}{r} \frac{\partial}{\partial r} + \frac{1}{r^2} \frac{\partial^2}{\partial \theta^2} + \frac{\partial^2}{\partial z^2} \right) (\sigma_r + \sigma_\theta + \sigma_z + \alpha ET) = 0 \dots\dots\dots 3.10$$

In addition, the stress, strain, and displacement fields must be such as to conform to the condition of loading imposed at the boundaries. This is known as satisfying the boundary conditions for a particular problem.

The third solid mechanics aspect is condition of Hook's law (stress strain relations). Material properties (constitutive relations, for example, Hook's law) must comply with the known behavior of the material involved. The total r, θ , and z strains ϵ_r , ϵ_θ and ϵ_z are obtained by adding to the thermal strains of the type described above and the strains due to stress resulting from external forces. From Hook's law for a homogeneous isotropic body in cylindrical coordinate system are :

$$\epsilon_{rr} = \frac{1}{E} [\sigma_{rr} - \nu(\sigma_{\theta\theta} + \sigma_{zz})] + \alpha \Delta T = \frac{1}{2G} (\sigma_{rr} - \frac{\nu}{1+\nu} \theta) + \alpha \Delta T \dots\dots\dots 3.11a$$

$$\epsilon_{\theta\theta} = \frac{1}{E} [\sigma_{\theta\theta} - \nu(\sigma_{rr} + \sigma_{zz})] + \alpha \Delta T = \frac{1}{2G} (\sigma_{\theta\theta} - \frac{\nu}{1+\nu} \theta) + \alpha \Delta T \dots\dots\dots 3.11b$$

$$\epsilon_{zz} = \frac{1}{E} [\sigma_{zz} - \nu(\sigma_{rr} + \sigma_{\theta\theta})] + \alpha\Delta T = \frac{1}{2G} (\sigma_{zz} - \frac{\nu}{1+\nu}\theta) + \alpha\Delta T \dots\dots\dots 3.11c$$

And

$$\epsilon_{r\theta} = \frac{\sigma_{r\theta}}{2G} \dots\dots\dots 3.12a$$

$$\epsilon_{\theta z} = \frac{\sigma_{\theta z}}{2G} \dots\dots\dots 3.12b$$

$$\epsilon_{zr} = \frac{\sigma_{zr}}{2G} \dots\dots\dots 3.12c$$

$$\theta = \sigma_{rr} + \sigma_{\theta\theta} + \sigma_{zz} \dots\dots\dots 3.13a$$

$$G = \frac{E}{2(1+\nu)} \dots\dots\dots 3.13b$$

$$\Delta T = T(z,t) - T_0 \dots\dots\dots 3.13c$$

With

E- Young's modulus

α - The coefficient of the linear thermal expansion

ν – The Poisson's ratio

G- Shear modulus

ΔT is the temperature change from the reference temperature to (where the reference temperature can be the temperature of the body in the unstrained state or the ambient temperature before a change of temperature).

Similar to other field problems in engineering science, the solution of thermal stress requires appropriate boundary conditions on the body under study. Thermal boundary conditions are stated in thermal analysis such as insulated surfaces and heat flux boundary conditions. In similar manner there are a number of structural boundary conditions as well as free surfaces from traction. The common types of boundary conditions for thermal stress applications normally include specification of how the body is being supported or loaded. This concept is mathematically formulated by specifying either the displacements or tractions at boundary points. A common example of this situation is shown in disc brake for a case involving a

surface of problem symmetry where the condition is one of a rigid-smooth boundary with zero axial and circumferential displacements and zero radial traction. Boundary conditions are normally specified using the coordinate system describing the problem and thus particular components of the displacements and tractions are set equal to prescribed values. For displacement-type conditions, such a specification is straightforward, and a common example includes fixed boundaries where the displacements are to be zero. In general three types of boundary conditions available in this analysis: circumferential, axial and radial constraints.

3.2.3.1. Circumferential Constraint

Circumferential boundary condition is due to geometrical symmetry of the rotor, and shown in figure 3.9 below. When temperature rises, and the material tries to expand freely along circumference, the circumferential compressive stress $\sigma = -\alpha E \Delta T$ suppresses the expansion which means fixed boundaries where the displacements are to be zero. The element can maintained in this condition by applying the distribution of compressive force given to the edges $\theta = \text{constant value}$.

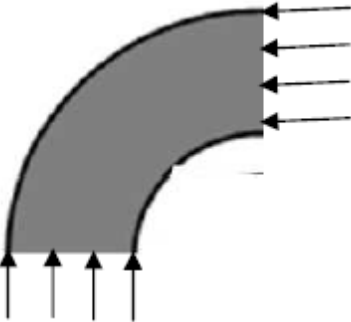


Figure 11: Circumferential Constraint (zero displacement)

3.2.3.2. Axial Constraint

Due to application of the pads from both side, free thermal expansion of the rotor in axial direction is suppressed, by compressive force $\sigma_z = -\alpha E \Delta T$ along axial direction, and there are two fixed boundaries where the displacements are to be zero. One is due to symmetry (the lower surface of the disc) and the other is due to pads axial displacement of the rotor (the upper surface of the rotor) is constrained to zero value

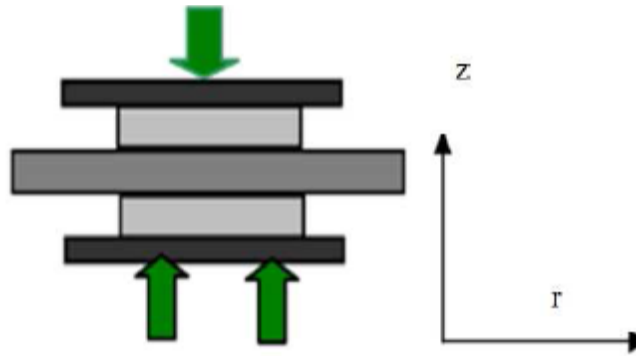


Figure 12: Axial compressive stresses

3.2.3.3. Radial Constraints

This is displacement boundary condition (fixed boundaries where the displacements are to be zero) which is applied at the inner radius of the rotor to prevent radial movement of the rotor. At the same time the external radius of the disc is free from stress, as well as displacement constraint .

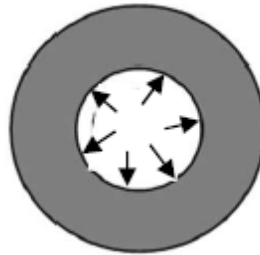


Figure 13: Radial Displacement Constraints

3.3. Analytical Analysis Methods in Disk Brake Temperature Distribution

To investigate the thermal stress behavior of brake discs under thermal load, it is necessary to obtain typical temperature distributions in this brake rotor as a function of time. Therefore, the objective of this section is to predict the temperature response of the brake disc design.

As it is shown in figure 3.8 below, disk is like an annulus and pad is like a partial annulus. The brake system clamps the pads through the caliper assembly by brake fluid pressure in the cylinder. Rotary motion of the disk causes the sliding contact between the disk and the pad and generates heat. For calculation of heat generation due to friction, rate of dissipated heat via friction should be taken in to account. This is all to do with the calculation of friction force and

the rate of work done by friction force. For the calculation of friction force, the pressure distribution at the contact surfaces of the disk and the pad should be determined.

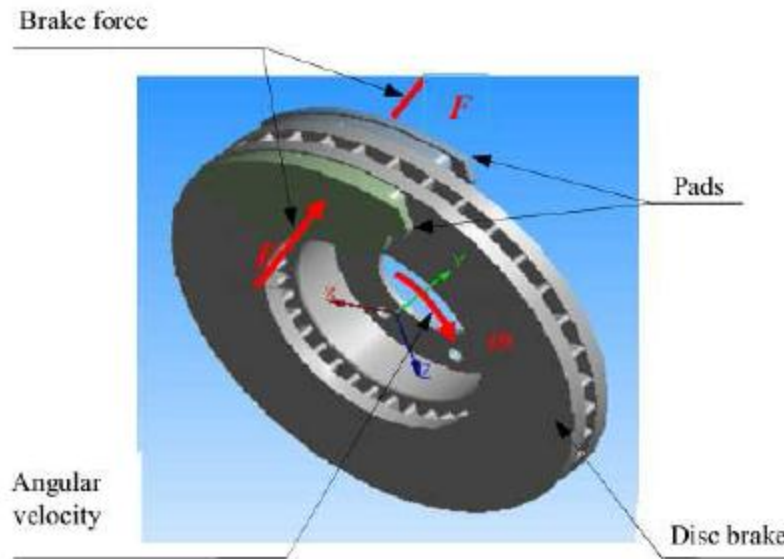


Figure 14:Schematic shapes of the disk and the pad in sliding contact

In the contact area of brake components, the pad and the disk, heat is generated due to friction. For calculation of heat generation at the interface of these two sliding bodies, two methods are suggested, macroscopic model and microscopic model. In case of macroscopic model analysis, brakes are essentially a mechanism to change the energy types. When a car is moving with speed, it has kinetic energy. Applying the brakes, the pads that press against the brake rotor convert this energy into thermal energy. The cooling of brakes dissipates the heat and the vehicle slows down. This is all to do with the first law of thermodynamics, known as laws of conservation of energy which states that energy cannot be created nor destroyed; it can only be converted from one form to another. In the case of brakes, it is converted from kinetic energy to thermal energy.

$$E_c = 0.5MV_o^2 \dots\dots\dots 3.14$$

Where M is total mass of the vehicle and V_o is the initial speed of the vehicle. To obtain the amount of heat dissipated by each of the disk will be

$$Q=0.25mV_o^2 \dots\dots\dots 3.15$$

Where, m is the amount of the distributed mass on the front axle of the vehicle. In addition air drags force, total mass of the rotating parts, and inclination of the roads are required.

The second method is Microscopic model. In this case, rate of generated heat due to friction is equal to the friction power. Some of this frictional heat is absorbed by the disk and the rest is absorbed by the pads. If it is supposed that the whole friction power is transferred to the heat energy and heat partition coefficient is stated by parameter γ . For this particular thesis the input data for analysis is taken from roller testing, which results application of microscopic model in this thesis.

3.3.1. Heat Partition Coefficient and Energy Input

The thermal energy generated at the brake friction Interface can be transferred to both the brake rotor and the pads. This partitioning of the thermal energy is dependent on the relative thermal resistances of the pad and brake rotor that are functions of their respective material densities, heat capacities and thermal conductivities as well as of the presence of any transfer film or third body layer at the rubbing interface. Theoretically, the pad thermal resistance should be higher than the rotor thermal resistance in order to protect the brake fluid from high temperatures but the value of the thermal resistance varies from one pad material to another. For the present analysis, the partitioning coefficient (γ) for thermal input to the brake disc was calculated as follows. The thermal effusivity ξ , for different material property is given by the following equation:

Table 3: The Material Property of the Pad

Material Properties	pad
<i>Thermal conductivity, k (W/m.c)</i>	5
<i>Density, ρ (kg/m³)</i>	1400
<i>Specific heat, C_p (J/kg.c)</i>	1000
<i>Poisson's Ratio, ν</i>	0.25
<i>Coeff. of expansion α (*10⁻⁶/c)</i>	10
<i>Elastic modulus, E(Gpa)</i>	1

Table 4: The Material Property of the Brake Assembly

properties	Cast iron	Maraging Steels	E-Glass	ALMMC
<i>Density, ρ (kg/m³)</i>	7100	8100	2580	2765.2
<i>Young's modulus, E(Gpa)</i>	125	210	72.3	85.5

<i>Thermal conductivity, k (W/m.k)</i>		25.5	1.3	181.5
<i>Specific heat, C_p (J/kg.k)</i>	586	813	810	826.8
<i>Poisson's Ratio, ν</i>	0.25	0.3	0.22	0.33
<i>Coeff. of expansion α (*10⁻⁶/k)</i>	8.1	11.5	5.4	17.5

$$\xi_d = \sqrt{k_d \rho_d c_d} \dots\dots\dots 3.16a$$

$$\xi_p = \sqrt{k_p \rho_p c_p} \dots\dots\dots 3.16b$$

$$S_p = \phi_o \int_{r_3}^{r_2} r dr = \phi_o / 2 (R_p^2 - r_p^2) = 65 \text{deg} / 2 * ((0.12)^2 - (0.06)^2) = 0.0061236 \text{m}^2 \dots\dots\dots 3.16c$$

$$S_d = 2\pi \int_{r_3}^{r_2} r dr = \pi (R_d^2 - r_d^2) = \pi * ((0.12)^2 - (0.06)^2) = 0.033912 \text{m}^2 \dots\dots\dots 3.16d$$

S_p and S_d are frictional contact surfaces of the pad and the disc, respectively.

For the given different material properties by using the values of table 3.3 and table 3.2 for the given values, we will get values of thermal effusivities of the pad and the disc from equation 3.16a and 3.16b as.

Therefore ;

A. thermal effusivities of the disc for Cast Iron Property is :

$$\xi_d = 14989.1$$

B. thermal effusivities of the disc for Maraging Steels Property is :

$$\xi_d = 12958.4$$

C. thermal effusivities of the disc for ALMMC Property is :

$$\xi_d = 20370.5$$

D. thermal effusivities of the disc for E-Glass Property is :

$$\xi_d = 5212.2$$

And

thermal effusivities of the pad for different material Properties are the same i.e;

$$\xi_p = 2645.75.$$

The total heat generated on the frictional contact interface q equals the heat flux into the disk q_d, and heat flux into the pad q_p.

The relative braking energy γ which is called heat partition coefficient is given by the following equation:

$$\gamma = \xi_d S_d / (\xi_d S_d + \xi_p S_p) \dots \dots \dots 3.17$$

Therefore;

A. heat partition coefficient for Cast Iron Property is :

$$\gamma = 0.969$$

B. heat partition coefficient for Maraging Steels Property is :

$$\gamma = 0.964$$

C. heat partition coefficient for ALMMC Property is :

$$\gamma = 0.977$$

D. heat partition coefficient for E-Glass Property is :

$$\gamma = 0.916$$

This partitioning of the thermal energy is dependent on the relative thermal resistances of the pad and brake rotor that are functions of their respective materials densities, heat capacities and thermal conductivities as well as of the presence of any transfer film or third body layer at the rubbing interface.

The heat flux generated by pressing the pad against the rubbing surface of the rotor is the only source of heat input to the model. The magnitude of this heat flux can be calculated from basic energy considerations. Energy input is a function of speed, coefficient of friction, radius of rotor, and pressure distribution.

In a braking system, the mechanical energy is transformed into a calorific energy. This energy is characterized by a total heating of the disc and pads during the braking phase. The heat quantity in the contact area is the result of plastic micro deformations generated by the friction forces. To obtain heat flux at the surfaces of two components of the brake system, we divide rate of thermal energy by the surface contact area of each component. Energy input is of two types: uniform pressure and uniform wear.

Contact surface element of the disc and the pad is shown on the figure 3.13. When disc slides over the pad, heat is generated at the interface due to friction and this heat is partitioned between the two bodies. The thermal energy generated at the brake friction interface can be transferred to both the brake rotor and the pads. The partitioning of heat is a function of the thermal properties

of the bodies, the contact geometry and the sliding speed . The rate of heat generated due to friction between these surfaces is calculated as follows:

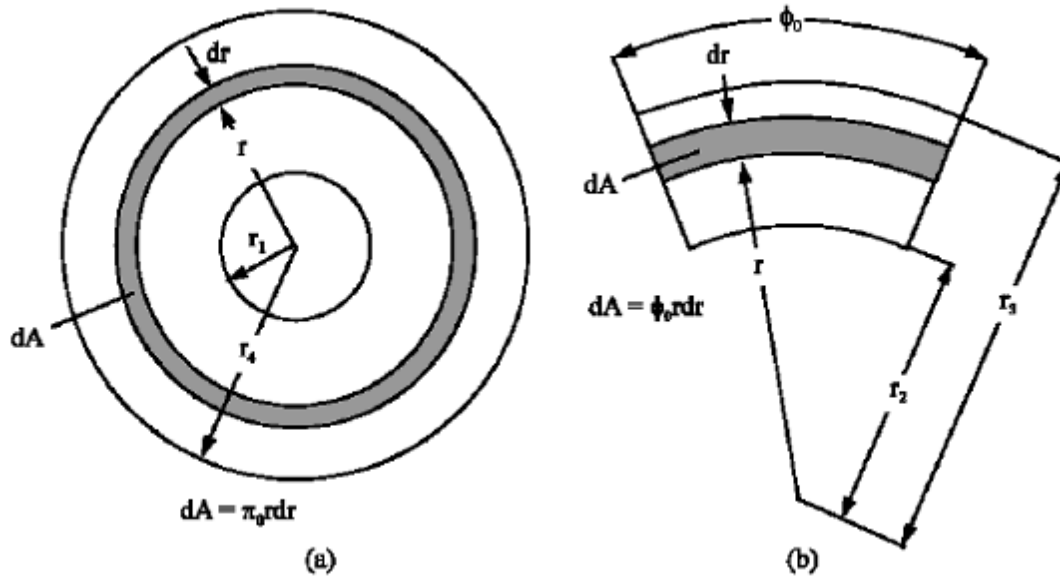


Figure 15: Contact surface elements of two components a) the disc and b) the pad.

$$d\dot{E} = dP = V dF_f = r \omega \mu p \phi_0 r dr \dots \dots \dots 3.18a$$

$$d\dot{E} = d\dot{E}_p + d\dot{E}_d \dots \dots \dots 3.18b$$

$$d\dot{E}_p = (1 - \gamma) dP = (1 - \gamma) \omega \mu p \phi_0 r^2 dr \dots \dots \dots 3.18c$$

$$d\dot{E}_d = \gamma dP = \gamma \omega \mu p \phi_0 r^2 dr \dots \dots \dots 3.18d$$

Where,

$d\dot{E}$ is the rate of heat generated due to friction between two sliding components

V is the relative sliding velocity and

dF_f is the friction force.

The terms $d\dot{E}_p$ and $d\dot{E}_d$ are the amount of absorbed heat by the pad and the disk, respectively.

Therefore, to calculate the frictional heat generation at the contact surfaces of two components of the brake system, parameters, e.g. the friction coefficient between two sliding components, relative sliding velocity, geometry of the disk brake rotor and the pad, and the pressure

distribution at the sliding surfaces must be available. There are two types of pressure distribution: uniform pressure and uniform wear pressure distribution.

In uniform pressure ($p = p_{max}$) heat flux q on a contact area is updated per the pressure distribution at every simulation step. Heat flux for uniform pressure is a function of time and space variable r ; the angular velocity decreases with time during braking action and the work done by friction force grows as radial space variable increases. This phenomenon is quite often when the pads are new.

Heat flux in the pad is given below.

$$q_p(r,t) = d\dot{E}_p/dS_p = (1 - \gamma)\omega\mu p\phi_o r^2 dr / \phi_o r dr = (1 - \gamma)\mu p r \omega(t) \dots\dots\dots 3.19a$$

$$q_{op}(r) = q_{o1}(r,0) = d\dot{E}_p/dS_p = (1 - \gamma)\omega\mu p\phi_o r^2 dr / \phi_o r dr = (1 - \gamma)\mu p r \omega_o \dots\dots\dots 3.19b$$

Similarly Heat flux in the disc is given below

$$q_d(r,t) = d\dot{E}_d/dS_d = \gamma\omega\mu p\phi_o r^2 dr / 2\pi r dr = \frac{1}{2\pi}\phi_o\gamma\mu p r \omega(t) \dots\dots\dots 3.19c$$

$$q_{od}(r) = d\dot{E}_d/dS_d = \gamma\omega\mu p\phi_o r^2 dr / 2\pi r dr = \frac{1}{2\pi}\phi_o\gamma\mu p r \omega_o \dots\dots\dots 3.19d$$

Where $ds_{d,p}$ is a surface contact area of disc and pads respectively.

In uniform wear ($P = p_{max}r_p/r$) however, assumption of uniform wear is more realistic after several braking application. This thesis focuses on uniform wear pressure distribution. Heat flux obtained for the uniform wear is just a function of time and it is independent of the space variable; the work done by friction force is the same at radial direction. This fact is seen by in pads as follows.

By inserting $P = p_{max}r_p/r$ in equation 3.19a, we will have

$$q_p(t) = (1 - \gamma)\mu p_{max} r \omega_o (1 - t/t_b) \dots\dots\dots 3.20a$$

And heat flux in the disc is obtained by inserting $P = p_{max}r_p/r$ in equation 3.19d, we will have

$$q_d(r,t) = q_{od}(r) * (1 - t/t_b) = \frac{1}{2\pi}\phi_o\gamma\mu p_{max} r_d \omega_o * (1 - t/t_b) \dots\dots\dots 3.20b$$

q_{op} , q_{od} is initial heat fluxes for pads and disc

γ - is the heat partitioning factor,

Φ_0 - is the cover angle of pad,

μ - is the friction coefficient,

ω - is the angular velocity,

r - is the radial coordinate,

z - is the axial coordinate,

r_p and R_p - are the internal and external radius of the pad.

The heat flux rate defined in Equations above is a function of vehicle speed but was otherwise assumed to apply uniformly over both rubbing surfaces of the disc. In reality, the generated heat flux in a disc brake is non-uniform and time-dependent over the rubbing surface.

This thesis focuses on uniform wear of heat flux distributions at $t=0$. These assumptions were made in order to simplify the thermal analysis which was only intended to predict typical temperature distributions for input to the thermal stress analysis. From equations 3.19d and 3.19b, Table 3.2 (for coefficient of friction), and 1Mpa pressure (from specification),

$$q_p(t) = (1 - \gamma)\mu p v_o (1 - t/t_b) = 0.09 * 0.35 * 1 * 10^6 * 0.0635 * 300 * (1 - t/t_b) \dots\dots\dots 3.20c$$

$$q_p(t) = 342900 * (1 - t/4.5) \sim 342900$$

Similarly Heat flux for the given different material properties of the the disc are given below;

$$q_d(r,t) = q_{od}(r) * (1 - t/t_b) = \frac{1}{2\pi} \Phi_0 \gamma \mu p_{max} r_d \omega_o * (1 - t/t_b) \dots\dots\dots 3.20d$$

Therefore ;

A. Heat flux for Cast Iron Property is :

$$q_d(t) = 668714.1 * (1 - t/4.5) \sim 668714.1 \text{ W/m}^2 \sim 0.668 \text{ W/mm}^2$$

B. Heat flux for Maraging Steels Property is :

$$q_d(t) = 665263.53 * (1 - t/4.5) \sim 665263.531 \text{ W/m}^2 \sim 0.665 \text{ W/mm}^2$$

C. Heat flux for ALMMC Property is :

$$q_d(t) = 674234.92 * (1 - t/4.5) \sim 674234.921 \text{ W/m}^2 \sim 0.674 \text{ W/mm}^2$$

D. Heat flux for E-Glass Property is :

$$q_d(t) = 632138.37 * (1 - t/4.5) \sim 632138.371 \text{ W/m}^2 \sim 0.632 \text{ W/mm}^2$$

3.4. Parametric Studies on Rotor Disc for Different Materials

3.4.1 Analytical Analysis Methods in Disk Brake Temperature Distribution

I) Vehicle specifications

Vehicle specifications is used for calculating the braking torque, heat flux and single stop temperature rise, we need vehicle specifications. The vehicle specifications include various parameters which are mentioned in below table I.

Table 3.5 : Vehicle parameters

Sr. No.	Description	values
1	Gross vehicle weight (M)	8,700kg
2	Wheel base (WB)	2.73 m
3	Maximum vehicle speed (V1)	200 (km/hr)
4	CG height (h)	0.915 m
5	Distance of CG from front axle (a1)	1.349 m
6	Distance of CG from rear axle (a2)	1.381 m
7	Tire rolling radius (Rt)	0.22 m
8	Stopping distance (Sd)	81 m

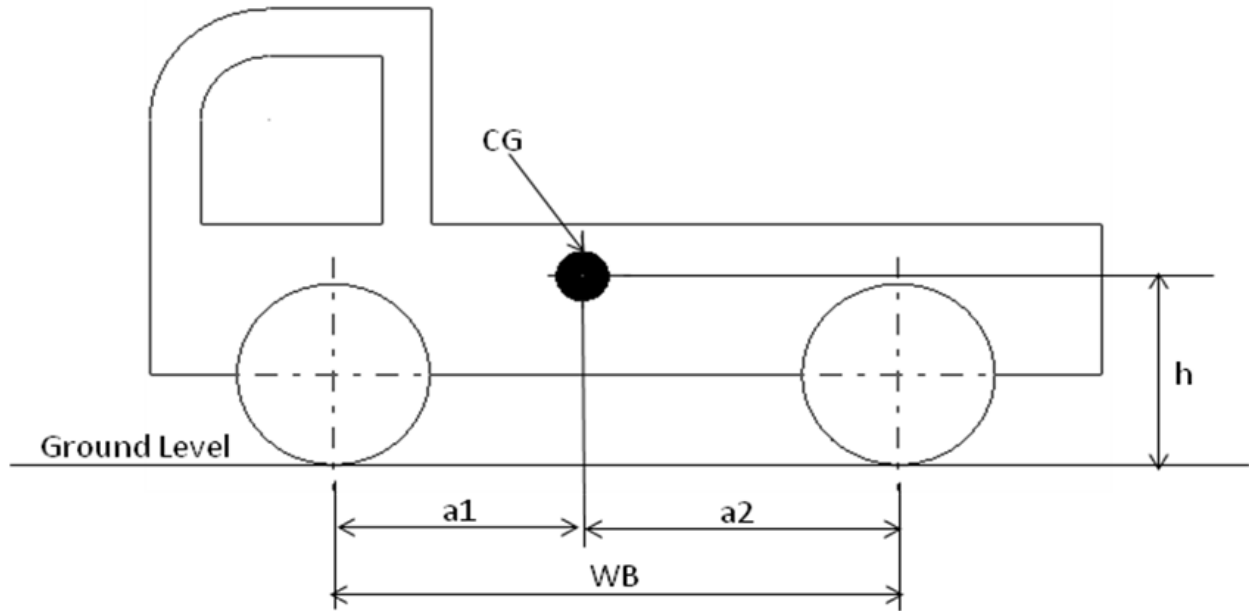


Figure 16: Vehicle dimensions

II. BRAKE TORQUE CALCULATION

The gross vehicle weight is 9.6 T and as per Indian Braking Standard IS: 11852, it falls under N2 category. For brake torque calculation following methodology is implemented.

- a. Static load distribution (R_f): - Static load distribution describes the weight distribution according to horizontal position of centre of gravity. Static load distribution on front axle can be calculated with the following equation.

$$R_f = M(a_2/a_1 + a_2) \dots \dots \dots 3.21$$

$$R_f = 8,700(1.381/2.73) = 4,400.982 \text{ kg}$$

Calculated static load distributions on front axle is 4,400.982 **kg**.

- b. Mean fully developed deceleration (MFDD):-MFDD can be calculated by considering the maximum test speed (V_1) of the vehicle in km/h. below equation is used to calculate MFDD.

$$\text{MFDD or } v = (V_b^2 - V_e^2) / 25.92(S_e - S_b) \text{ m/s}^2 \dots \dots \dots 3.22$$

Whereas,

V_b is the 80% of V_1 in km/h,

V_e is final speed of the vehicle after braking in km/h as 10% of V_1 ,

S_e is the total distance travelled by the vehicle in meters during braking and

S_b is the final distance travelled in meters i.e. zero.

Then,

$$V_b = 0.8 * 200 = 160 \text{ km/hr}$$

$$V_e = 0.1 * 200 = 20 \text{ km/hr}$$

$$v = 4.5 \text{ m/s}^2$$

c. Dynamic load distribution after braking (F_{zf}):- The vehicle is considered as one rigid body which moves along an ideally even and horizontal road. At each axle the force in the wheel are combined actions of normal and longitudinal force. In dynamic load distribution of the vehicle after braking, centre of gravity height (h in meters) plays an important role and influence dynamic part of the axle loads. Dynamic load distribution for front axle can be calculated by below equation

$$F_{zf} = M g \left(\frac{h}{a_1 + a_2} \right) \left(\frac{v}{g} \right) \dots \dots \dots 3.23$$

Whereas, g is acceleration due to gravity **9.81 m/s²**. The calculated dynamic load distribution for front axle is **8820 kg**.

c. Total load on front axle due to braking (T_f): -While decelerating, the total load is the sum of static load and dynamic load. And front axle is subjected to maximum dynamic load during braking. So calculation is done only for front axle. It can be calculated with help of below equation [5]

$$T_f = R_f + F_{zf} \dots \dots \dots 3.24$$

Whereas T_f is the total load acting on front axle. The calculated values for front and rear axle are **13221 kg**.

d. Brake force on front axle (B_f): -After deciding the static loading, dynamic loading and total loading, the brake force acting on front axle can be calculated with the help of below equation

$$B_f = T_f \mu_r \dots \dots \dots 3.25$$

Whereas, μ_r is the coefficient of road adhesion and varies according to road conditions. The calculated value for front axle is **5288 kg** considering as Asphalt μ_r as **0.55**.

The brake force acting on front axle is the function of total load acting and coefficient of adhesion (μ_r). Below table II shows the different values of coefficient of adhesion as per different road conditions .

Table 5: coefficient of adhesion

Surface	Values
Asphalt and concrete (dry)	0.8 - 0.9
Asphalt (wet)	0.5 - 0.6
Concrete road	0.75
Earth road (dry)	0.68
earth road (wet)	0.55
Gravel	0.6
Tar road	0.4
Ice surface	0.1
Snow (hard packed)	0.2

- e. Brake force acting on per wheel of front axle (B_{fw}): - Brake force on each wheel of front axle is calculated with following equation

$$B_{fw} = B_f / N_w \dots\dots\dots 3.26$$

Whereas, N_w is the number of wheels on front axle.

Considering number of wheels on front axle as 2, then brake force on per front wheel is **2644 kg**.

- f. Brake torque acting on per wheel of front axle (T_{bw}):-The brake torque acting on per wheel of

front axle is the function of brake force and tire rolling radius (R_t) can be calculated with the help of following equation

$$T_{bw} = B_{fw} R_t \dots\dots\dots 3.27$$

$$= 2644 * 0.22$$

The brake torque on per front wheel is **582 kg-m**.

The brake will need to overcome this load before it can start to slow down the vehicle. But, if the load is at rest, the static brake torque will prevent the load from moving. In practice, a safety

factor should be used in the case where the brakes is called upon only to hold this load and is only infrequently used in a dynamic manner. In this case a safety factor of **1.5** is used to calculate final brake torque on the disc. By considering the safety factor, the final braking torque will be **900 kg-m**.

III. HEAT FLUX AND TEMPERATURE CALCULATION

Frictional heat is generated at the rubbing surface due to the interactions between the pad and disc. The energy must be quickly dissipated to the surrounding air. Radiation also helps to dissipate the heat energy stored within the rotor when the temperature is high. The non-uniform heat flux input to the disc brake is calculated from the non-uniform pressure distribution, friction coefficient and sliding velocity along the disc-pad interface. The amount of heat flux that flow into each component depends on the disc and pad material.

Following steps are followed to calculate heat flux and single stop temperature rise.

a .Kinetic energy (KE):- Following equation is used to calculate the kinetic energy of the vehicle travelling with 100 km/h, .i.e. **27.77 m/s**.

$$KE = \left(\frac{1}{2}\right)Mv^2$$

Whereas, v is the speed of vehicle in m/s. The calculated kinetic energy is **13447416 J**.

b. Rotational energy (RE):-Rotational energy is the energy needed to slow down the rotating parts. It varies for different vehicles and which gear is selected. However taking 3% of kinetic energy is a reasonable assumption. The calculated rotational energy for the vehicle considered is **403422 J**.

c. Total energy (TE):-Total energy is the sum of kinetic energy and rotational energy. It can be expressed with below equation

$$TE=KE+RE \dots\dots\dots 3.27$$

The calculated total energy is **13850838 J**.

d. Disc usable area (Ad):-Size of the brake disc considered for 8.7 T vehicle is, outer diameter (OD) as 0.24 m and inner diameter (ID) as 0.12 m. The usable area of the brake disc can be calculated with the help of below equation

$$A_d = \left(\frac{\pi}{4}\right) * (OD)^2 - (ID)^2 \dots\dots\dots 3.28$$

The disc usable area will be **0.034 m²**

e. Time required to stop the vehicle (ts):-Time required to stop the vehicle is calculated with the help of following equation

$$t = \frac{v}{u} \dots\dots\dots 3.29$$

The time required to stop the vehicle is **4.6sec**.

f. Braking power (Pb) and highest braking power (Pb(0)):-Braking power is the ratio of total energy to time required to stop the vehicle. It can be expressed in below equation

$$P_b = \frac{TE}{t} \dots\dots\dots 3.30$$

The calculated braking power is **2991541 Watt**.

And highest brake power (Pb(0)) produced at the onset of braking can be calculated with the below equation and can be also shown in fig.3.15.

$$P_{b(o)} = 2P_b \dots\dots\dots 3.31$$

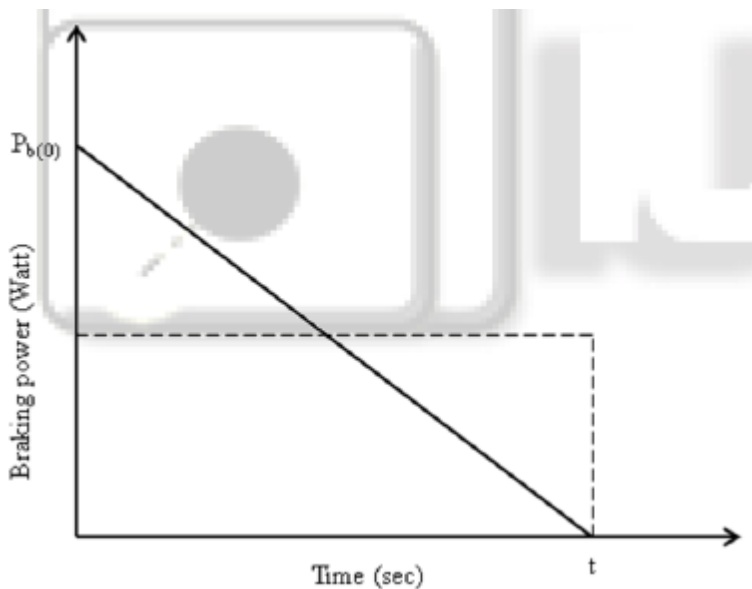


Figure 17:Plot for brake power vs. Time

The calculated onset of braking power is **5983083 Watt**.

g. Power distributed per disc (Pd):-The commercial vehicle of 8.7 T is two axle vehicle and as stated earlier front and rear axle is equipped with disc brake assembly. The braking power distributed per brake is calculated with the help of below equation .

$$P_d = 0.25 * P_{b(o)} \dots\dots\dots 3.32$$

The value of power distributed per disc is **1495770 Watt**.

a. Heat flux calculation (q):-Heat flux or thermal flux is the rate of heat energy transfer through a given surface. The brake calliper applies the brake force on effective radius on both the surface of brake disc .

The heat flux for the brake disc can be calculated with the help of below equation .

$$q = p_d / 2A_d \dots\dots\dots 3.33$$

i. Single stop temperature rise (Ts):-Single stop temperature rise depends on the time required (t) to stop the vehicle, heat flux and material properties. This is due to single braking condition.

Finally, single stop temperature rise can be calculated based on the material properties. This temperature is calculated for the required deceleration to stop at the distance of 81m. Following equation is used to calculate the temperature rise in °K or °c.

$$T_s = \left(\frac{0.527q\sqrt{t}}{\sqrt{(\rho * c * k)}} \right) \dots\dots\dots 3.34$$

Whereas, ρ is density of material in kg/m³, Cp is specific heat in J/kg-k and k is thermal conductivity of in W/m-k.

Performanceevaluation: Due to the application of brakes on the car disk brake rotor, heat generation takes place due to friction and this thermal flux has to be conducted and dispersed across the disk rotor cross section. The condition of braking is very much severe and thus the thermal analysis has to be carried out.

Therefore for calculating Single stop temperature rise(Ts), and compressive stresses the following material Properties were selected for the modified Disc Brakes.

Following material Properties were selected for the modified Disc Brakes.

A. Cast Iron Properties:

Table 6:Cast Iron Properties

properties	Cast iron
<i>Density,ρ (kg/m³)</i>	7100
<i>Young's modulus,E(Gpa)</i>	125
<i>Thermal conductivity,k (W/m.k)</i>	54
<i>Specific heat, C_p (J/kg.k)</i>	586
<i>Poisson's Ratio,ν</i>	0.25
<i>Coeff. of expansion α (*10⁻⁶/k)</i>	8.1

Therefore Single stop temperature rise depends on the time required (t) to stop the vehicle, heat flux and material properties.

$$T_s = \left(\frac{0.527q\sqrt{t}}{\sqrt{(\rho*c*k)}} \right)$$

$$T_s = 188.1^\circ\text{C}$$

B. Maraging Steels Properties:

Table 7:Maraging Steels Properties

properties	Maraging Steels
<i>Density,ρ (kg/m³)</i>	8100
<i>Young's modulus,E(Gpa)</i>	210
<i>Thermal conductivity,k (W/m.k)</i>	25.5
<i>Specific heat, C_p (J/kg.k)</i>	813
<i>Poisson's Ratio,ν</i>	0.3
<i>Coeff. of expansion α (*10⁻⁶/k)</i>	11.5

Therefore Single stop temperature rise depends on the time required (t) to stop the vehicle, heat flux and material properties.

$$T_s = \left(\frac{0.527q\sqrt{t}}{\sqrt{(\rho*c *k)}} \right)$$

$$T_s = 263.48^\circ\text{C}$$

C. ALMMC(Aluminum metal matrix composites) Properties:

Table 8: ALMMC(Aluminum metal matrix composites) Properties

properties	ALMMC
<i>Density, ρ (kg/m³)</i>	2765.2
<i>Young's modulus, E (Gpa)</i>	85.5
<i>Thermal conductivity, k (W/m.k)</i>	181.5
<i>Specific heat, C_p (J/kg.k)</i>	826.8
<i>Poisson's Ratio, ν</i>	0.33
<i>Coeff. of expansion α (*10⁻⁶/k)</i>	17.5

Therefore Single stop temperature rise depends on the time required (t) to stop the vehicle, heat flux and material properties.

$$T_s = \left(\frac{0.527q\sqrt{t}}{\sqrt{(\rho*c *k)}} \right)$$

$$T_s = 166.97^\circ\text{C}$$

D. E-Glass Properties:

Table 9: E-Glass Properties

properties	E-Glass
Density, ρ (kg/m ³)	2580
Young's modulus, E (Gpa)	72.3
Thermal conductivity, k (W/m.k)	1.3
Specific heat, C_p (J/kg.k)	810
Poisson's Ratio, ν	0.22
Coeff. of expansion α (*10 ⁻⁶ /k)	5.4

Therefore Single stop temperature rise depends on the time required (t) to stop the vehicle, heat flux and material properties.

$$T_s = \left(\frac{0.527q\sqrt{t}}{\sqrt{(\rho*c*k)}} \right)$$

$$T_s = 393.74 \text{ } ^\circ\text{C}$$

NB. All the above calculated Single stop temperature T rise is the temperature rise due to single braking condition.

The relative brake temperature after the nth brake application can be calculated using relation,

$$T_{roa} - T_i = \frac{\left[1 - e^{(-nhAt_c)/(\rho cv)} \right] [\Delta t]}{1 - e^{(-hAt_c)/(\rho cv)}} \dots\dots\dots 3.35$$

Further these respective temperatures are applied on the respective disc's material in steady state thermal analysis using ANSYS 14.5 workbench.

3.5. Methods of Analyzing Disc Stress Components

We consider that the disc is made of a homogeneous isotropic material. The disc is assumed as sandwiched between the two pads, in which temperature variation occurs only along thickness of the disc. Analytical solution for thermal stress components during thermal transients will be done only for areas where exposed to high temperature variation during brake application, this specifically include surface of the rotor closest to the pads. Due to symmetry only cross section of the thickness and circumferential slice of the rotor is used for analytical reasoning. It is assumed that the thermo mechanical properties do not change during a thermal transient and that the strain rates due to the thermal loading are small, so both the inertia and thermo mechanical coupling terms in the thermo elasticity governing equations can be neglected.

The compressive stresses ‘ σ ’ developed in the surface of a disc from sudden temperature increases is

$$\sigma = \frac{E}{1-\nu} * \alpha * \Delta T \dots\dots\dots 3.36$$

Where

E Young’s modulus

ν Poisson’s Ratio,

α Coefficient of expansion

Therefore ;

A. compressive stresses for Cast Iron Properties is :

$$\sigma = 197 \text{Mpa}$$

B. compressive stresses for Maraging Steels Properties is :

$$\sigma = 211 \text{Mpa}$$

C. compressive stresses for ALMMC Properties is :

$$\sigma = 186 \text{Mpa}$$

D. compressive stresses for E-Glass Properties is :

$$\sigma = 242 \text{Mpa}$$

3.5.1. Von Mises Theory Analysis and Fatigue Life Time Estimation

Fatigue life

Fatigue resistance is the resistance which lowers the mechanical properties of a material such as strength and stiffness due to cyclic loading, such as due to take off and landing of a plane, vibrating a plate . It is estimated that 50-90% of structural failure is due to fatigue loading.

Factors affecting fatigue life are:

- Cyclic stress state
- Geometry
- Surface quality
- Material type
- Residual stresses
- Direction of loading
- Grain size
- Temperature

Stress life approach has been adopted for conducting a fatigue analysis.

In order to use stress/life information for design purposes, a common procedure is to cross-plot the data to show the expected life (expected stress for some particular probability of failure) for a given combination of the alternating component of stress (σ_{alt}), defined as half the stress range, $\frac{1}{2}(\sigma_{max} - \sigma_{min})$, and the mean stress (σ_m) which is $\frac{1}{2}(\sigma_{max} + \sigma_{min})$. The stress ratio (R) is $\sigma_{min} / \sigma_{max}$. In metallic fatigue it is frequently assumed that compression stresses were of no significance because they acted only to close fatigue cracks, unlike tensile forces. Master diagrams of this kind are presented in a variety of forms, all more or less equivalent, but the most familiar is that which is usually referred as the Goodman diagram as shown in figure below. For design purposes, it was useful to have an equation to represent the fail/safe boundary in this diagram, and it is the linear relationship of Figure 3.16 that is associated with the name of Goodman (1899) although others have been proposed, including the earlier parabolic relationship of Gerber (1874). The linear and parabolic laws have been modified to include safety factors on one or both of the stress components. For metals as well as for composites, relates to the minimum amount of test data that is needed to define the failure envelope with a level of reliability sufficient for engineering design of critical components.

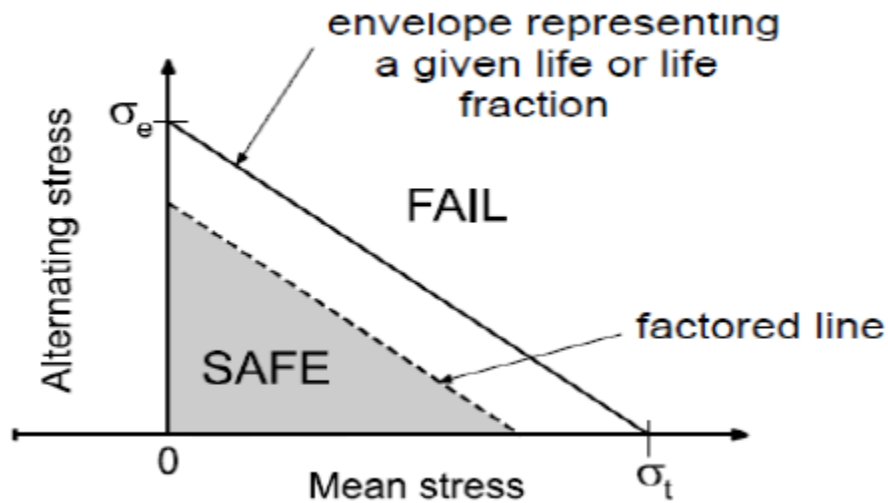


Figure 18: Schematic illustration of a constant life or Goodman diagram

The stress σ_e is the endurance or fatigue limit, and σ_t is the material tensile strength

In inelastic stress analysis, a mathematical equation involving the three principal normal stresses, known as a yield function, is generated. If the calculated yield function is greater than the yield strength of a material, plastic straining and subsequent strain softening or hardening occurs. Generally, there are several yield functions available to check whether the stress state is beyond the elastic region. These include the von Mises stress criterion, the maximum shear stress criterion and the maximum normal stress criterion. If a material is subjected to stresses beyond the elastic region, change of the yield surface occurs due to the development of plastic strain. There are two basic types of change of the yield surface. One is based on the assumption that the centre of the yield surface remains fixed whilst, at the same time, the yield surface expands without changing shape. This is known as isotropic hardening. The other, known as kinematic hardening, is based on the assumption that the yield surface translates within the stress space but does not change size or shape. Both the maximum shear stress (Tresca) and von Mises stress criteria are widely used to predict the yield surfaces of ductile materials because they have been found to fit the experimental results of ductile materials. In contrast, the maximum normal stress criterion is commonly used to predict fracture for brittle materials because their yield stresses occur at the low strain levels and are difficult to define.

Tresca and von Mises are generally applied when structural material is ductile. The von Mises theory generally predicts failure more accurately, but the Tresca theory is often used in design because it is simpler to apply and is more consecutive.

Von Mises theory relates the distortional energy of a point under a general state of stress to that of the tensile specimen at yielding . A hydrostatic state of stress occurs when all three principal stresses are equal. In this situation, the normal strains on all directions are equal and there is no shear stress due to symmetry as well. Consequently, no distortion of the stressed element occurs. Any deviation from this state will cause distortion. A general state of stress can be considered as the superposition of a pure hydrostatic state.

To evaluate the thermal stresses caused by temperature distributions, the elastic von Mises stress (σ_e) is defined in equation 3.43 below was considered, since this parameter, which combines the three principal stresses, was assumed to determine yield (onset of plastic deformation) in metals:

$$\sigma_e = \frac{1}{\sqrt{2}} \left[(\sigma_r - \sigma_\theta)^2 + (\sigma_\theta - \sigma_z)^2 + (\sigma_z - \sigma_r)^2 \right]^{1/2} \dots\dots\dots 3.37$$

Where σ_r , σ_θ , and σ_z are principal stresses in a cylindrical axis system. Since the elastic stresses and strains are completely reversible and non-cumulative, the brake disc model was investigated for one cycle of the braking and cooling period only.

Even though the Von Mises theory is stated above, the failure analysis of the material property is given in tensile strength only. The given materials its compressive strength is typically three to four times more than its tensile strength. The lack of graphite associated volume changes allows for a similar Poisson’s ratio to other engineering metals. Poisson’s ratio remains constant over a large compressive stress range and increases at higher stress levels.

CHAPTER FOUR

4. Finite Element Analysis Methods and Conditions

4.1. Material properties

The same material is used both in analytical and finite element method. The detail thermal properties and mechanical properties of those material is discussed in analytical analysis of section 3.3. Thermal properties of this materials , which are thermal conductivity, specific heat capacity, and thermal expansion coefficient, are used as an input for thermal stress analysis. Again mechanical properties such as Poisson's ratio and modulus of elasticity are used in stress analysis depending up on temperature distributions. These thermal properties and mechanical properties are taken from table 3 and 4 .

4.2. ANALYSIS USING ANSYS

Dr. John Swanson founded ANSYS. Inc in 1970 with a vision to commercialize the concept of computer simulated engineering, establishing himself as one of the pioneers of Finite Element Analysis (FEA). ANSYS is general-purpose finite element analysis (FEA) software package. Finite Element Analysis is a numerical method of deconstructing a complex system into very small pieces (of user-designated size) called elements. The software implements equations that govern the behaviour of these elements and solves them all; creating a comprehensive explanation of how the system acts as a whole. These results then can be presented in tabulated or graphical forms.

Steps in ANSYS:

To solve any problem in ANSYS it mainly follows the following steps. These are common steps to all problems except material properties and type of analysis used.

1) Preliminary decisions

- a. Analysis type
- b. Model
- c. Element type

2) Pre processing

- a. Material
- b. Create or import the model geometry
- c. Mesh the geometry

3) Solution

- a. Apply loads
- b. Solve

4) Post processing

- a. Review results
- b. Check the validity of the solution.

4.3. Finite Element Method Conditions

4.3.1. Requirements Of Brake Disc

The important requirements of the brake disc are as follows:-

- It should provide a surface having well anti wear qualities.
- It should allow the optimum rate of heat transfer.
- Heat is generated at every cycle of brake application and must be dissipated to the atmosphere..
- Sufficient strength and minimum weight.
- It must be accommodate within the minimum space available.

4.3.2. Structural Analysis

Structural analysis of brake disc is probably the most common application of finite element method (FEM). Because the brake disc is subjected to high stresses during braking. ANSYS is useful software for design engineers. This software uses the finite element method to simulate the working conditions of any component and predicts the results about their behavior. FEM requires the solution of large system of equations. It is powered by various types of solvers. ANSYS make it possible to designers to check and verify the results for their design.

The procedure for developing the brake disc includes the following steps:-

- Build the model in any CAD software. Even designers can model the brake disc in ANSYS.
- Import the model in ANSYS workbench.
- Decide the suitable element size and mesh the model.
- Apply boundary conditions.

- Evaluate the result.
- Modify the design as per result.

4.3.3. Thermal Analysis

Thermal analysis is used to determine the temperature distribution, thermal gradient, rate of heat flow and heat flux in an object that occurred due to thermal loads. Such load includes the following parameters :-

- Convection
- Radiation
- Heat flow rates
- Heat flow per unit is i.e. Heat Flux.
- Heat flow per unit volume i.e. Heat Generation Rate.
- Constant temperature boundaries.

The thermal analysis may be either linear or nonlinear. Linear includes with material properties and nonlinear includes material properties that depend on temperature. The thermal properties of most material vary with nonlinear.

4.3.4. Finite Element Method Model

The first step was to prepare a structure model of the brake disc with pads. This was carried out using finite element software.

3-D model developed for the analysis is given below (figure 4.1). Numerical simulations using the ANSYS finite element software package were performed in this study for a simplified version of a disc brake system which consists of the two main components contributing for thermal structural analysis, the disc and the pads. The dimensions and the parameters used in the thermal stress calculation are recapitulated in Table 3.2

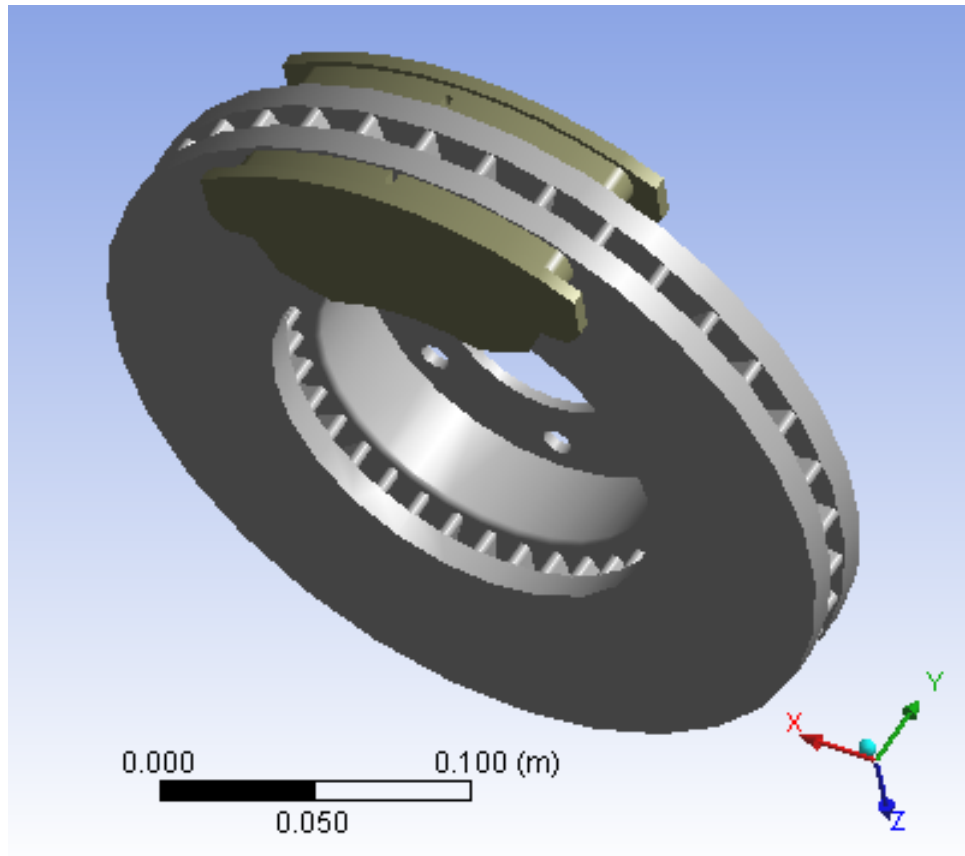
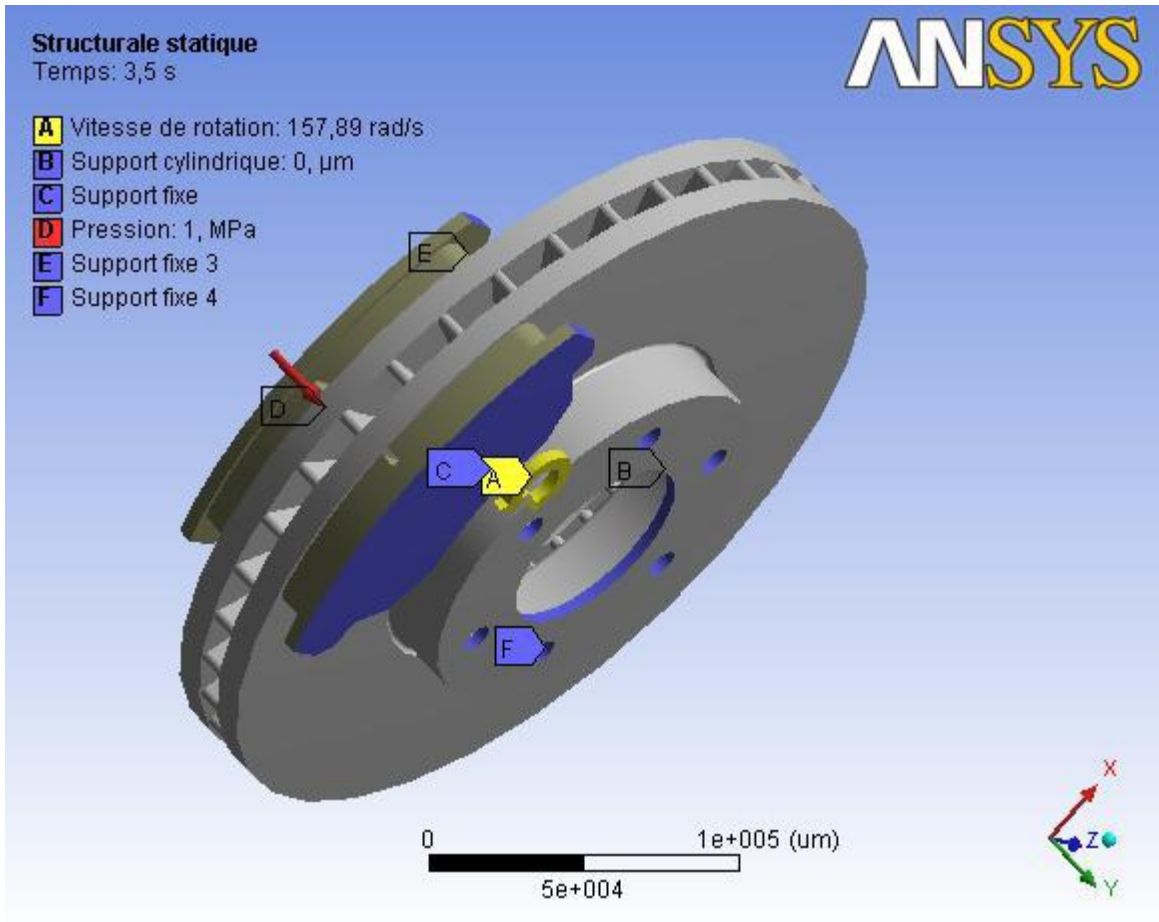


Figure 19:FEM model creation on ANSYS WB of 24mm Disc Brake.

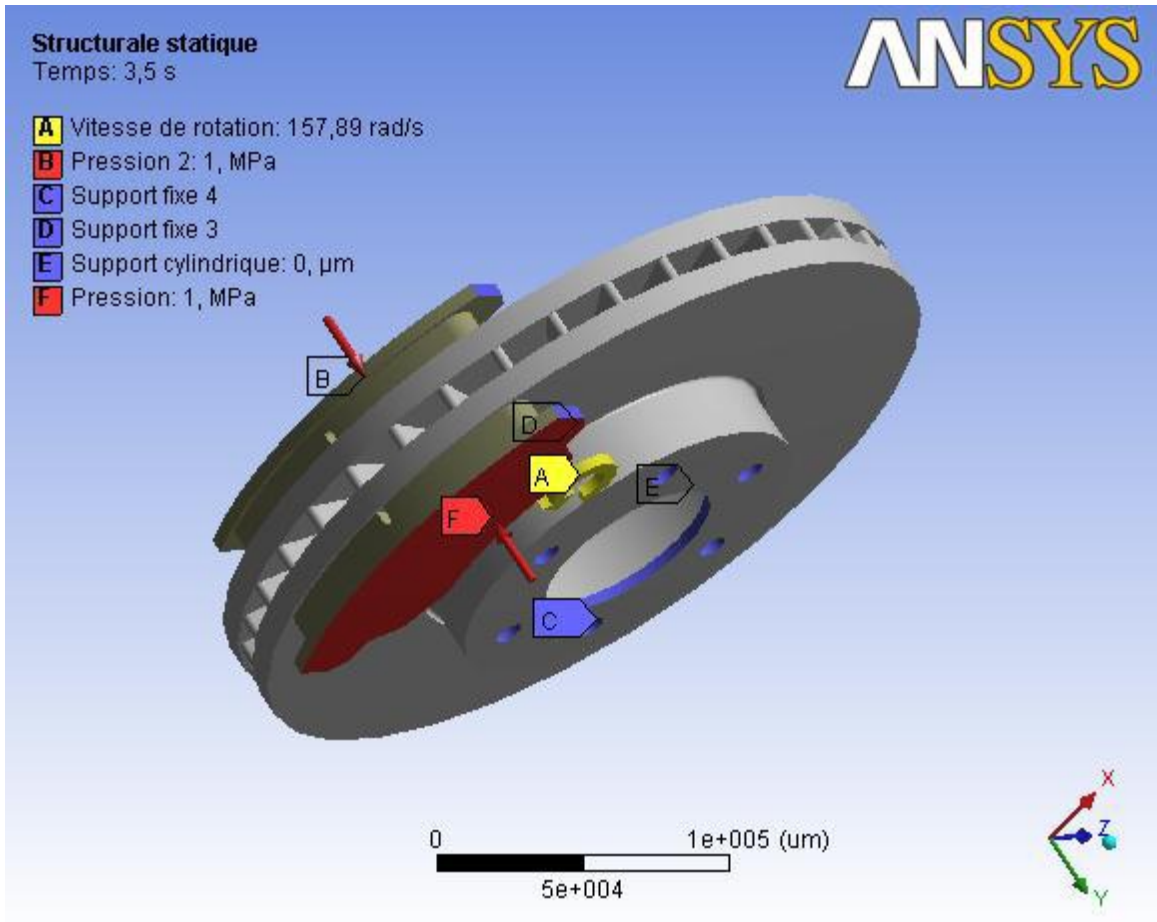
4.3.5. Boundary conditions and loading of the disc and pads

In order to accurately conduct the heat transfer and thermal analysis of the vented rotor design chosen for this study, a 3-D model of the brake disc was developed. Since the purpose is to predict typical temperature data for investigating the thermal stress behavior, only the area where the brake disc is subjected to high thermal load was modeled in detail (rotor). The model and analysis of wheel hub is omitted due to the fact that no thermal related problems created in wheel hub, because it is far away from disc pad contact.

In this FE model, boundary conditions in embedded configurations are imposed on the models (disc-pad) as shown in Fig. 4.2(a) for applied pressure on one side of the pad and Fig. 4,2(b) for applied pressure on both sides of the pad. The disc is rigidly constrained at the bolt holes in all directions except in its rotational direction. Meanwhile, the pad is fixed at the abutment in all degrees of freedom except in the normal direction to allow the pads move up and down and in contact with the disc surface.



(a) Applied pressure on one side of the pad



(b) Applied pressure on both sides of the pad
 Figure 20: Boundary conditions and loading imposed on model the disc-pads

4.3.6. Thermal boundary conditions

To express the heat transfer in the disc brake model, thermal boundary conditions and initial condition have to be defined. As shown in Figure 4.3, at the interface between the disc and brake pads, heat is generated due to sliding friction, which is shown as dashed lines. In the exposed region of the disc and brake pads, it is assumed that heat is exchanged with the environment through convection [28]. Therefore, the convection surface boundary condition is applied there. On the surface of the back plate, adiabatic or insulated surface boundary condition is used as presented in Figure 4.3. The vehicle speed decreases linearly with respect to time where the variation of heat flux during the simulation is represented in Fig. 4.4.

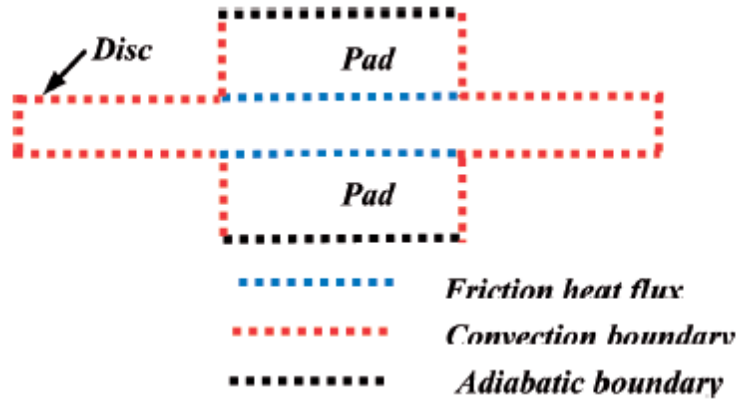


Figure 21: Thermal boundary conditions applied on disc brake

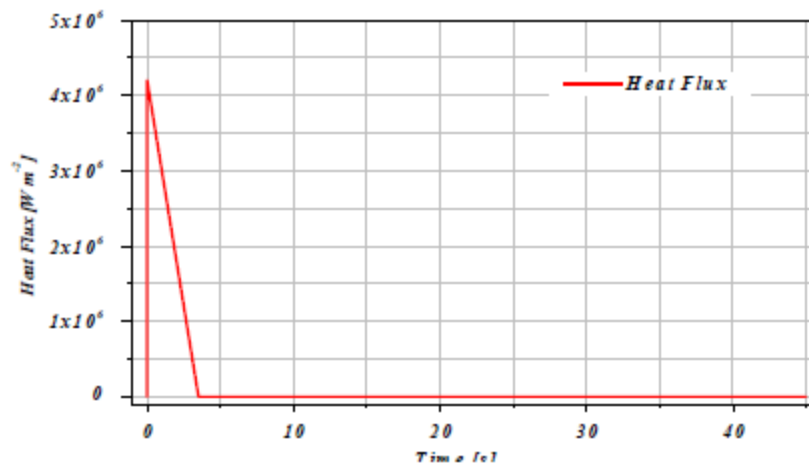


Figure 22: Heat Flux versus time

4.3.7. Meshing and Loading Conditions the Disc

The goal of meshing in Workbench is to provide robust, easy to use meshing tools that will simplify the mesh generation process. The model using must be divided into a number of small pieces known as finite elements. Since the model is divided into a number of discrete parts, in simple terms, a mathematical net or "mesh" is required to carry out a finite element analysis. A finite element mesh model generated is shown in fig.4.5. The mesh results are as shown in table No 2. The elements used for the mesh of the model are tetrahedral three-dimensional elements with 8 nodes (Figure 4.10), both thermally and structurally.

In this simulation, the meshing was refined in the contact zone (disc-pad). This is important because in this zone the temperature varies significantly. The disc is meshed using nearly seven

thousand and two hundred 8 noded ventilated elements with a quadratic interpolation function as shown in Figure 4.5 below.

The first step was to prepare a structure model of the brake disc with pads. This was carried out using finite element software (Fig. 5). Then it was meshed and defined by boundary conditions to put on ANSYS Multiphysics and to initialize the calculation. In this work, a three-dimensional FE model consists of a ventilated disc and two pads as illustrated in Figure 4.5. Whilst, Figure 4.6 shows contact zone between the disc and pad. A frictional contact pair was defined between disc-pad interfaces. the element of contact where the element types used were Quadratic Quadrilateral Contact (Conta 174) and Quadratic Quadrilateral Target (Targe 170) are also shown in fig. 4.6.

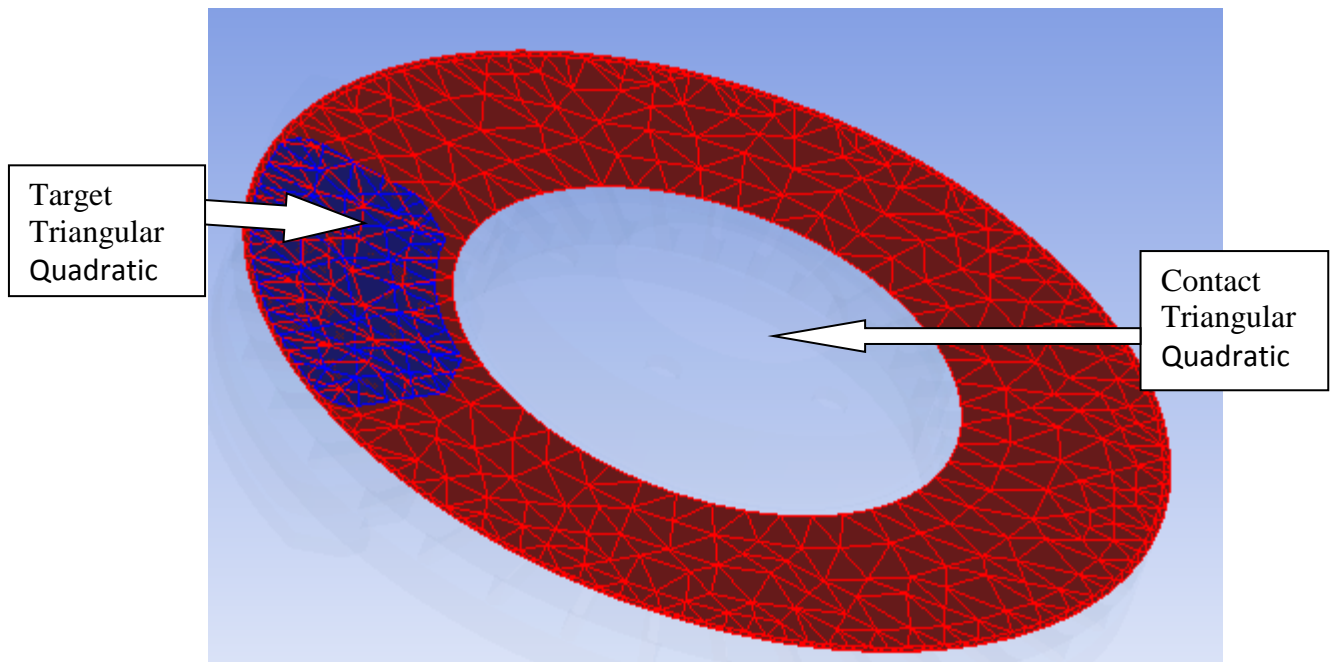


Figure 23:Contact zone of the disc and pad

The mesh of the finite elements was selected due to the difference of the obtained peak values of temperature relating to the finest mesh i.e. model with the 16 elements in the circumference and 32433 nodes was used in the thermal analysis. As the mesh should be capable to reproduce the rapid temperature variations in the immediate vicinity of the contact surface, the size of the finite element increased with the distance from the region of generated surface of friction. To avoid inaccurate or unstable results, a proper fixed time step associated with spatial mesh size is essential .

The thermal loading is characterized by the heat flux entering the disc through the real contact area (two sides of the disc). We consider heat flux during application of brake (deceleration period) only. Again we consider convection when the car accelerates only. The initial and boundary conditions are introduced into module ANSYS. The thermal calculation will be carried out by choosing the transient state and by introducing physical properties of the materials. The selected data for the numerical application are summarized as follows:

- ✓ Total time of simulation = 4.5 s
- ✓ Increment of time = 0.025s
- ✓ Number of sub steps=300
- ✓ Number of load steps=1

4.4. Methods of Finite Element Analysis

Before the age of computers, analytical methods were used as engineering tools for determining the integrity of a design. For example, Dike [30] illustrated that the mathematical equations for conduction of heat in an isotropic solid could be used to investigate the temperature response of brake disc designs by simplifying complicated parameters such as temperature dependent material properties, real brake disc geometry and complex boundary conditions. However, for real problems involving complex material properties and boundary conditions, a numerical method of analysis is more suitable. The most popular of the various numerical methods that have been developed is the finite element (FE) method. Two types of FE analysis are widely used in brake design: heat transfer analysis to determine transient temperature distributions and thermal stress analysis to determine stresses and strains due to these non-uniform temperature distributions.

Mechanical components in the form of simple bars, beams, etc., can be analyzed quite easily by basic methods of mechanics that provide closed-form solutions. Actual components, however, are rarely so simple, and the designer is forced to less effective approximations of closed-form solutions, experimentation, or numerical methods. There are a great many numerical techniques used in engineering applications for which the digital computer is very useful. In mechanical design, where computer-aided design (CAD) software is heavily employed, the analysis method that integrates well with CAD is finite-element analysis (FEA). The mathematical theory and applications of the method are vast.

Mechanical component is a continuous elastic structure. FEA divides the structure into small but finite, well-defined, elastic substructures called elements. By using polynomial functions, together with matrix operations, the continuous elastic behavior of each element is developed in terms of the element's material and geometric properties. Loads can be applied within the element, on the surface of the element, or at the nodes of the element. The element's nodes are the fundamental governing entities of the element, as it is the node where the element connects to other elements, where elastic properties of the element are eventually established, where boundary conditions are assigned, and where forces (contact or body) are ultimately applied. A node possesses degrees of freedom. Degrees of freedom are the independent translational and rotational motions that can exist at a node. At most, a node can possess three translational and three rotational degrees of freedom. Once each element within a structure is defined locally in a matrix form, the elements are then globally assembled through their common nodes into an overall system matrix. Applied loads and boundary conditions are then specified and through matrix operations the values of all unknown displacement degrees of freedom are determined. Once this is done, it is a simple matter to use these displacements to determine strains and stresses through the constitutive equations of elasticity.

The establishment of the finite element model and the finite element calculation of this thesis work were conducted through the software package, ANSYS. There are also a number of commercial FEA software packages that are available, such as NASTRAN, Algor, LSDYNA, etc. ANSYS is a combined interactive/batch type computer aided design software package, which contains many mechanical analysis programs developed, commercialized and marked by ANSYS.inc. ANSYS mechanical is a self-contained analysis tool incorporating pre-processing such as creation of geometry and meshing, solver and post processing modules in a unified graphical user interface. In addition, it is advanced level of others finite element software. ANSYS is the name commonly used for ANSYS mechanical, general-purpose finite element analysis (FEA) computer aided engineering software tools.

4.4.1. Coupled-Field Analyses and Methods

A coupled-field analysis is a combination of analyses from different engineering disciplines (physics fields) that interact to solve a global engineering problem, hence, we often refer to a coupled-field analysis as a multiphysics analysis. When the input of one field analysis depends on the results from another analysis, the analyses are coupled. The procedure for a coupled field

analysis depends on which fields are being coupled, but two distinct methods can be identified: direct and sequential (load transfer).

The direct method usually involves just one analysis that uses a coupled-field element type containing all necessary degrees of freedom. Coupling is handled by calculating element matrices or element load vectors that contain all necessary terms. An example of a direct method coupled-field analysis is a piezoelectric analysis using the PLANE223, SOLID226, or SOLID227 elements.

The sequential method involves two or more sequential analyses, each belonging to a different field. You couple the two fields by applying results from the first analysis as loads for the second analysis. An example of this is a sequential thermal-stress analysis where nodal temperatures from the thermal analysis are applied as "body force" loads in the subsequent stress analysis. With a physics file-based load transfer, you must explicitly transfer loads using the physics environment. An example of this type of analysis is a sequential thermal-stress analysis where nodal temperatures from the thermal analysis are applied as "body force" loads in the subsequent stress analysis. The physics analysis is based on a single finite element mesh across physics. You create physics files that define the physics environment; these files configure the database and prepare the single mesh for a given physics simulation. The general process is to read in the first physics file and solve. Then read in the next physics field, specify the loads to be transferred, and solve the second physics.

The term sequentially coupled refers to solving one physics simulation after another. Results from one analysis become loads for the next analysis. If the analyses are fully coupled, results of the second analysis will change some input to the first analysis. The complete set of boundary conditions and loads consists of the following:

- **Base physics loads**, which are not a function of other physics analyses. Such loads also are called nominal boundary conditions.
- **Coupled loads**, which are results of the other physics simulation.

Typical applications you can solve with ANSYS include the following:

- ✓ Thermal stress
- ✓ Induction heating
- ✓ Induction stirring

- ✓ Steady-state fluid-structure interaction
- ✓ Magneto-structural interaction
- ✓ Electrostatic-structural interaction
- ✓ Current conduction-magneto statics

The ANSYS program can perform multiphysics analyses with a single ANSYS database. A single set of nodes and elements will exist for the entire model. What these elements represent are changes from one physics analysis to another, based on the use of the physics environment concept. There are basically two methods of coupling distinguished by the finite element formulation techniques used to develop the matrix equations: Strong (also matrix, simultaneous, or full) coupling, and Weak (also load vector or sequential) coupling. These are illustrated here with two types of degrees of freedom ($\{X1\}$, $\{X2\}$):

In strong coupling the matrix equation is of the form:

$$\begin{bmatrix} [k_{11}] & [k_{12}] \\ [k_{21}] & [k_{22}] \end{bmatrix} \begin{Bmatrix} \{x_1\} \\ \{x_2\} \end{Bmatrix} = \begin{Bmatrix} \{F_1\} \\ \{F_2\} \end{Bmatrix} \dots\dots\dots 4.1$$

and the coupled effect is accounted for by the presence of the off-diagonal submatrices [K12] and [K21]. This method provides for a coupled response in the solution after one iteration.

In weak (also load vector or sequential) coupling, the coupling in the matrix equation is shown in the most general form:

$$\begin{bmatrix} [k_{11}(\{x_1\}, \{x_2\})] & 0 \\ 0 & [k_{22}(\{x_1\}, \{x_2\})] \end{bmatrix} \begin{Bmatrix} \{x_1\} \\ \{x_2\} \end{Bmatrix} = \begin{Bmatrix} \{F_1(\{x_1\}, \{x_2\})\} \\ \{F_2(\{x_1\}, \{x_2\})\} \end{Bmatrix} \dots\dots\dots 4.2$$

and the coupled effect is accounted for in the dependency of [K11] and {F1} on {X2} as well as [K22] and {F2} on {X1}. At least two iterations are required to achieve a coupled response. Note that both method of couplings are used in thermal structural analysis, unlike others coupled fields.

4.4.2. Thermal-Structural Analysis

To investigate the thermal stress behavior of brake discs under cyclic thermal load, it is necessary to obtain typical temperature distributions in these brake discs as a function of time.

Therefore, the objective of this section is to predict the temperature response of the disc. The material properties required for the temperature analysis in brake discs include the density, specific heat capacity and thermal conductivity. To determine the temperature distribution, the physical conditions existing at the boundaries must be defined such as surface heat fluxes and convective heat transfer coefficients at free surfaces.

The same brake rotor model was analyzed for thermal stress at each time step of the thermal analysis for both finite element method and analytical method. The predicted non-uniform temperature distributions from the thermal analysis were used as the input data in this analysis.

To evaluate the thermal stresses caused by these temperature distributions, stress components (axial, radial and circumferential stresses) and the elastic von Mises stress was considered, since these parameter, which combines the three principal stresses. These parameters are assumed to determine yield (onset of plastic deformation) in metals. Elastic stresses and strains are completely reversible and non cumulative in disc brake [4], therefore the brake disc model was investigated for only one cycle of the braking period.

The descriptions Thermal-Structural coupling phenomena includes applicable analysis types, applicable element types, and basic matrix equations, including the matrix and/or vector terms possible in each analysis type.

Element types: SOLID186, PLANE13, SOLID98, PLANE223, SOLID226, SOLID227

Matrix equation:

(a) Strong coupling

$$\begin{bmatrix} [M] & [0] \\ [0] & [0] \end{bmatrix} \begin{Bmatrix} \{\ddot{u}\} \\ \{\ddot{T}\} \end{Bmatrix} + \begin{bmatrix} [C] & [0] \\ [C^{tu}] & [C^t] \end{bmatrix} \begin{Bmatrix} \{\dot{u}\} \\ \{\dot{T}\} \end{Bmatrix} + \begin{bmatrix} [k] & [0] \\ [k^{tu}] & [k^t] \end{bmatrix} \begin{Bmatrix} \{u\} \\ \{T\} \end{Bmatrix} = \begin{Bmatrix} \{F\} \\ \{Q\} \end{Bmatrix} \dots\dots\dots 4.3$$

(b) Weak coupling

$$\begin{bmatrix} [M] & [0] \\ [0] & [0] \end{bmatrix} \begin{Bmatrix} \{\ddot{u}\} \\ \{\ddot{T}\} \end{Bmatrix} + \begin{bmatrix} [C] & [0] \\ [0] & [C^t] \end{bmatrix} \begin{Bmatrix} \{\dot{u}\} \\ \{\dot{T}\} \end{Bmatrix} + \begin{bmatrix} [k] & [0] \\ [0] & [k^t] \end{bmatrix} \begin{Bmatrix} \{u\} \\ \{T\} \end{Bmatrix} = \begin{Bmatrix} \{F\} + \{F^{th}\} \\ \{Q\} + \{Q^{ted}\} \end{Bmatrix} \dots\dots\dots 4.4$$

Where: $[k_t] = [k_{tb}] + [k_{tc}]$

$$\{F\} = \{F_{nd}\} + \{F_{pr}\} + \{F_{ac}\}$$

$$\{Q\} = \{Q_{nd}\} + \{Q_g\} + \{Q_c\}$$

$\{u\}$ is displacement vector

$\{T\}$ is thermal potential (temperature) vector

\dot{u} is time derivative of displacement

\ddot{u} is second time derivative of displacement

$[M]$ is structural mass matrix (Coefficient matrices of second time derivatives of unknowns.)
(discussed in Derivation of Structural Matrices)

$[C]$ is structural damping matrix (Coefficient matrices of first time derivative of unknowns)
(discussed in Derivation of Structural Matrices)

$[C^t]$ is thermal specific heat matrix (discussed in Derivation of Heat Flow Matrices)

$[C^{tu}]$ is thermoelastic damping matrix (discussed in Thermoelasticity)

$[K]$ is structural stiffness matrix (Coefficient matrices of unknown) (discussed in Derivation of Structural Matrices)

$[K^t]$ is thermal conductivity matrix (may consist of 1, 2, or 3 of the following 3 matrices)
(discussed in Derivation of Heat Flow Matrices)

$[K^{tb}]$ is thermal conductivity matrix of material (discussed in Derivation of Heat Flow Matrices)

$[K^{tc}]$ is thermal conductivity matrix of convection surface (discussed in Derivation of Heat Flow Matrices)

$[K^{ut}]$ is thermoelastic stiffness matrix (discussed in Thermoelasticity)

$\{F^{nd}\}$ is applied nodal force vector (discussed in Derivation of Structural Matrices)

$\{F^{pr}\}$ is pressure load vector (discussed in Derivation of Structural Matrices)

$\{F^{ac}\}$ is force vector due to acceleration effects (i.e., gravity) (discussed in Derivation of Structural Matrices)

$\{F^{th}\}$ is thermal strain force vector (discussed in Derivation of Structural Matrices)

$\{Q^{nd}\}$ is applied nodal heat flow rate vector (discussed in Derivation of Heat Flow Matrices)

$\{Q^c\}$ is convection surface vector (discussed in Derivation of Heat Flow Matrices)

$\{Q^g\}$ is heat generation rate vector for causes other than Joule heating (discussed in Derivation of Heat Flow Matrices)

$\{Q^{ted}\}$ is heat generation rate vector for thermo elastic damping

4.4.3. Element used in thermal analysis

SOLID90 is used for thermal analysis of the rotor . SOLID90 is a higher order version of the 3-D eight node thermal element (SOLID70). The element has 20 nodes with a single degree of freedom, temperature, at each node. The 20-node elements have compatible temperature shapes and are well suited to model curved boundaries. The 20-node thermal element is applicable to a 3-D, steady-state or transient thermal analysis. If the model containing this element is also to be analyzed structurally, the element should be replaced by the equivalent structural element (such as SOLID186).

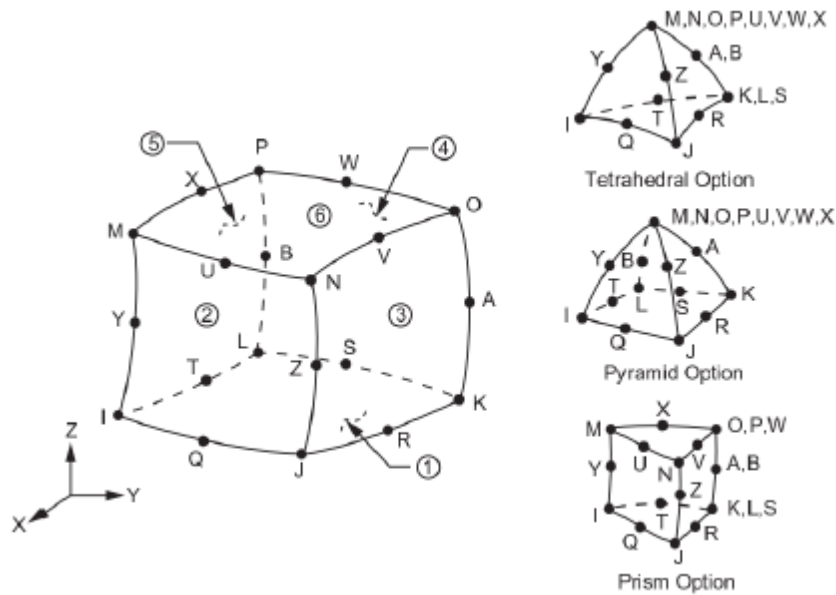


Figure 24: SOLID90 Geometry

The geometry, node locations, and the coordinate system for this element are shown in Figure 4.7 . The element is defined by 20 node points and the material properties. A prism-shaped element may be formed by defining duplicate K, L, and S; A and B; and O, P, and W node numbers. A tetrahedral-shaped element and a pyramid-shaped element may also be formed as shown in Figure 4.10.

There is nodal loading condition in this element. Convection or heat flux (but not both) may be input as surface loads at the element faces as shown by the circled numbers on Figure 4.10. Heat generation rates may be input as element body loads at the nodes. If the node I heat generation rate HG (I) is input, and all others are unspecified, they default to HG (I). If all corner node heat generation rates are specified, each midside node heat generation rate defaults to the average heat

generation rate of its adjacent corner nodes. The solution output associated with the element is in nodal temperatures included in the overall nodal solution.

4.4.4. Element Used in Stress Analysis

SOLID186 is a higher order 3-D 20-node solid element that exhibits quadratic displacement behavior. The element is defined by 20 nodes having three degrees of freedom per node: translations in the nodal x, y, and z directions. The element supports plasticity, hyperelasticity, creep, stress stiffening, large deflection, and large strain capabilities. It also has mixed formulation capability for simulating deformations of nearly incompressible elastoplastic materials, and fully incompressible hyperelastic materials. SOLID186 is available in two forms: Homogenous Structural Solid (KEYOPT(3) = 0, the default) and Layered Structural Solid (KEYOPT(3) = 1) [31]. SOLID186 Homogenous Structural Solid is well suited to modeling irregular meshes. The element may have any spatial orientation.

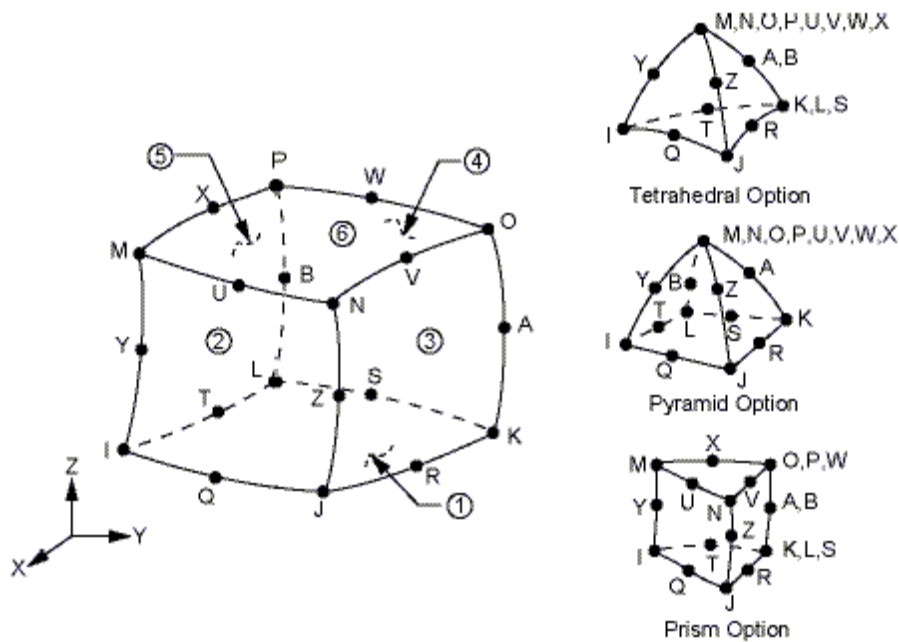


Figure 25: SOLID186 Homogenous Structural Solid Geometry

The geometry, node locations, and the element coordinate system for this element are shown in Figure 4.8. A prism-shaped element may be formed by defining the same node numbers for nodes K, L, and S; nodes A and B; and nodes O, P, and W. A tetrahedral-shaped element and a pyramid-shaped element may also be formed as shown in Figure 4.11. SOLID187 is a similar,

but 10-node tetrahedron element. In addition to the nodes, the element input data includes the anisotropic material properties. Anisotropic material directions correspond to the element coordinate directions.

Element loads are described in nodal loading. Pressures may be input as surface loads on the element faces as shown by the circled numbers on Figure 4.11. Positive pressures act into the element. Temperatures may be input as element body loads at the nodes. The node I temperature T(I) defaults to TUNIF (uniform temperature). If all other temperatures are unspecified, they default to T(I). If all corner node temperatures are specified, each midside node temperature defaults to the average temperature of its adjacent corner nodes. For any other input temperature pattern, unspecified temperatures default to TUNIF. SOLID186 homogenous structural solid input summary is listed below.

Nodes

I, J, K, L, M, N, O, P, Q, R, S, T, U, V, W, X, Y, Z, A, B

Degrees of Freedom: - UX, UY, UZ

Real Constants: - None

Material Properties: - EX, EY, EZ, ALPX, ALPY, ALPZ, PRXY, PRYZ, PRXZ (or NUXY, NUYZ, NUXZ), DENS, GXY, GYZ, GXZ, ALPD, BETD

Surface Loads: - Pressures

face 1 (J-I-L-K), face 2 (I-J-N-M), face 3 (J-K-O-N),

face 4 (K-L-P-O), face 5 (L-I-M-P), face 6 (M-N-O-P)

CHAPTER FIVE

5. Results and Discussion

In this section, results of finite element approach for temperature and thermal stress estimation in ANSYS and analytical method is compared. The result of the analysis summarized as follow. Temperature distribution of analytical analysis is almost the same to that of ANSYS. But, thermal stress of analytical analysis is somewhat greater than ANSYS both in compressive as well as tensile stresses. Analytical and ANSYS temperature distribution whether the similarity of the input for thermal stress analysis in ANSYS and analytical analyses is maintained. Unless the thermal analysis is approach.

5.1. Results of Thermal Analysis

5.1.1. Temperature Distribution for Grey Cast Iron Rotor Disc

Figures 5.1 show temperature Distribution for Grey Cast Iron Rotor Disc predicted by the FE analysis in brake application. In order to investigate the temperature and von Mises stress histories, surface of the disc is selected, because surface areas are subjected to high temperatures and stresses and these parameters are reduced through the thickness to the contour plot result .

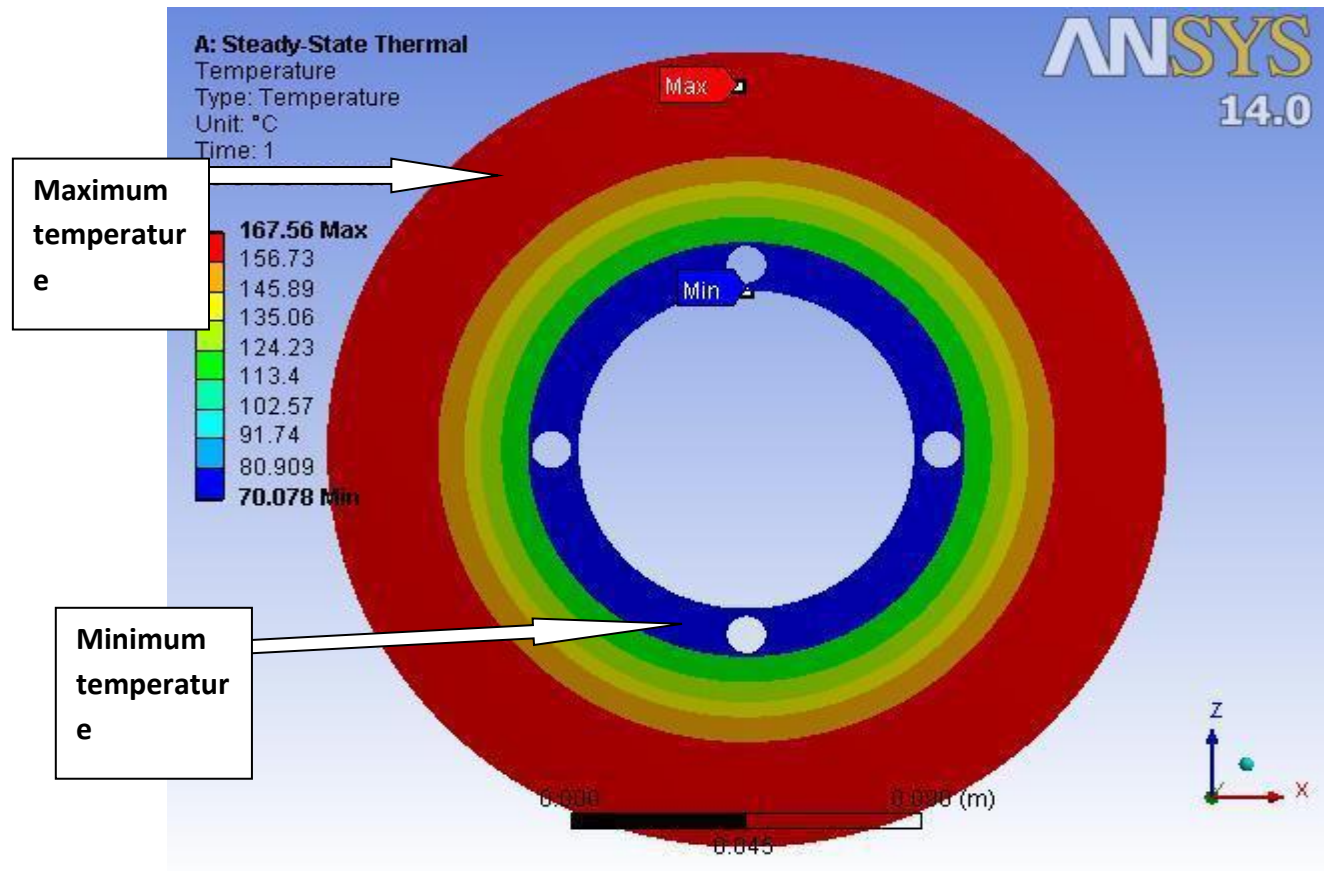


Figure 26: Temperature Distribution for Grey Cast Iron Rotor Disc

5.1.2. Temperature Distribution for maraging steel Rotor Disc

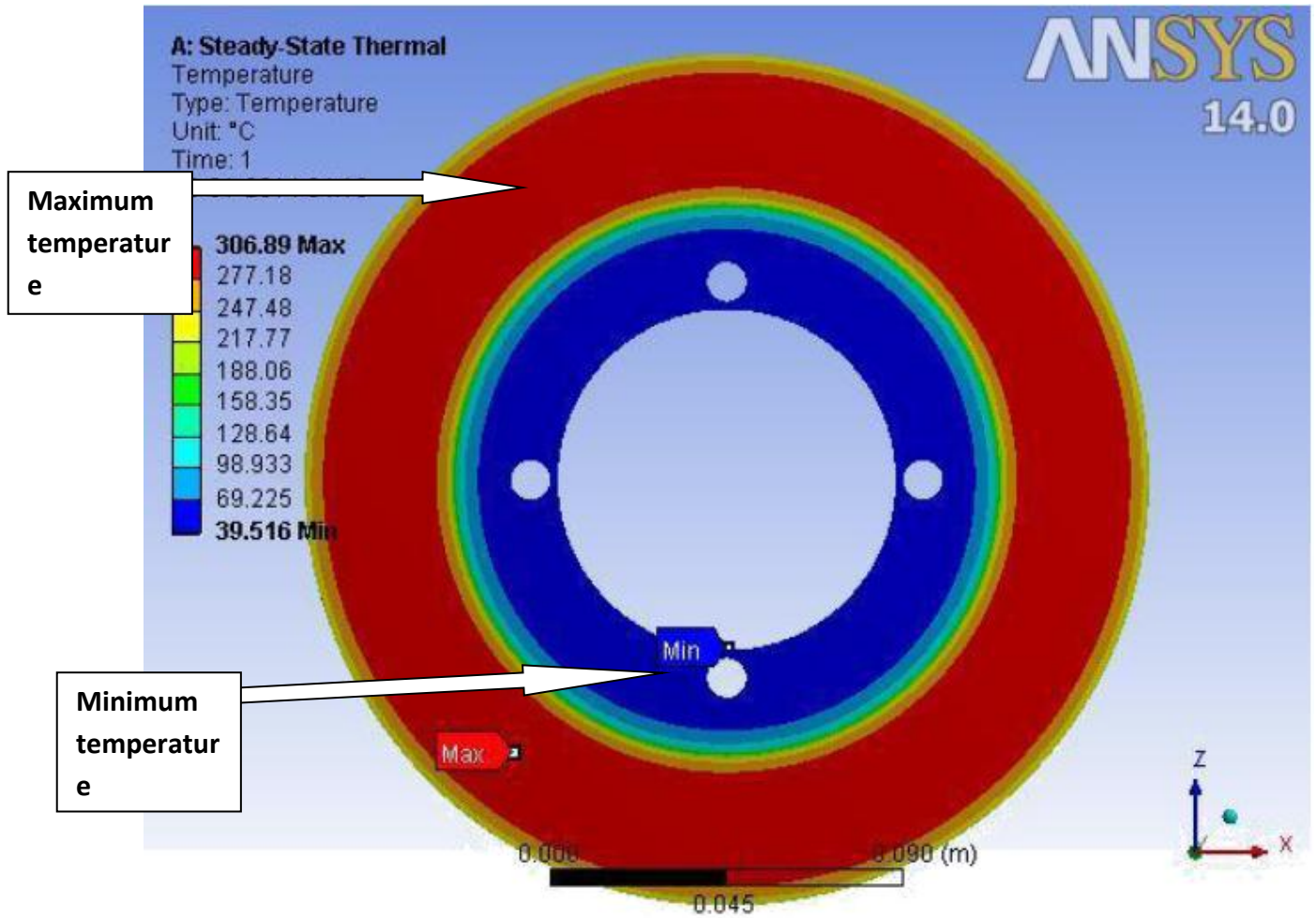


Figure 27: Temperature Distribution for maraging steel Rotor Disc

5.1.3. Temperature Distribution for ALMMC Rotor Disc

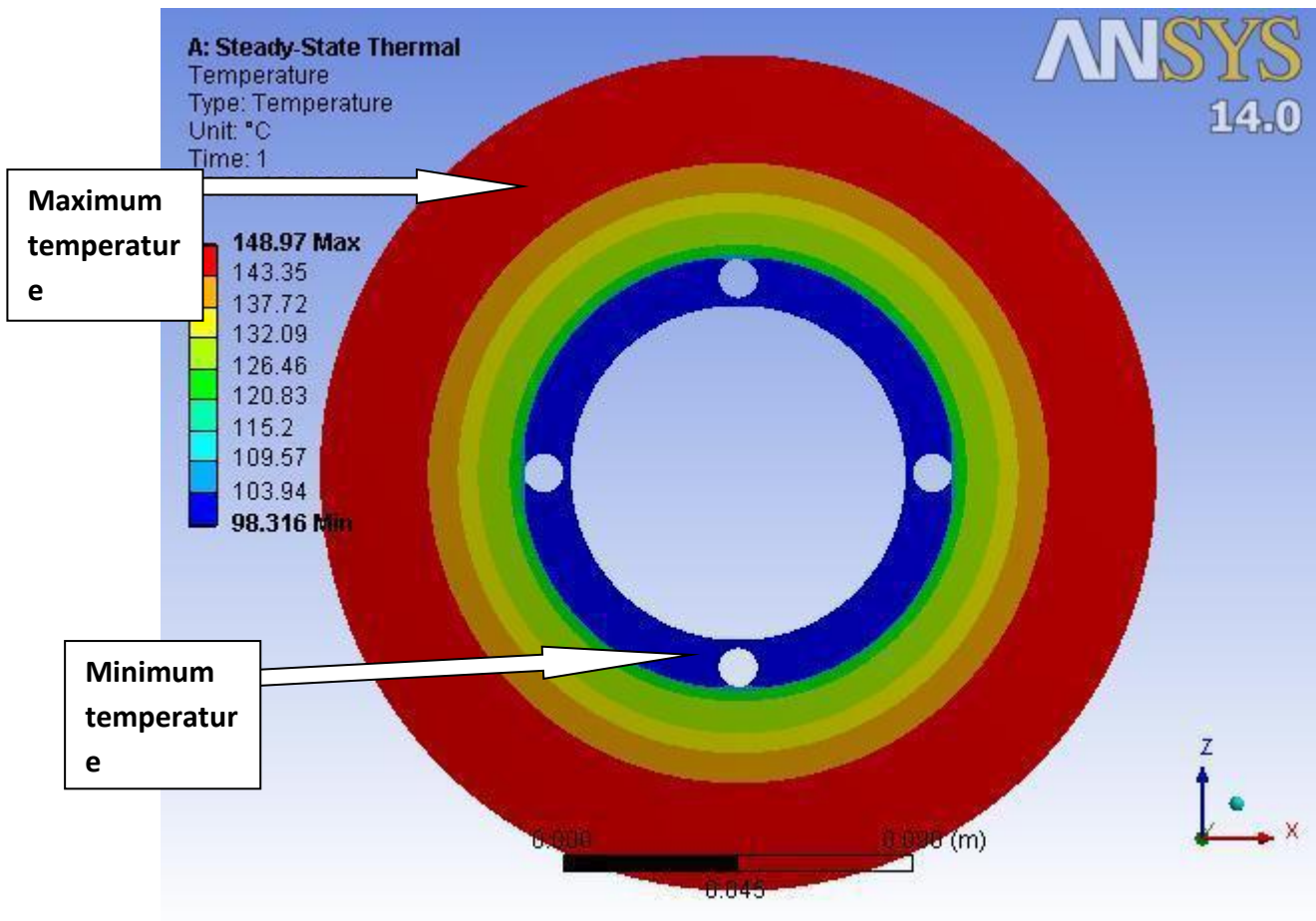


Figure 28: Temperature Distribution for ALMMC Rotor Disc

5.1.4. Temperature Distribution for E-Glass Rotor Disc

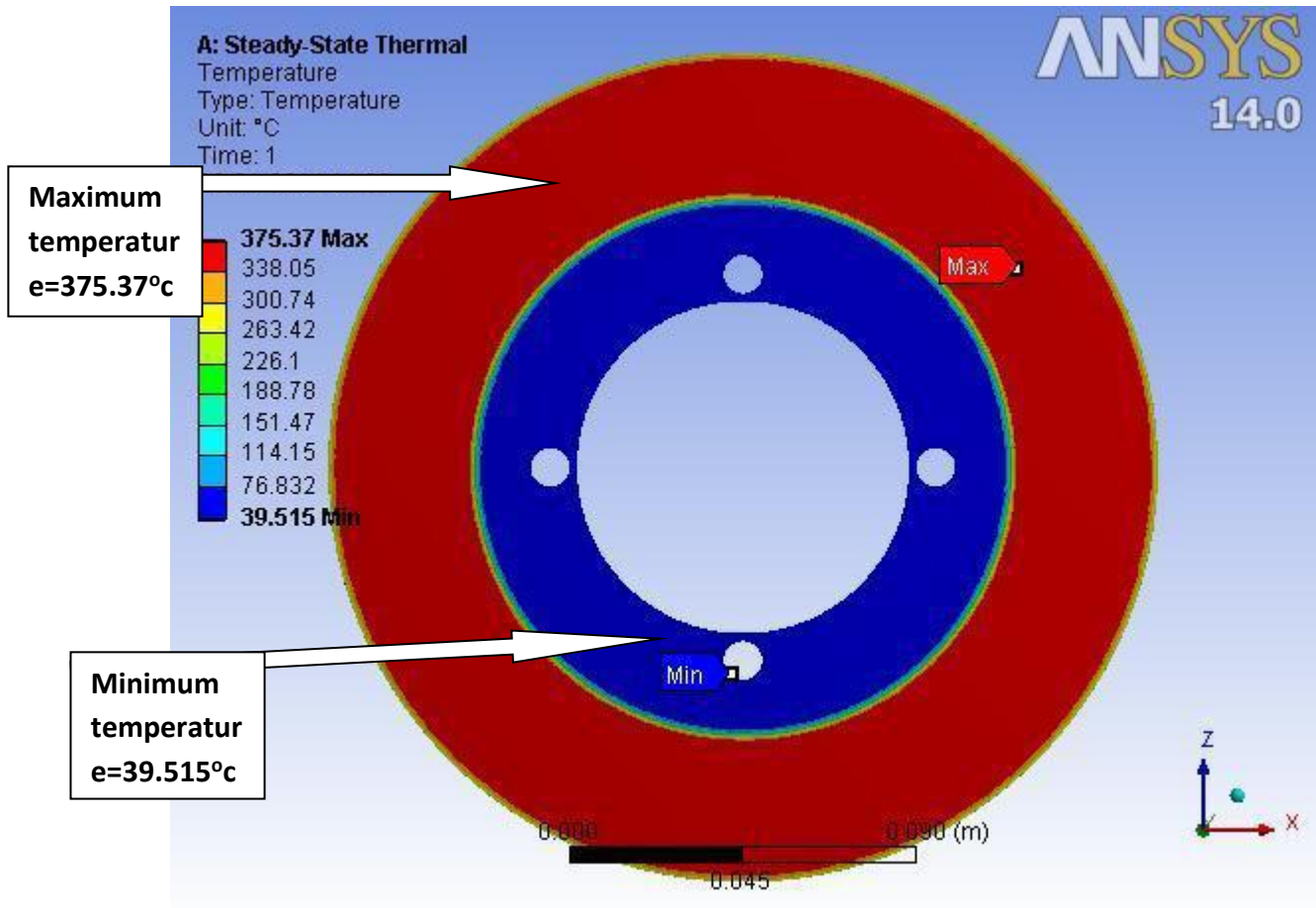


Figure 29: Temperature Distribution for E-Glass Rotor Disc

Table 10: Temperature Distribution during Braking in Various Materials: Results Comparison

S.No.	Material	Max. Temp. (°C)	Min. Temp. (°C)
1	Grey Cast Iron	167.56	70.078
2	Maraging steel	245.46	39.75
3	ALMMC	148.97	98.316
4	E-Glass	375.37	39.51

Therefore Thermal analysis is carried out for the application of braking force because of friction for the time duration of 4.5 seconds. The maximum temperature obtained in ALMMC rotor disc is at rubbing surface & is observed to be 148.97 °c. By comparing the different results obtained

from FEA & analytical analysis it is concluded that rotor disc of grey cast iron having 24mm thickness & 120mm diameter is the best suitable combination for the present application.

5.1.5. Total heat flux analysis for gray cast iron

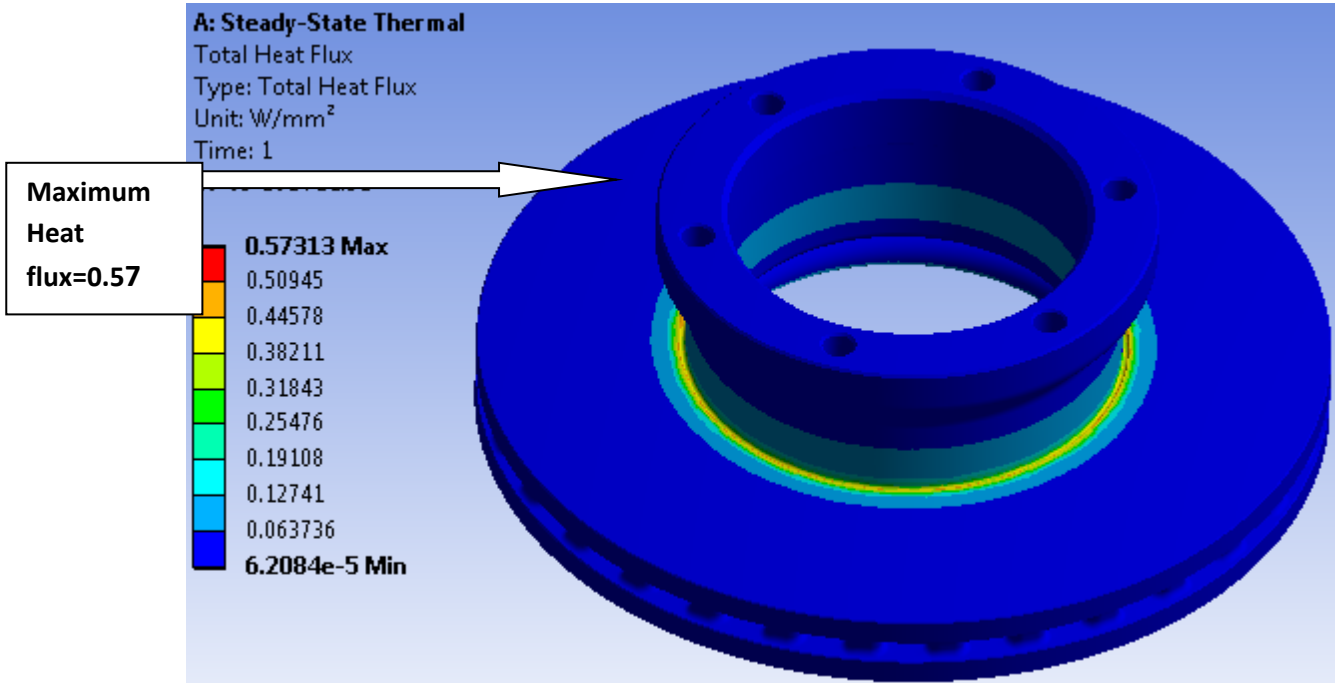


Figure 30: Total heat flux analysis

5.1.6. Total heat flux analysis for ALMMC

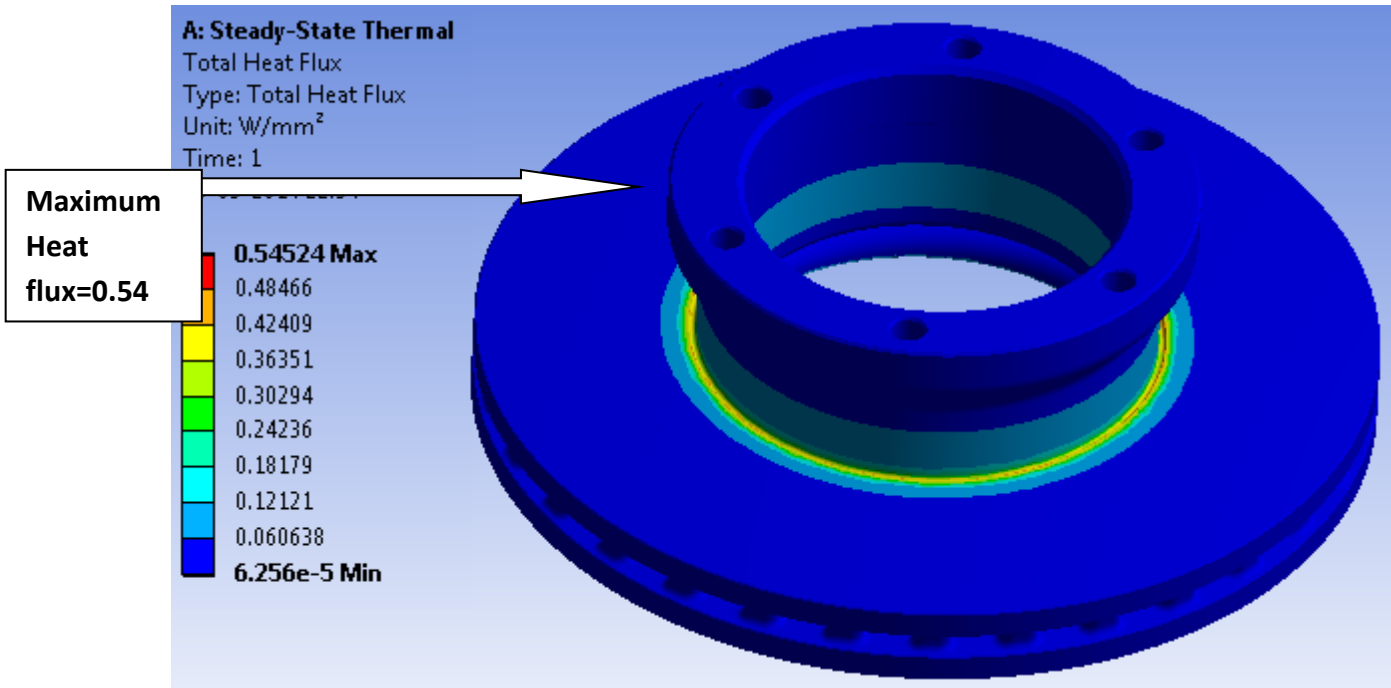


Figure 31: Total heat flux analysis

5.2. RESULTS OF STRUCTURAL ANALYSIS

5.2.1. principal stress and deformation through surface and thickness of the disc

The same brake rotor finite element model of brake disc was analyzed for thermal stress at each time step of the thermal analysis. The predicted non-uniform temperature distributions from the thermal analysis were used as the input data in this analysis. To evaluate the thermal stresses caused by these temperature distributions, circumferential, radial, as well as the elastic von Mises stress defined in equation 3.43 was considered.

A. Results for Gray cast iron

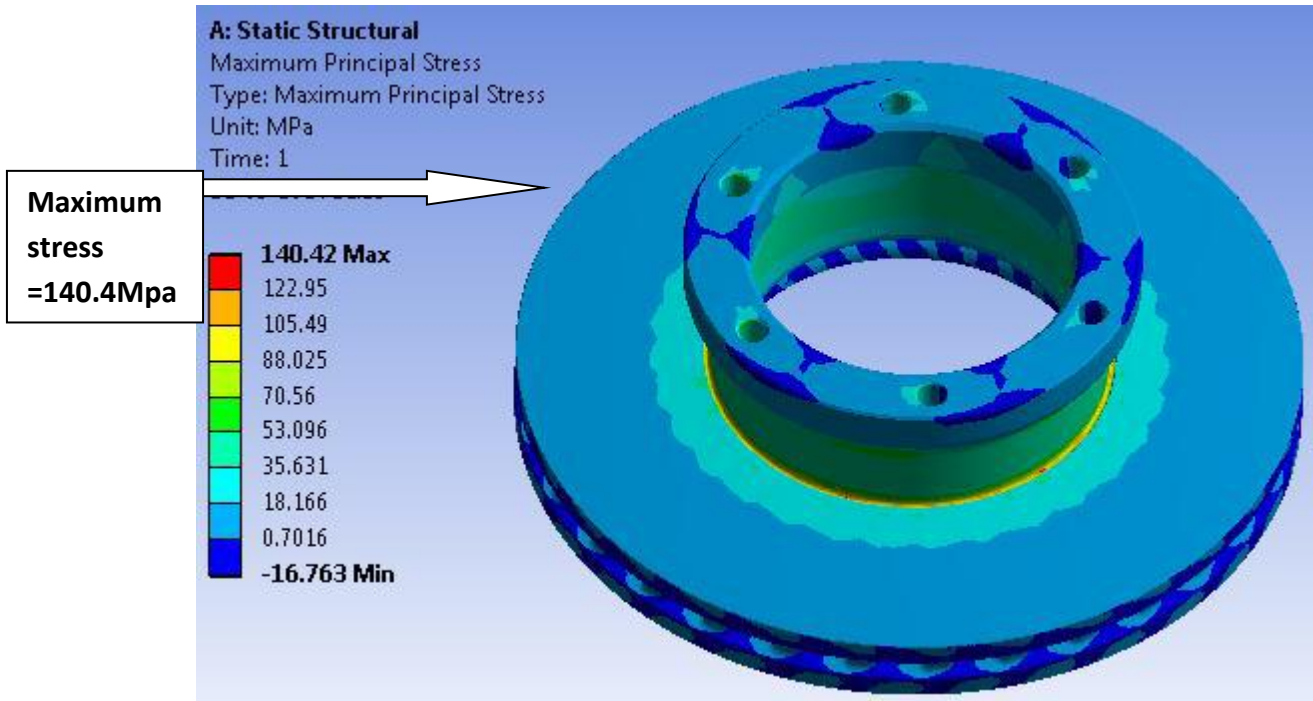


Figure 32:Maximum principle stress

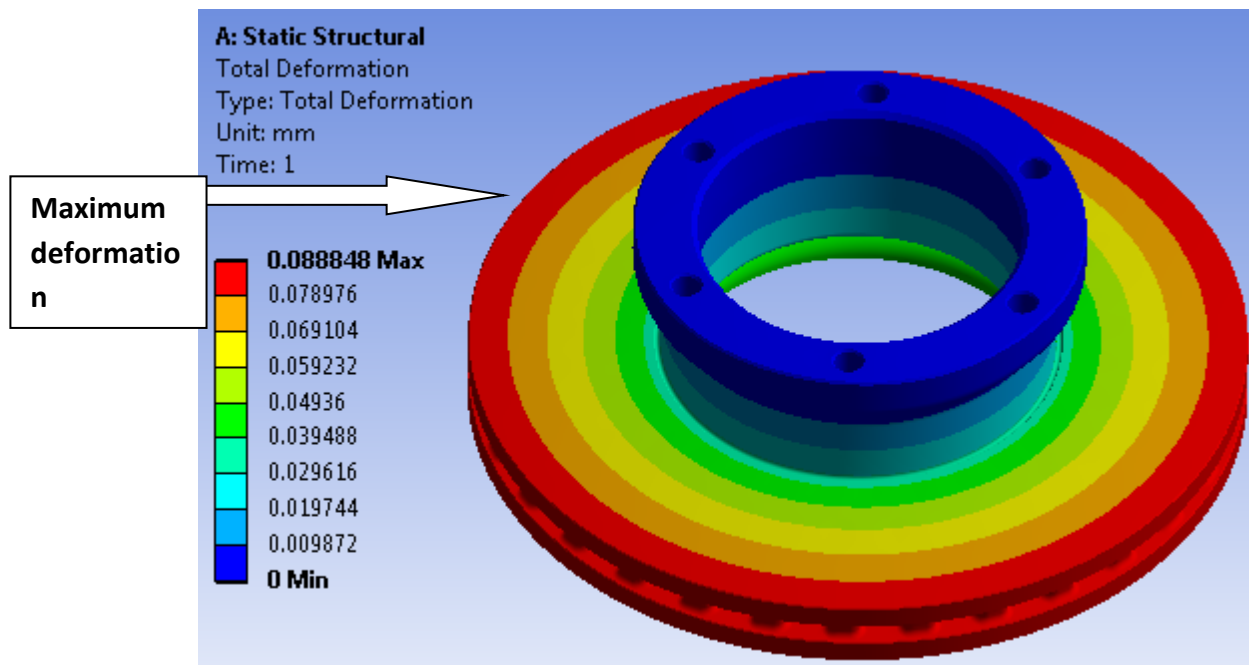


Figure 33:Total deformation

B. Results for ALMMC

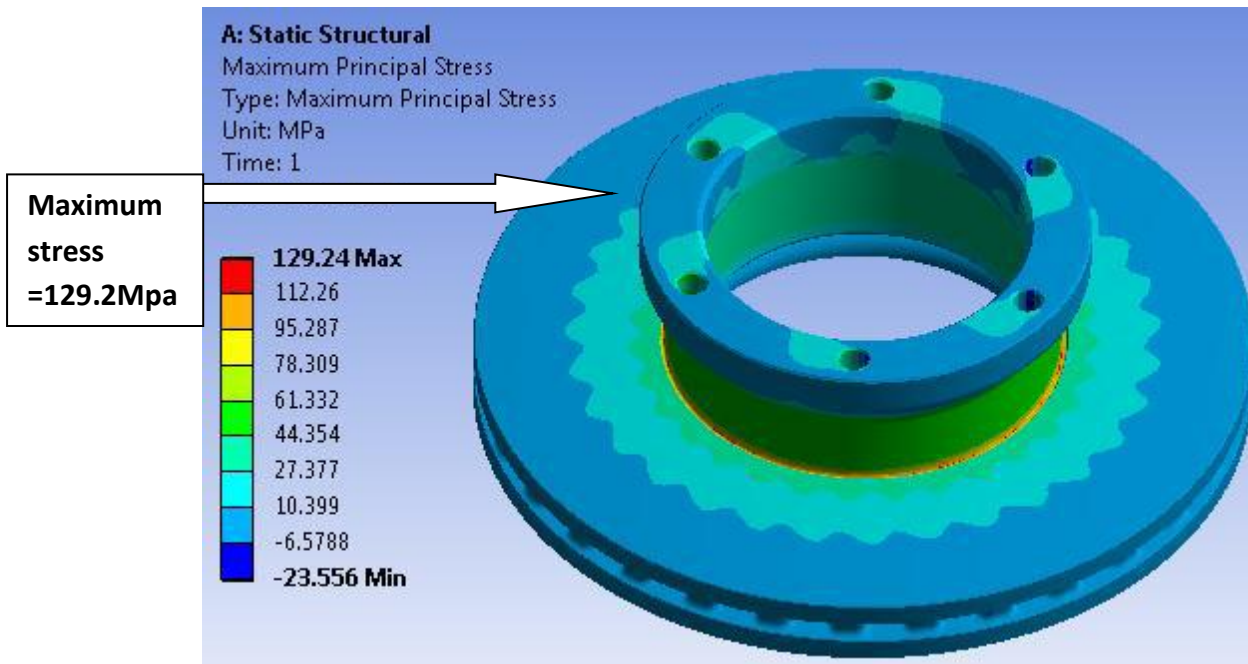


Figure 34: Maximum principle stress

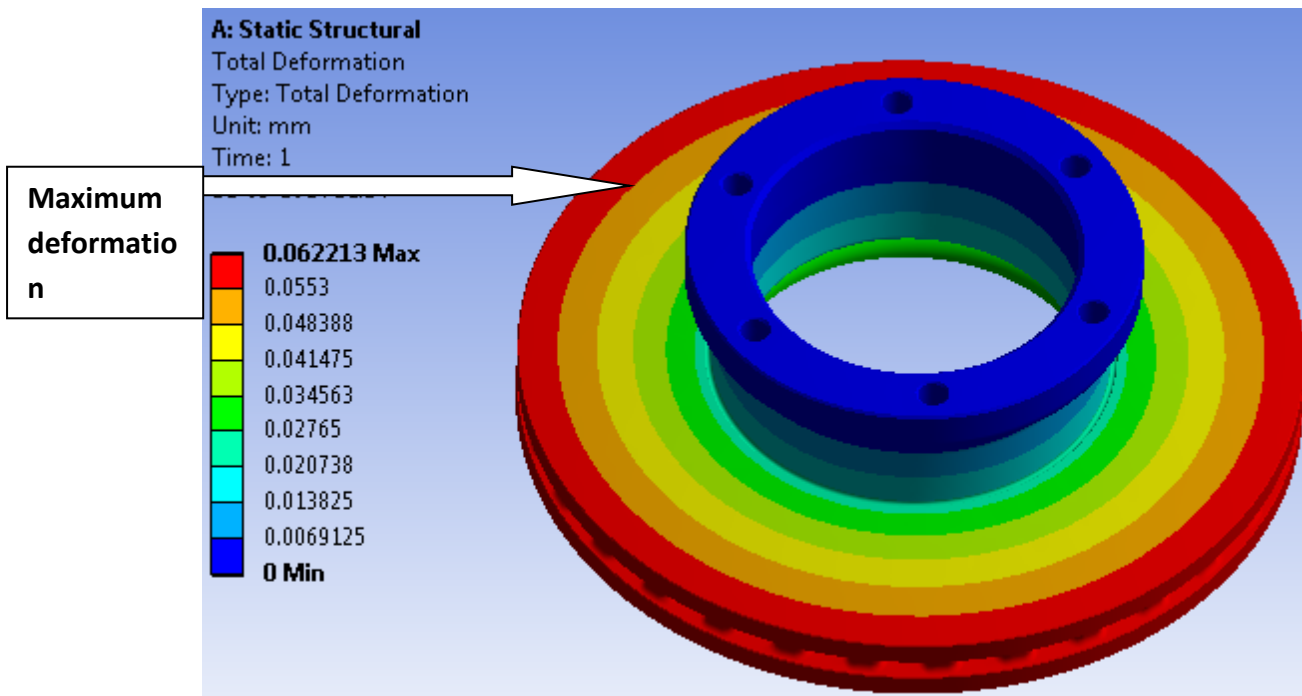


Figure 35: Total deformation

Summary of structural analysis is tabulated in table 5.2

Table 11:Results Comparison of materials

S.No.	Material	Max. principle stress (Mpa)	Total deformation (mm)
1	Grey Cast Iron	140.42	0.0888
2	Maraging steel	154.35	0.0986
3	ALMMC	129.24	0.0622
4	E-Glass	185.81	0.152

Analytically by equation 3.43 maximum von Mises stress is 186Mpa and ANSYS predicts 129.24Mpa with 21% error. This error is minimized as we reduce the size of symmetry and increase mesh density.

The table 5.2 gives the results of the four materials Grey cast iron, Maraging Steel ,ALMMC and E-Glass proposed and shows that cast iron gives less deformation and Max. stress when the loads are applied. Therefore ALMMC material is preferred over the existing materials.

Table 12:Comparison the Results of brake Disc by analytical and FEM

S. NO	Material	Analytical Max. Temp °c	FEM Max. Temp °c	Analytical Von mises Stress Mpa	FEM Von mises Stress Mpa
1	Cast iron	185.41	167.56	197	140.42
2	Maraging steel	263.62	245.46	211	154.35
3	ALMMC	166.85	148.97	186	129.24
4	E-Glass	411.74	375.37	242	185.81

CHAPTER SIX

6. Conclusions and Recommendation

6.1. Conclusion

In this thesis work, FEA analysis procedure developed to study temperature and thermal stress in disc brake. The method developed in this thesis work can be used to analyze temperature and thermal stress in sliding contact mechanical components. Comparison of FEA result with analytical method is done and similar result is obtained with reasonable accuracy. Therefore, users may use FEA using ANSYS to estimate temperature and thermal stress developed in any mechanical components related to thermal stress. Generally the present study can provide a useful design tool and improve the brake performance of disk brake system. From the above Table 12 we can say that all the values obtained from the analysis are less than their allowable values. Brake disk design is safe based on the strength and rigidity criteria and also Braking torque, heat flux and single stop temperature rise are calculated with the help of vehicle specifications.

Maximum temperature rise are calculated for four different materials, i.e. Gray cast iron(185.41 & 167.56 °c) , maraging steel(263.62 & 245.46 °c) ,ALMMC(166.85 & 148.97 °c) and E-Glass (411.74 & 375.37 °c) for both Analytical and FEA respectively. Also FEA of maximum principle stress for the material Gray cast iron, maraging steel ,ALMMC and E-Glass are 140.42Mpa , 154.35Mpa ,129.24Mpa , , and 185.81 Mpa respectively and Analytical analysis of maximum principle stress for the material Gray cast iron, maraging steel ,ALMMC and E-Glass are 197Mpa,211Mpa ,186Mpa and 242Mpa respectively. Comparing the different results obtained from the analysis, it is concluded that ALMMC is the best possible combination for the present application. The analysis led to aluminum metal matrix composite as the most appropriate material for brake disc system

Comparing the different results of temperature rise and stress field obtained from analysis it shows that in the ventilated ALMMC reduction in temperature and stresses than the other materials. All the values obtained from the analysis are less than their allowable values. Hence the brake disk design is safe based on the strength and rigidity criteria.

6.2. Recommendation

From analytical analysis and Finite element analysis observations, it can be concluded that high temperature induced in disc/brake interface can result in rotor fade, surface rupture and high stress, again which reduces life of the brake.

Different researchers specify different ways to eliminate thermal related problems in brake rotors. According to [1], increase in yield and fatigue strength of the rotor material, is one aspect. Even though the detail of increasing yield and fatigue strength was not given, it has direct influence on surface rupture, fade, and fracture of the rotor. In addition, decreasing brake temperature and redesigning the hub-rotor unit to eliminate constraint stresses were set as ways to improve brake performance in terms of life, failure and surface tribology.

The degree of increase of surface temperature depended on the thermal conductivity of the brake disc material. If the material had low thermal conductivity, the temperature gradient across the brake disc thickness was high. As a result, the surface temperature rose faster than that of the brake disc body, resulting in different thermal expansions between the surface and body of the brake disc. This problem is solved by gray cast iron material quality improvement: proportions of chemical compositions of the constituent. Increasing the carbon content in cast iron has the effect of increasing thermal conductivity. Fatigue life, as well as the behavior during cyclic loading, varies widely for different constituents of Carbon, Silicon, Manganese, and Sulfur and phosphorus.

Brake fade and rotor warping can be reduced through proper braking technique; when running down a long downgrade that would require braking simply select a lower gear (for automatic transmissions this may necessitate a brief application of the throttle after selecting the gear).

Also, periodic, rather than continuous application of the brakes will allow them to cool between applications. Continuous light application of the brakes can be particularly destructive in both wear and adding heat to the brake system.

Another technique employed to prevent brake fade is the incorporation of fade stop brake coolers. Like titanium heat shields the brake coolers are designed to slide between the brake pad backing plate and the caliper piston. They are constructed from a high thermal conductivity, high yield strength metal composite which conducts the heat from the interface to a heat sink which is

external to the caliper and in the airflow. They have been shown to decrease caliper piston temperatures by over twenty percent and to also significantly decrease the time needed to cool down.

6.3. Future Work

In this thesis work temperature and thermal stress distribution along thickness of the disc is studied. Other influencing factors are not studied. So this work is restricted to the specified cases. However, this paper can be extended to other situation listed below. Further numerical method investigations should be conducted on:

- ✓ Fatigue analysis of disc brake under repeated brake application with time varying heat flux applied at the disc surface
- ✓ Fracture mechanics approach to study surface stress related to initiation and propagation of cracks by stress varying along radius of the disc.
- ✓ Hot spots analysis as a result of high local temperatures on the brake disc, hot spots may form and lead to undesirable performance hindrances such as brake fade or vibrations and judder.
- ✓ Vibration analysis caused by stress components
- ✓ Wear and noise analysis of disc brake caused by thermally induced surface stress
- ✓ Tribology and vibrations study of the contact disc-pads
- ✓ Experimental study to verify the accuracy of the numerical model developed
- ✓ Study of dry contact sliding under the macroscopic aspect (macroscopic state of the disc and pad surfaces).

REFERANCE

- Samic , & Sheridan. (2012). effects of friction on the pressure distribution between the rotor and the pads. Product Development and Materials Engineering. *MSc Thesis, School of Engineering in Jönköping*.
- A.Floquet . (2010). “temperature distribution and comparison of simulation results and experimental results in the disc by 2D thermal analysis using axis-symmetric model.”. *International Journal of Automotive Technology*,, 11(1), 133-138.
- Babukanth, & Vimal. (2013). “transient Analysis of disk brake using ANSYS Software”. *International Journal of Latest Trends in Engineering and Technology*, 2(3), 18-25.
- Belhocine, & Bouchetara. (2010). “simulation of fully coupled thermomechanical analysis of disc brake rotor caused by frictional heat generated during braking application”. *Journal of Mechanical Science and Technology*, 24, 81-84.
- Choi , & Lee. (1998). ‘finite element analysis of transient thermoelastic behaviors in disc brakes’,. *Vehicle Noise and Vibration, IMechE Conference Transactions*. doi:C521/009/98
- Hassan , & Li . (2011). “the temperature distribution for disc brakes by carrying out a coupled thermal–mechanical analysis as a part of their works”. *World Academy of Science, Engineering and Technology*, 60(12), 1411-1414.
- Hogskolan. (2012). “simulation of thermal fatigue stresses in a disc brake with Frictional Heat Generation “. *New York Science Journal*, 10(5), 39-43.
- Kang, & Cho . (2010). “the geometry of vents in motorcycle disc brakes which affects the surface of the disc and the thermal characteristics of disc brakes”. *International Journal of Automotive Technology*, 11(1), 133-138.
- Kim, S. W. (2012). “the temperature distribution, the thermal deformation, and the thermal stress of automotive brake disks have quite close relations with car safety”. *Journal of Mechanical Science and Technology*, 26(7), 2133-2137.
- lee. (2012, July-Sept.). pressure distribution between the rotor and the pads including the friction force. *International Journal of Advanced Engineering Research and Studies*, 1 (4), 39.
- Nackatsuji. (2013). “the initiation of hair-like cracks which formed around small holes in the flange of one-piece discs during overloading conditions”. *International Journal of Emerging Technology and Advanced Engineering*, 3(9), 383-389.

- Noyes, & Vickers. (2013). "the temperature response on the rubbing surfaces of a brake disc, using the assumption of a uniform heat flux". *Advances in Materials Science and Engineering*, 1-9.
- S.Koetnuyom. (2014). "Thermal stress Analysis of Automotive Brake Rotors.". *International Journal of Current Engineering and Technology*(3), 129-132.
- Yano, & Murata. (2000). 'experimental work to determine the amount of heat flow from the frictional interface into the rotor by conduction. 36, 857–862.

Appendix I: Specification of SUV Car

Specification	SUV
Performance	<ul style="list-style-type: none"> - Min. steering diameter (m)----- 12 - Max. speed km/hr ----- 130 - Fuel tank capacity (L) ----- 90 - AC capacity (kpa) -----0.55 - Braking distance (km/hr) ----- 25/60 - Parking brake grade angle (min) -----20⁰ 5min. not move - Idling speed (rpm) ----- 800 - Emission ----- Euro III -ON roadspeed performance-----130 OFF road speed performance-----90
Dimension	<ul style="list-style-type: none"> - Over all (l x w x h) mm ----- 4620 x 180 x 1830 - Frame (L x W) mm ----- 4470 x 1740 - Cabin (l x h x w) mm ----- - Wheel base (mm) -----2730 - Wheel track front/rear (mm) ----- 1480/1492 - Min ground clearance (mm) ----- 220
Electrical system	<ul style="list-style-type: none"> - Type single line negative grounded - Generator ----- 12v/100A - Battery ----- 12V/90A - Starter ----- 12V

Mass	<ul style="list-style-type: none"> - Curb weight of chassis (kg) -----910 - Axle load distribution front (kg) ----- 1150 - Axle load distribution rear (kg) -----1360 - G.V.W (kg) ----- 1860 - Complete vehicle weight (kg) -----2510 - Max load capacity (kg) ----- 2510
Engine	<ul style="list-style-type: none"> - Model ----- R425DOHC - 4 cylinder in line, 4 stroke , turbo charger, water cooled, inter cooler, electric control, common rail diesel engine -1 cylinder with 4 valves - Displacement -----2499cc -Max output power (kw/r/min) ----- 105/4000 - Max torque (Nm/r/min) -----340/2000 - Min fuel conception (g/kwh) ----- 210 - Fuel conception (L/km) ----- off road (L/100km)90km/h 10L on road 120km/h 12L
Clutch	<ul style="list-style-type: none"> - Single disc, dry type, friction clutch
Gear Box	<ul style="list-style-type: none"> - Mechanism ----- 5 gear, reverse gear - Manual operated ----- 4 WD and 2 WD - Gear ratio --- I:4.016;II:2.318;III:1.401;IV:1.000;V:0.778;R:3.549
Steering mechanism	<ul style="list-style-type: none"> - Model ----- ZDZ7 - Circulating ball power steering, hydraulic assisted

Rack	- Front over suspension ----- Dual cross member
Wheel	<p>independent, torsion bar</p> <p>- Rear cover suspension ----- torsion bar,5 bar coil spring</p> <p>- Rim ----- Aluminum type,17 inch</p> <p>- Tire -----235/75R Spare tire</p>
cab	<p>- Type ----- all metal closed with AC</p> <p>- Seats ----- 5 seats</p> <p>- electronic type AC and DVD entertainment system with Bluetooth</p> <p>- Door ----- has indicator light</p> <p style="padding-left: 40px;">has remote control</p> <p>- Seat cloth ---- leather laminated</p> <p>- Remote control of rear view mirror</p> <p>- Motor operated window glass</p> <p>- Electrical control of side indicator light under rear view mirror</p>
Frame	- Mitsubishi tech.
Wheel Alignment	<p>- Camber angle ----- $10^{\circ} - 1^{\circ} 10^{\circ}$</p> <p>- Caster angle ----- $2^{\circ} - 4^{\circ}$</p> <p>* The gap should be in – out (3 – 5) (mm)</p>
others	<p>- Car model ----- DD6470C</p> <p>- Color ----- Silver/black</p> <p>- Safety energy absorbing steering column</p> <p>-Air bag</p>

	-camera capacity on Reverses gear----- -Mediaplayer-----DVD+Bluetooth+GPS
Breaking	- Parking brake ----- Handle cable, central control,Drum type - Front brake ----- Disc type - Rear brake ----- Disc type -Brake type-----ABS+EBD
Over all weight weight	-Only vehicle (kg)-----1860 -Vehicle and load and also passenger + deriver (2510)